Journal of Petroleum Science Research (JPSR) Volume 3 Issue 1, January 2014 www.jpsr.org
doi: 10.14355/jpsr.2014.0301.01

Experimental Investigation of Crude Oil–Xanthan Emulsions Flow Behavior

Mamdouh T. Ghannam, Basim Abu-Jdayil, and Nabil Esmail*

Department of Chemical and Petroleum Engineering, College of Engineering, United Arab Emirates University, P.O. 15551, Al-Ain, United Arab Emirates

*Department of Mechanical Engineering, Concordia University,
1455 de Maisonneuve Boulevard W., Montreal, Quebec, Canada M3G 1M8

mamdouh.ghannam@uaeu.ac.ae; esmail@encs.concordia.ca

Abstract

The rheological behaviors of crude oil-xanthan gum emulsions were studied in terms of viscosity-shear rate and shear stress-shear rate to understand the flow behavior of these emulsions. Understanding the interaction of oil droplets phase within the aqueous continuous phase is necessary for the oil displacement mechanism by polymer solution during the enhanced oil recovery stage, thus flow behaviors of crude oil-xanthan gum emulsions were experimentally investigated. The observed rheological behavior was modeled using available mathematical models. Rheostress RS100 was employed throughout this investigation for measuring and analyzing the experimental measurements. A cone and plate of RS100 rheometer was utilized for this investigation. During the shear rate sweep over the range of 0.1-1000 s^{-1}, the measurements of shear stress and viscosity of different emulsions were investigated versus shear rate. The xanthan gum concentration range of 500-10^4 ppm (i.e. 0.05-1.0 wt %) was examined. Different crude oil concentrations over the range of 25–75% by volume were tested. A detailed investigation of the flow behavior of crude oil-xanthan gum emulsions was completed. Light concentration of crude oil-water emulsion exhibited Newtonian behavior, however the medium and high crude oil-water emulsions concentrations showed non-Newtonian of shear thinning behavior. All examined aqueous solutions of xanthan gums showed non-Newtonian profile in which their measured viscosity decreased with shear rate. The flow behavior of crude oil-gum emulsion exhibited non-Newtonian of shear thinning behavior that can be presented by Casson model.

Keywords

Crude Oil; Xanthan Gum; Emulsion; Shear Stress; Shear Rate; Viscosity

Introduction

A significant percentage of crude oil, around 40 – 50 % of the original crude oil, remains or traps in an oil well and cannot be produced by the conventional techniques. Enhanced oil recovery is a recommended technique to extract this residual crude oil. The utilization of polymer aqueous solutions in the enhanced oil recovery stage is very beneficial to keep the crude oil production rate at the required economical level after the conventional methods have been exhausted. In several enhanced oil recovery applications, polymers are utilized as thickeners to alter the rheology of the aqueous phase in order to improve mobility ratio, sweep efficiency, and increase recovery and oil production rates.

One important application of polymer solution in the enhanced oil recovery process is either to recover the oil remaining in the oil reservoir or to push surfactant solutions in the tertiary oil recovery stage.[1] This process normally leads to the formation of crude oil–aqueous polymer emulsion, i.e., the presence of an immiscible oil dispersed phase into another continuous liquid phase. Emulsions can be encountered in several important industrial applications such as food, paper, pharmaceutical, and crude oil industries. One principal type of polymer being used in the polymer flooding stage is the polysaccharide biopolymer or xanthan gum; it is a high molecular weight extracellular polysaccharide produced by bacteria of the genus Xanthomonas campestris. Xanthan gum has enormous industrial importance with applications in the food, pharmaceutical and oil industries.[2-3]

Many biopolymers can be utilized in oil recovery processes, while xanthan gum has been the most employed biopolymer.[4] Xanthan gum is a polysaccharide produced by fermentation of the microbe Xanthomonas compestris, and has been investigated by both chemical and physical techniques.[5] Solutions of xanthan are highly pseudoplastic and show very good suspending properties. This makes xanthan very useful as a suspending, stabilizing, thickening and emulsifying agent for food, cosmetics, pharmaceuticals and oil recovery, among other applications.[6] Rodd et al.[7]

reported that the xanthan gum solutions are one of the most intensively studied polysaccharide systems both in terms of physical chemistry and rheological properties. Numerous experimental studies have been published for the viscosity investigation of the xanthan gum aqueous solution. Some examples of the previous published work: Whistler and BeMiller[8] found greater pseudoplasticity results from xanthan gum solutions due to the formation of high molecular weight aggregates of stiff rod molecules. Milas and Rinaudo[9] reported that the xanthan macromolecules in the ordered helical structure would stiffen the polysaccharide solution, and this makes xanthan one of the stiffest natural biopolymers.[10] Morris[11] and Sato et al.[12] reported that the xanthan molecules behave as a rigid rod at low molecular weights whereas the shape would be a stiff wormlike coil at high molecular weight. Therefore, the shape of the xanthan molecules in solution depends on the molecular weight of the polysaccharide.

Several experimental studies are done on the rheological measurements of emulsions in which the continuous phase is Newtonian fluid.[13-15] For a very dilute concentration of oil phase into aqueous phase, viscosity increases linearly with oil concentration. For medium oil phase concentration, viscosity increases nonlinearly while the emulsion is still Newtonian. However, at a high oil phase concentration, emulsions behave in non-Newtonian pseudoplastic fashion with associated yield stress at oil concentration higher than 75%.[16-18] Few experimental rheological investigations on oil–aqueous phase emulsion have been found in which a non-Newtonian polymeric solution is employed as a continuous phase.[19-22] Sosa-Herrera et al.[22] studied the rheological properties of oil-in-water prepared with 30% sunflower oil and different sodium caseinate/gellan gum mixtures at 25 ^{o}C. They reported low viscosity values and almost Newtonian behavior for caseinate, gellan gum, and caseinate/gellan mixture aqueous solutions. Also, they noticed that the emulsions without gellan exhibited almost Newtonian behavior. However, when gellan concentration of 0.03% or higher was added into the emulsion, shear thinning non-Newtonian behavior was observed. There is a large number of published data available on the rheology of dispersed solid particle in liquid emulsion.[23-27]

The fluid viscosity of a Newtonian behavior is independent of shear rate or shear stress and depends only on the material and its temperature and pressure. The plot of shear stress versus shear rate for a Newtonian fluid, the so called flow curve or rheogram, is a straight line passing through the origin with slope equal to the fluid viscosity. However, a non-Newtonian fluid behavior is one whose flow curve is non-linear or does not pass through the origin, i.e., fluid viscosity is not constant at a given temperature and pressure but it is dependent on flow conditions such as flow geometry, shear rate and others.

Modeling analysis was utilized to find a rheological model that can be employed to fit the experimental measurements. Three rheological models of Casson, Bingham, and Power law, Equations 1-3, were investigated to study which relationship will be more suitable to present the experimental measurements.[28] Where τ is the applied shear stress in Pa and $\dot{\gamma}$ is the corresponding shear rate in s^{-1}, the τ_o and η of Equations 1-2 are the apparent yield stress in Pa and the apparent viscosity in Pas. The m and n of Equation 3 are consistency index in Pa.s^n and flow behavior index, respectively. If the flow behavior index, n, equals 1 the fluid behavior shows Newtonian profile. When n is less than 1, the fluid exhibits non-Newtonian of shear- thinning properties. However, if n is greater than 1, the fluid shows non-Newtonain of shear-thickening behavior.

$$\tau = (\tau_o^{0.5} + (\dot{\gamma}\ \eta)^{0.5})^2 \quad (1)$$

$$\tau = \tau_o + \eta\,\dot{\gamma} \quad (2)$$

$$\tau = m\ \dot{\gamma}^{n} \quad (3)$$

Experimental Work

One important application of natural and synthetic polymers such as polysaccharides, polyacrylamides, polyethylene oxide is in the enhanced oil recovery processes. The objective of the current investigation is to study the flow behavior of crude oil-xanthan gum emulsions using RheoStress RS 100 rheometer. This investigation examined a wide range of concentrations of xanthan gum, crude oil, two types of xanthan gums, and a wide range of shear rate.

Rheometer

Rheostress RS100 rheometer from Haake was used to study the flow behavior of different crude oil-xanthan gum emulsions. All measurements were carried out at a room temperature of 22 ^{o}C. A water bath was employed to control the applied temperature in the RS100 system. The control rate, CR-Mode, of RS100 was utilized for all measurements. Cone-plate sensor was used with a cone angle of 4^{o}. The cone diameter was 35 mm with gap of 0.137 mm at the cone tip. A controlled variable lift speed was used to locate the

cone in the right position over the plate. All operation procedures, rheological measurements, and data analysis were controlled and carried out by Haake software package.

Crude Oil

Crude oil–xanthan gum emulsions were prepared from crude oil, xanthan gum aqueous solution, and surfactant material. Crude oil from North Sea was employed in all experimental measurements with viscosity equal to 7.16 mPas at 40 ^{o}C, density equal to 880.6 kg/m^3 at 15 ^{o}C, and acid value of 0.0012 Kg KOH/ Kg. The crude oil was supplied by Shell Canada Limited.

Surfactant Material

Triton X-100 from Sigma-Aldrich Canada Ltd. was utilized as a surfactant with specific gravity of 1.07 and flash point of 113 ^{o}C. A surfactant material was required to prepare the oil emulsions. A surfactant is usually added into oil–aqueous phase system as an emulsifying agent to accomplish two roles. The first role is to lower the oil–aqueous solution interfacial tension, therefore, assisting in the formation of the emulsion system. The second role of the surfactant material is to stabilize the presence of the oil droplets phase within the aqueous continuous phase to avoid the oil droplets coalescence mechanism.[13]

Xanthan Gums

Two xanthan gums were employed for this investigation. The first one was a chemical grade from Sigma-Aldrich Canada Ltd (Oakville, Ontario L6H 6J8, Canada), product # G1253 under the product name of Sigma. The other one was an industrial grade of xanthan gum from CP Kelco (Atlanta-GA 30339, USA) with product # 10040282, product name Kelzan. Both products are white to tan colored powders and they are intended for use in non-food applications such as a thickener and rheology control agents. The tested solutions were prepared by dispersing the xanthan gum powder slowly in 0.25 liter of warm distilled water to the required concentration. The solutions were gently stirred until all the xanthan gum completely dissolved. Since xanthan solution is biodegradable, 1.0 gm formaldehyde was added and the solutions were stored at 4 ^{o}C until use to avoid bacterial growth.

Results and Discussion

Flow Behavior of Crude Oil-water Emulsions

The apparent viscosity of crude oil–water emulsions in the absence of polymer materials was carried out under a wide range of shear rates (0.1–1000 s^{-1}) and crude oil concentrations (10-75% by volume) to examine the flow characteristic.[21] The low concentration of crude oil of 10% reported Newtonian behavior with constant viscosity. For the medium concentration range of 25–50 % crude oil, the apparent viscosity showed a gradual reduction with shear rate exhibiting non-Newtonian of shear thinning behaviors. The flow curve of 50% crude oil showed more shear thinning behavior than the 25% emulsion. The reported shear thinning was attributed to the gradual breakup of inter-particle structures. At a shear rate of 100 s^{-1}, medium concentrations showed a little jump which was also reported by Lee et al.[29] Some crude oil droplets exercise self restructuring during the breakup of interparticle forces process to form flocculated droplets up to 200 s^{-1}, which suffer gradual shear thinning till 1000 s^{-1}. However, for 75% crude oil emulsion, a strong shear thinning of non-Newtonian behavior was reported over the whole range of shear rate.

In general, the apparent viscosity of crude oil–water emulsion increased gradually with crude oil concentration due to droplet–droplet interactions. With the increase of the crude oil concentration, the number of oil droplets increases within the continuous phase. Therefore, the separation distance between the crude oil droplets will reduce. This situation increases the droplet–droplet interaction and collision, which eventually enhances the apparent viscosity of crude oil–water emulsion.

Flow Behavior of Xanthan-gum Solutions

Figures 1-a and 1-b display the flow behaviors of xanthan solutions for Sigma and Kelzan types respectively. These figures show the apparent viscosity profile of different xanthan solutions against four decades of shear rates. Xanthan solutions exhibit the characteristic plateau behavior of polymeric solutions. In general, over the range of 500-10^4 ppm, as the xanthan gum concentration increases the apparent viscosity enhances strongly. Increase in gum content from 0 to 1000 ppm slightly increased the viscosity throughout the shear rate range. While at 5000 ppm a sudden increase in the viscosity was encountered. Further addition of the gum content to 10^4 ppm increased the viscosity of the xanthan solution even more. All solutions presented in Figures 1-a & 1-b show a non-Newtonian shear thinning in which the measured apparent viscosity decreases with shear rate.

For example, the apparent viscosity of the 10^4 ppm Sigma xanthan solutions records 36,235 mPas at shear rate of 0.3 s^{-1} and it decreases significantly to 38 mPas at 750 s^{-1}. Similar behaviors were reported by other researchers such as Lopez et al.,[30] Martinez-Padilla et al.,[31] and Kayacier and Dogan.[32]

Flow Behavior of Crude Oil-gum Emulsions and the Effect of Gum Concentration

Two xanthan gums of Sigma and Kelzan types over concentration range of 0-10^4 ppm were used to study the flow behaviors of crude oil–xanthan gum emulsions. Two concentrations of 25 and 75% by volume of crude oil were examined. The flow behavior of crude oil-xanthan gum emulsions were investigated in terms of shear stress in Pa-shear rate in s^{-1} (i.e. τ versus $\dot{\gamma}$) and apparent viscosity in mPas-shear rate in s^{-1} (i.e. η versus $\dot{\gamma}$).

Figures 2-a and 2-b show the rheogram behavior and viscosity profile versus shear rate for 25% crude oil and different concentrations of Sigma xanthan gum. Figure 2-a shows nonlinear behavior on log-log scale for all the gum concentrations. Shear stress increases gradually and significantly with shear rate and gum concentration of Sigma type. It is important to mention that the influence of gum concentration is more noticeable at low shear rate than at higher shear rate. As can be seen from Figure 2-a, the different rheogram curves are approaching each other by increasing shear rate, which means that the hydrodynamic effect is more dominant than the gum concentration at high shear rate. For further investigation of the rheograms experimental data of crude oil-xanthan gum emulsions, a fitting analysis is carried out to predict which rheological model can be utilized to present the flow behavior of crude oil-xanthan gum emulsions. The well-known Casson model[28], Eq. (1), sufficiently fits the flow behavior of crude oil–xanthan emulsions. Table I reports the regression analysis of the 25% crude oil-xanthan gum emulsions for different gum concentration. The solid curves in Figure 2-a are plots of the Casson model predictions. Therefore, Casson model (i.e. solid curves in Figure 2-a) very adequately fits the flow curves of the above mentioned solutions over the entire range of the examined shear rate.

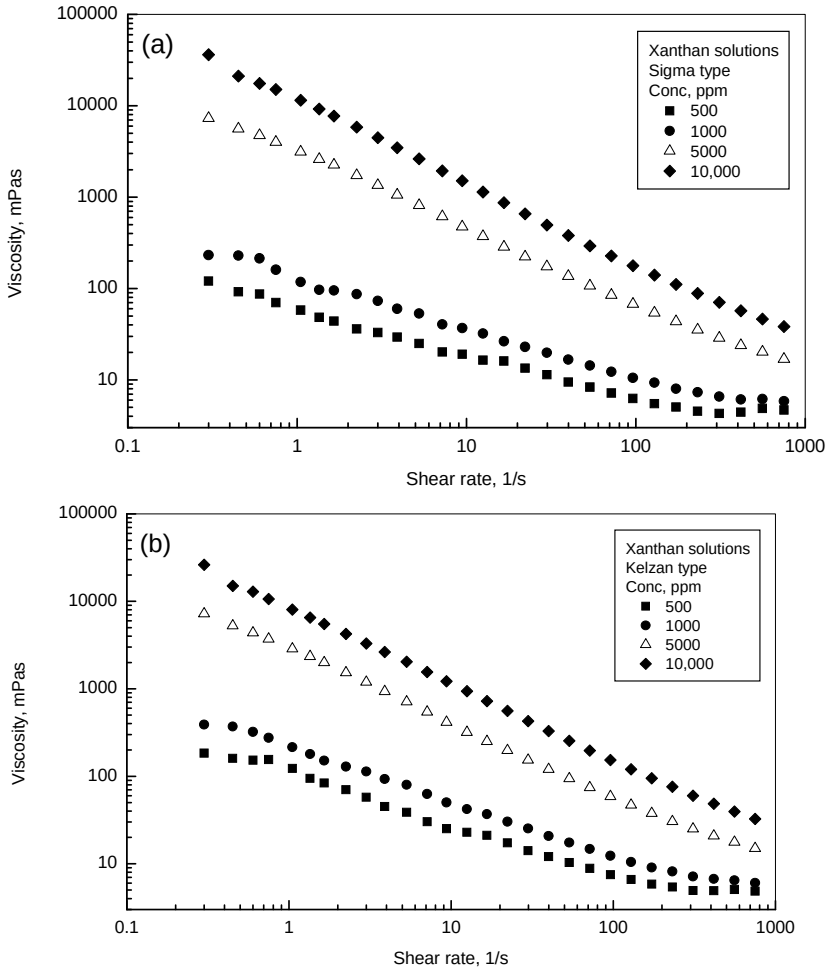

Figure 1. Apparent viscosity versus shear rate for different xanthan solutions.

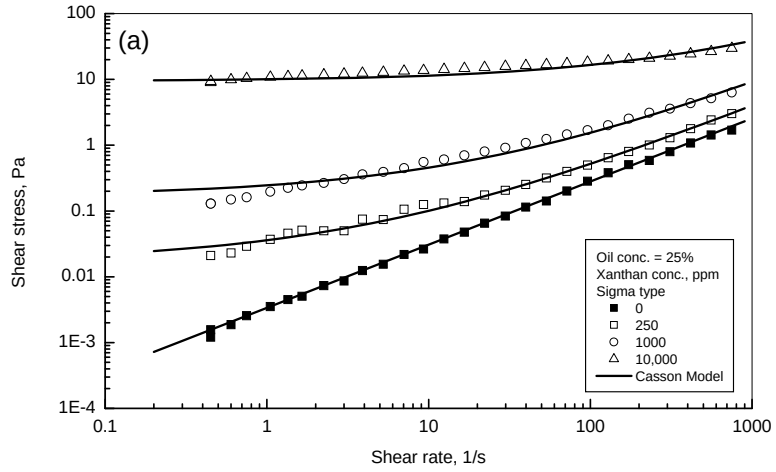

Figure 2-a. Rheogram behavior of 25% oil-sigma xanthan emulsions.

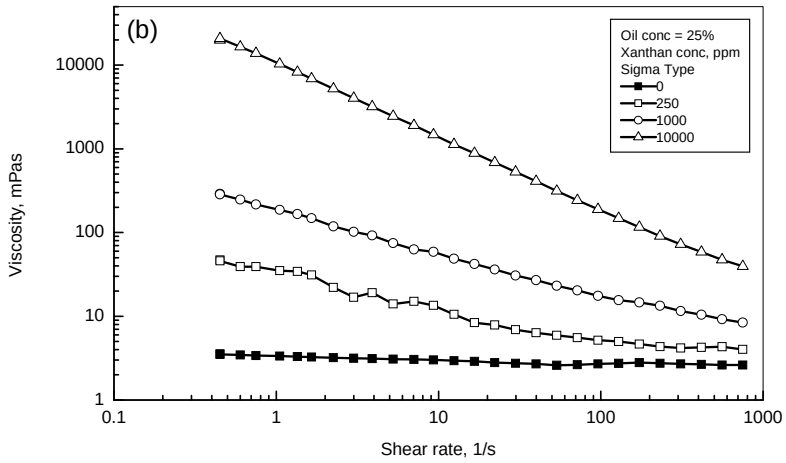

Figure 2-b. Viscosity profile of 25% oil-sigma xanthan emulsions.

TABLE I 25% CRUDE OIL–SIGMA XANTHAN GUM EMULSIONS REGRESSION ANALYSIS

Gum Concentration	τ_o	η_c
ppm	Pa	Pas
250	0.017	0.0035
500	0.057	0.0060
1000	0.170	0.0055
5000	3.100	0.0075
10,000	9.400	0.0100

Figure 2-a shows that the Casson model can be utilized with enough confidence to present the flow behavior of 25% crude oil-Sigma xanthan gum emulsions. The first term in the Casson model is yield stress τ_o, which can be considered as the transition border between solid–like emulsion behavior and liquid–like emulsion behavior. Below the yield stress value, the emulsion deforms elastically with recoverable deformation. However, above the yield stress value, the emulsion deforms continuously like a viscous liquid with non-recoverable deformation.

Figure 2-b shows a typical example of viscosity flow behavior for crude oil–xanthan gum emulsions. Several remarks can be withdrawn from Figure 2-b, viscosity decreases gradually and strongly with shear rate showing a non-Newtonian behaviors for all the examined concentrations of Sigma xanthan gum. The viscosity of 25% crude oil-xanthan gum emulsion increases steadily and significantly with xanthan gum concentrations from 0 to 10^4 ppm. As can be seen from Figure 2-b the effect of gum concentration on viscosity profile is more pronounced at low shear rate, whereas at higher shear rate, the hydrodynamic effect is more dominant causing all viscosity flow curves approach each other. Figure 2-b shows that the increasing the xanthan concentration enhances the emulsion rheological behavior through granting a higher apparent viscosity of the continuous phase and generating a network structure within the continuous phase (Cao et al.[33], Dickinson et al.[34], Yaseen et al.[35]). The contribution of the continuous phase higher viscosity and the presence of the network structure within the continuous phase will slow down the kinetic, diffusion and protecting the oil droplets phase coalescence, which improves the stability and viscosity of the crude oil-xanthan emulsions. Furthermore, the theory of oil depletion flocculation suggests that increasing the continuous phase viscosity enhances the inter droplet attraction leading to higher viscosity as well.

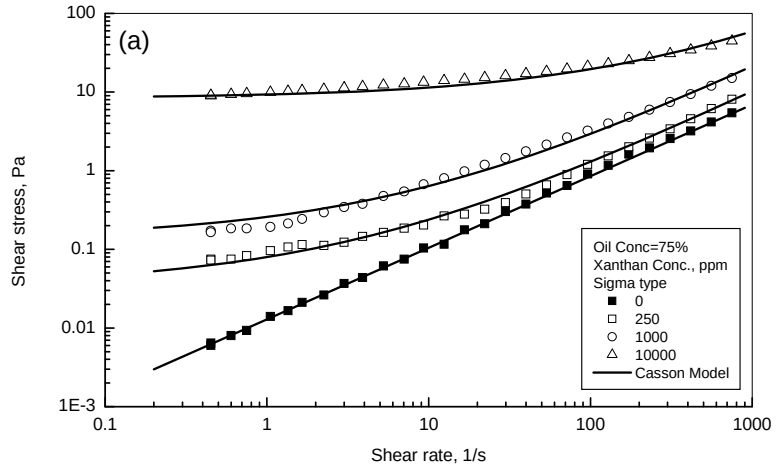

Figure 3-a. Rheogram behavior of 75% oil-sigma xanthan emulsions.

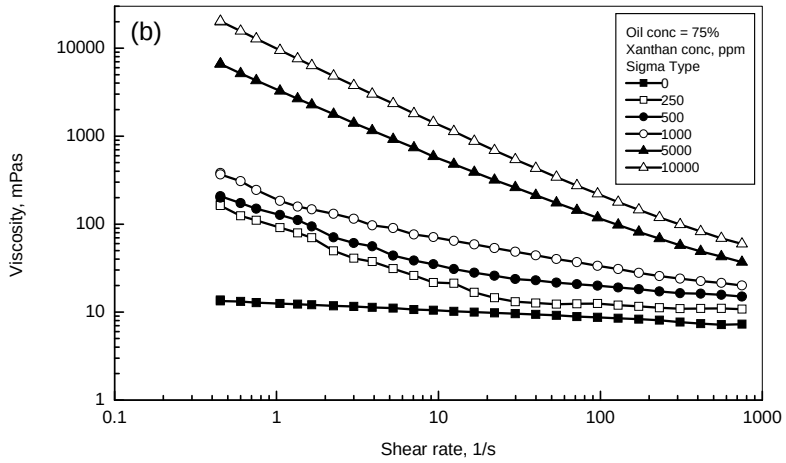

Figure 3-b. Viscosity profil of 75% oil-sigma xanthan emulsions.

Figures 3-a and 3-b show flow behaviors of higher crude oil emulsions, i.e. 75% crude oil, in the presence of different Sigma xanthan gum concentrations (i.e. 0 to 10^4 ppm). In general, these figures show similar flow behaviors to the emulsions of 25% crude oil. Fitting analysis was completed for the 50% and 75% crude oil-Sigma xanthan gum emulsions. The results of these analyses are reported in Table II.

TABLE II CRUDE OIL–SIGMA XANTHAN GUM EMULSIONS REGRESSION ANALYSIS

	50% oil		75% oil	
Gum Concentration	τ_o	η_c	τ_o	η_c
ppm	Pa	Pas	Pa	Pas
250	0.007	0.0072	0.035	0.0091
500	0.038	0.0098	0.053	0.0130
1000	0.150	0.0100	0.140	0.0180
5000	3.300	0.0120	3.100	0.0200
10,000	9.000	0.0150	8.400	0.0230

Figures 4-a and 4-b display the rheogram behaviors of two different emulsions of 25% and 75% crude oil concentrations. These emulsions were prepared from crude oil and different gum concentrations of an industrial grade of Kelzan. A wide range of Kelzan concentration was examined over the range of 0-10^4 ppm to study the effect of industrial gum concentration on the flow behavior of crude oil-xanthan gum emulsions. From a general observation, Figures 4-a and 4-b provide almost similar behaviors to the crude oil-gum emulsions in which chemical grade of Sigma xanthan was utilized. To extract some information about the flow behavior of crude oil-industrial gum emulsions, a fitting analysis was completed according to the Casson model of Equation 1. The results of the regression analysis for the 25% and 75% crude oil emulsions are reported in Table III. The solid curves in Figure 4 are the Casson model predictions.

TABLE III CRUDE OIL–KELZAN XANTHAN GUM EMULSIONS REGRESSION ANALYSIS

	25% oil		75% oil	
Gum Concentration	τ_o	η_c	τ_o	η_c
ppm	Pa	Pas	Pa	Pas
250	0.023	0.0051	0.018	0.0087
500	0.084	0.0052	0.030	0.0130
1000	0.170	0.0053	0.220	0.0170
5000	3.500	0.0062	3.300	0.0180
10,000	8.100	0.0100	8.500	0.0250

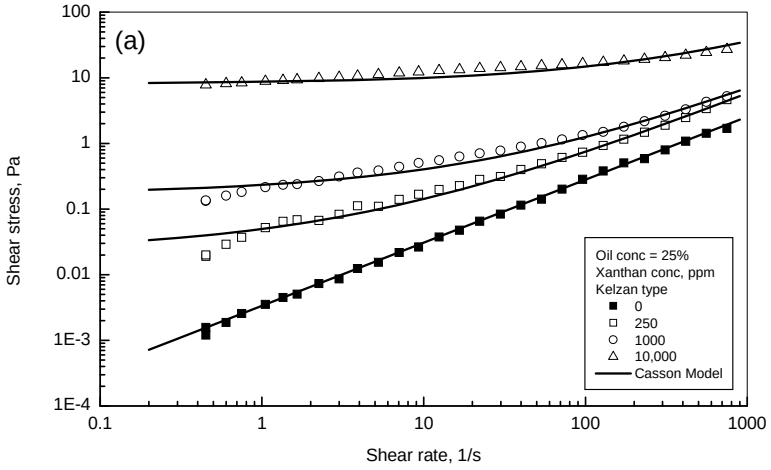

Figure 4-a. Rheogram behavior of 25% oil-kelzan xanthan emulsions.

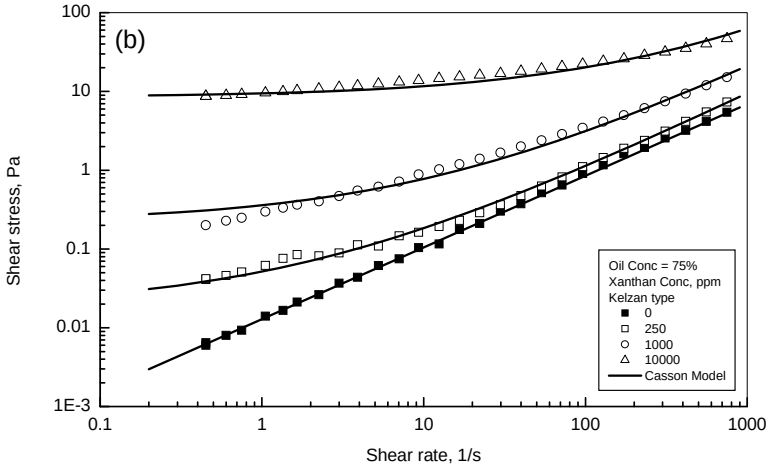

Figure 4-b. Rheogram behavior of 75% oil-kelzan xanthan emulsions.

Effect of Oil Concentration on the Emulsion Flow Behavior

The apparent viscosities of crude oil-Sigma xanthan emulsions are shown in Figures 5-7. Four decades of shear rate (0.1-1000 s^{-1}) were covered to examine the flow characteristic of crude oil-xanthan emulsions. These figures show the effect of the addition of different amounts of crude oil (i.e. from 0 to 75% by volume) into three Sigma xanthan aqueous solutions with concentrations of 500, 1000 and 5000 ppm respectively. In general, Figures 5-7 show that the apparent viscosities of the emulsions are higher than their corresponding aqueous solutions. In addition, the apparent viscosity increases gradually with the crude oil concentration. Figures 5-6 present two distinct regions depending upon the gum concentration: the lower shear rate region where the apparent viscosities increase significantly with the crude oil dispersed phase concentration, and the higher shear rate region where the apparent viscosities of the different crude oil emulsions are almost similar but above the aqueous solutions. The limit between the two distinct regions depends upon the gum concentration. Figures 5-6 with the gum concentrations of 500 and 1000 ppm, the limits between the two regions are around 10 and $1s^{-1}$, respectively. Figure 7 for the gum concentration of 5000 ppm does not show noticeable influence for the crude oil concentration since all viscosities behaviors fall on top of each other. Therefore, an important remark that can be concluded from Figures 5-7 is the gradual reduction of the crude oil influence on the emulsion viscosity with gum concentration, i.e., the higher the gum concentration we add, a lesser viscosity enhancement of crude oil will result. This can be concluded by comparing Figures 5-7 of different gum concentrations. The effect of oil concentration is more noticeable in the low shear rate region. However, the different viscosity curves are approaching each other at higher shear rate region indicating that the hydrodynamics is more dominant than the oil concentration at high shear rate region. For gum concentrations of 500 & 1000 ppm, during the higher shear rate region, all the viscosity curves show no effect for oil concentration with almost Newtonian flow behavior.

The presence of the crude oil dispersed phase within the aqueous phase of xanthan solution will gradually enhance the apparent viscosity of the emulsions with crude oil concentration. This enhancement can be attributed to the interactions and collisions between the droplets of the crude oil dispersed phase. These interactions and collisions will increase the apparent viscosity of the emulsions. Within the higher shear rate region, the observed phenomenon can be explained by the flocculation–deflocculation mechanism of crude oil dispersed phase within the aqueous phase of the xanthan solution. The more crude oil was added, the more response of flocculation–deflocculation mechanism and consequently higher viscosities.

More elaboration on the role of the presence of crude oil within the emulsions can be highlighted through the discussion of relative viscosity of crude oil–xanthan emulsions. Relative viscosity can be defined by the ratio

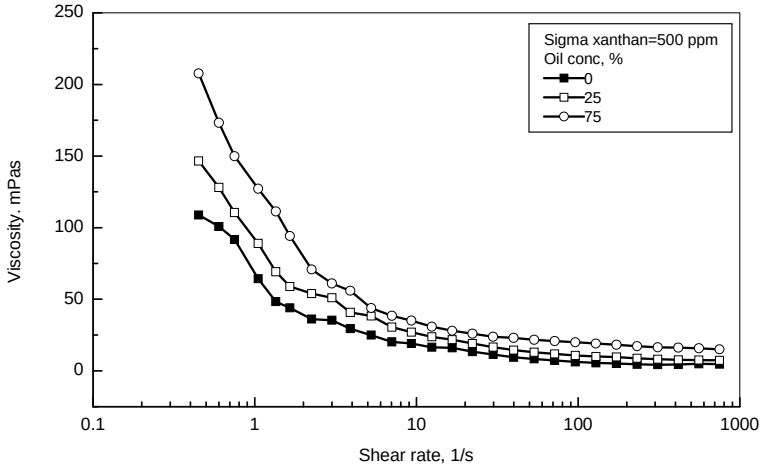

Figure 5. Effect of the oil concentrations on the 500 ppm xanthan emulsions.

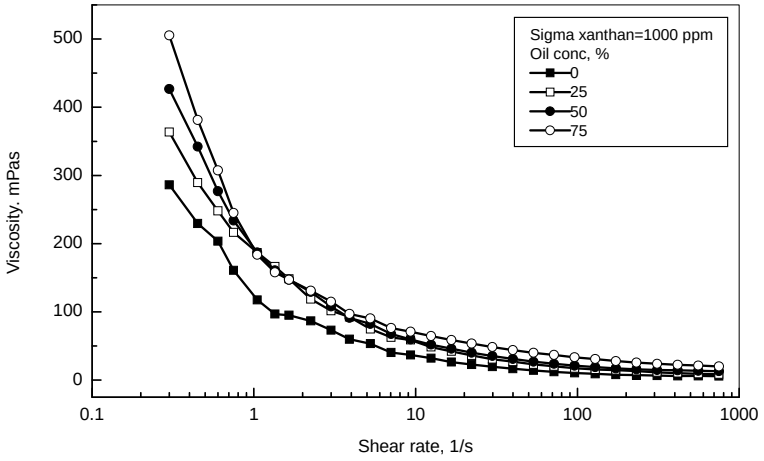

Figure 6. Effect of the oil concentrations on the 1000 ppm xanthan emulsions.

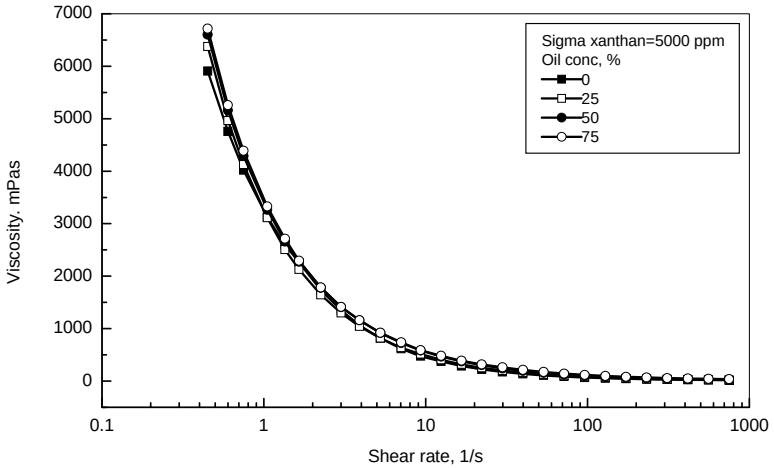

Figure 7. Effect of the oil concentrations on the 5000 ppm xanthan emulsions.

between the emulsion viscosity and the continuous phase viscosity at the same shear rate. Relative viscosity was investigated for all examined emulsions with different concentrations of crude oil and xanthan gums. To investigate the effect of oil concentration, Figures 8a-8d display the relative viscosity profiles of crude oil–Sigma xanthan versus shear rate for four different xanthan concentrations of 500, 1000, 5000, and 10,000 ppm respectively. Figures 8a-8d show that the relative viscosity increases significantly with crude oil concentration and it increases as well with shear rate. As can be concluded from these figures, the dependence of relative viscosity on shear rate relies on the xanthan concentration. For xanthan concentration ≤1000 ppm, the relative viscosity increases gradually and significantly with a shear rate up to 300 s^{-1} and then it starts to reduce gradually. Whereas, for xanthan concentrations of higher than 1000 ppm, the relative viscosity of the emulsions increase slightly and continuously with shear rate.

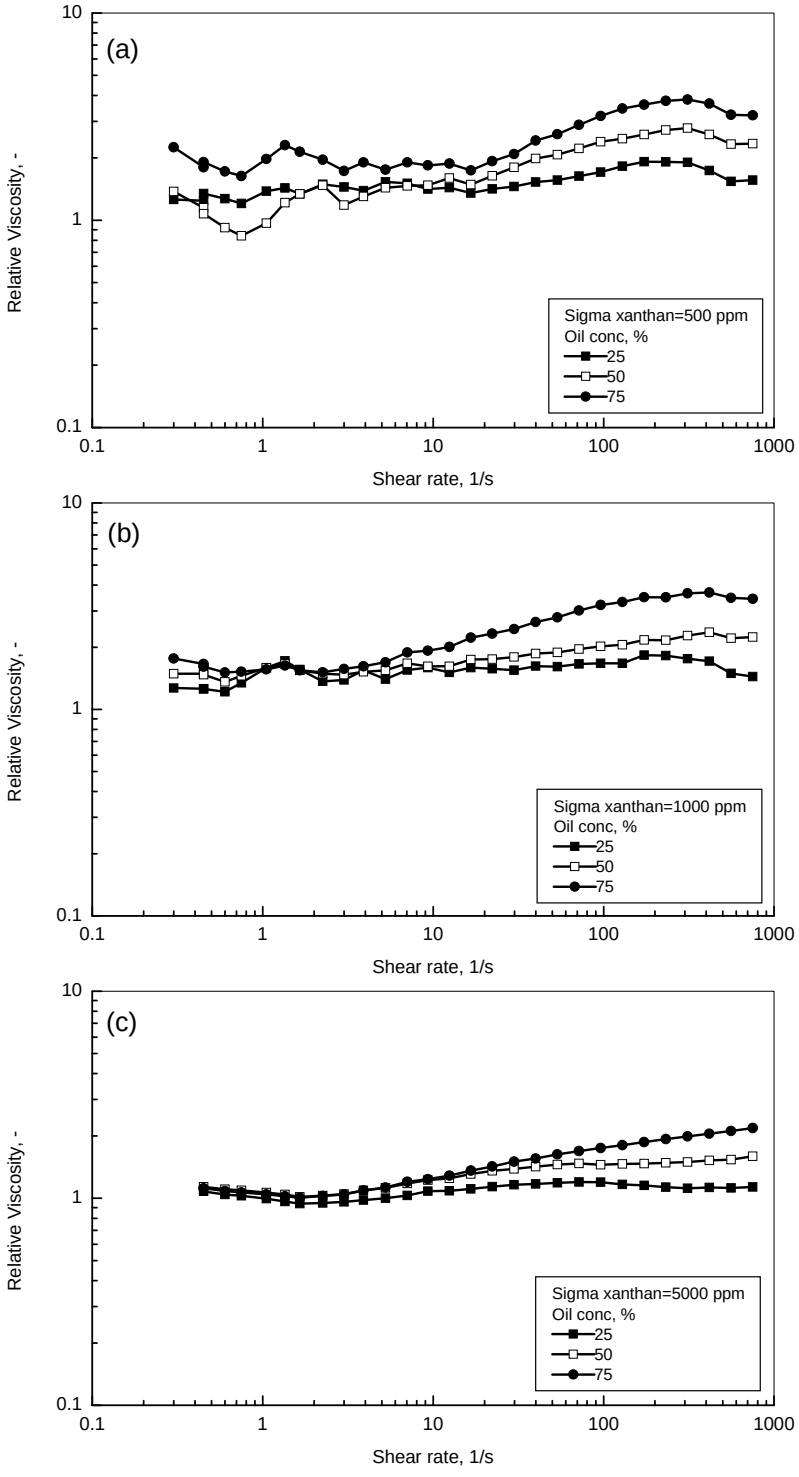

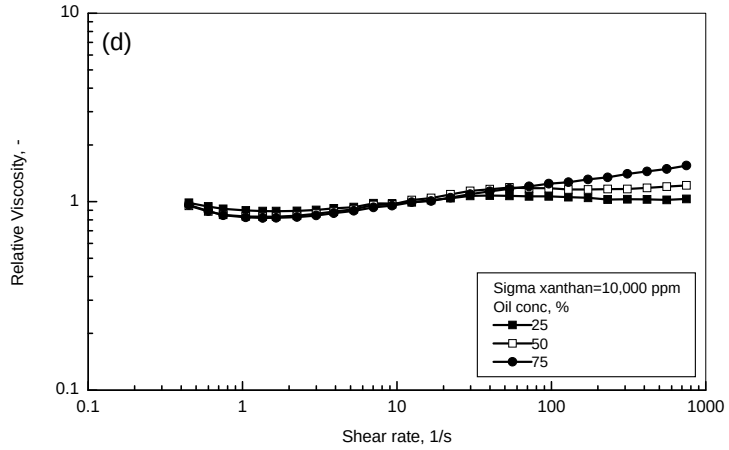

Figure 8. Reelative viscosity behavior for different oil and sigma xanthan concentrations.

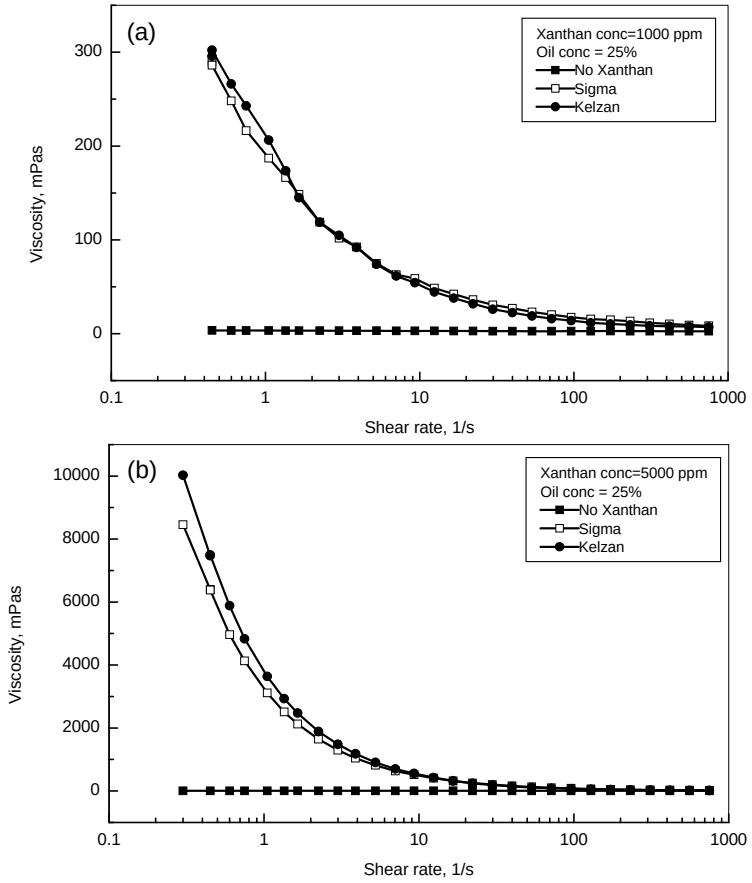

Figure 9. Comparison between the viscosity behaviors of different emulsions for 25% crude oil.

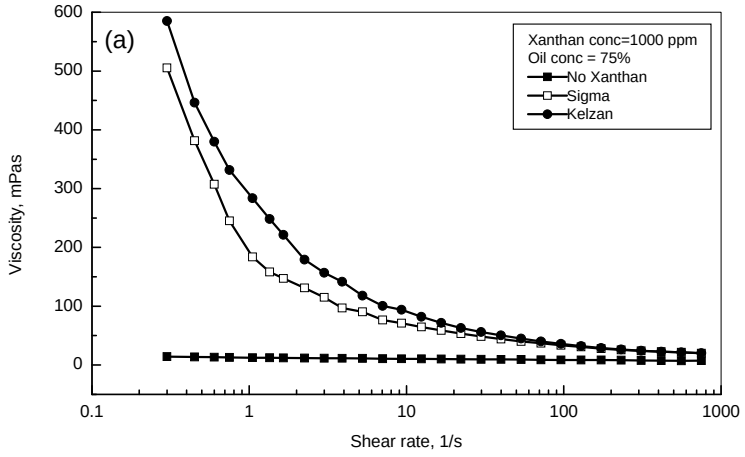

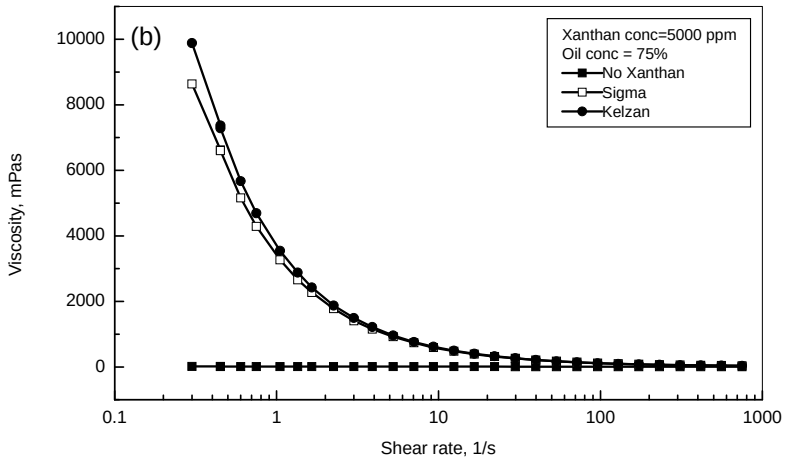

Figure 10. Comparison between the viscosity behaviors of different emulsions for 75% crude oil.

Effect of Gum Type on the Emulsion Flow Behavior

The comparison between the viscosity behaviors of Sigma and Kelzan xanthan gums are presented in Figures 9-10 for two concentrations of crude oil and two concentrations of xanthan gums. Figure 9 shows the comparison for low concentration of 25% crude oil, whereas Figure 10 is for the higher crude oil concentration of 75%. Figure 9-a shows the emulsion viscosity behavior for 25% crude oil concentration and 1000 ppm of gum concentration. As expected, the viscosity curves for crude oil– gum emulsions are much higher than the viscosity curve for crude oil-water emulsion at shear rate < 100 s^{-1}. For gum concentration of 1000 ppm and 25% crude oil, Figure 9-a shows almost similar behavior for both Sigma and Kelzan emulsions. For higher gum concentration of 5000 ppm, Kelzan emulsion show a slightly higher viscosity profile than Sigma emulsion for shear rate < 10 s^{-1}. However, for shear rate > 10 s^{-1} the three curves are combined together into one curve showing Newtonian behavior in which viscosity was determined only by hydrodynamics effect. For the higher crude oil concentration of 75% crude oil, Figures 10-a and 10-b show that the Kelzan viscosity profiles are significantly higher than the Sigma emulsions. The differences between Sigma and Kelzan emulsions gradually reduce with gum concentration until the two curves of 10^4 ppm gum concentration and 75% crude oil completely coincide.

Figures 11-12 show a more detailed comparison between the performance of the two gum materials of Sigma and Kelzan in terms of relative viscosity versus shear rate for 25% and 75% crude oil concentrations respectively. In each figure, a-d respectively, four different xanthan concentrations were investigated over the range of 500 to 10,000 ppm. Up to the gum concentration of ≤ 1000 ppm, Figures 11a, 11b, 12a, and 12b show that the relative viscosity curves of the Sigma xanthan type are positioned higher than the relative viscosity curves of the Kelzan xanthan type. However for higher gum concentrations of 5000 and 10,000 ppm, Figures 11c, 11d, 12 c and 12d show that the relative viscosities for Kelzan emulsions are slightly higher than the Sigma emulsions.

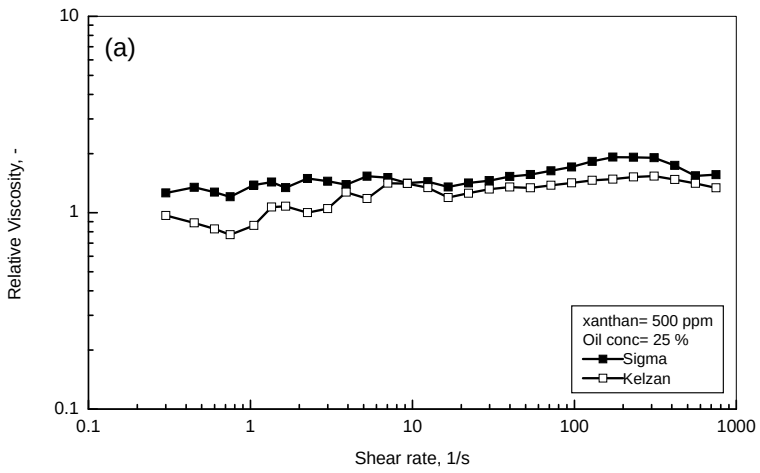

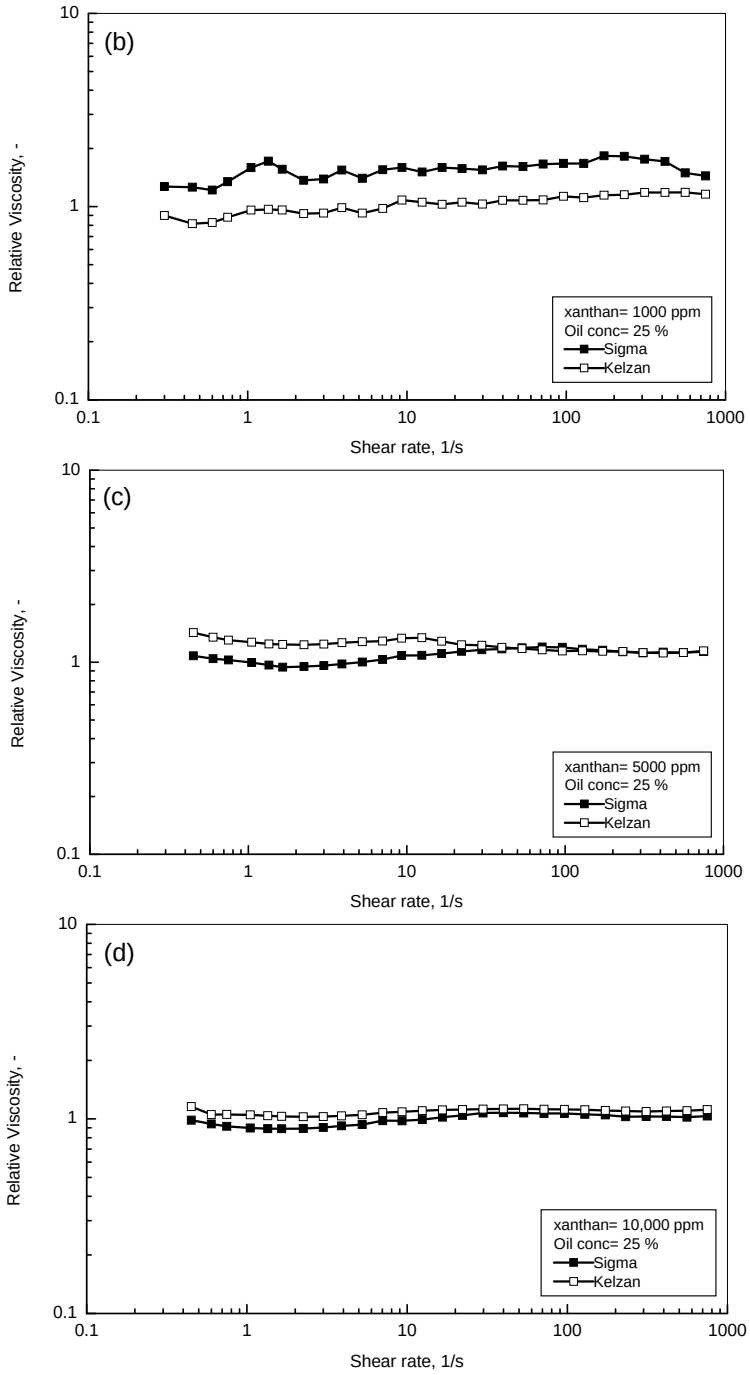

Figure 11. Comparison between the relative viscosity of 25% emulsions.

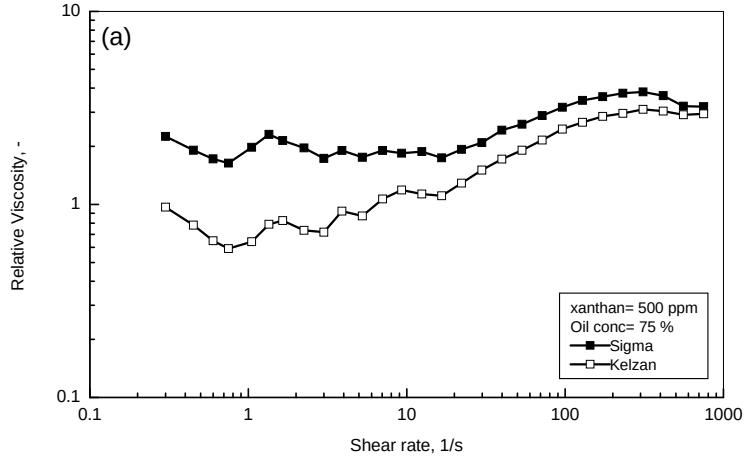

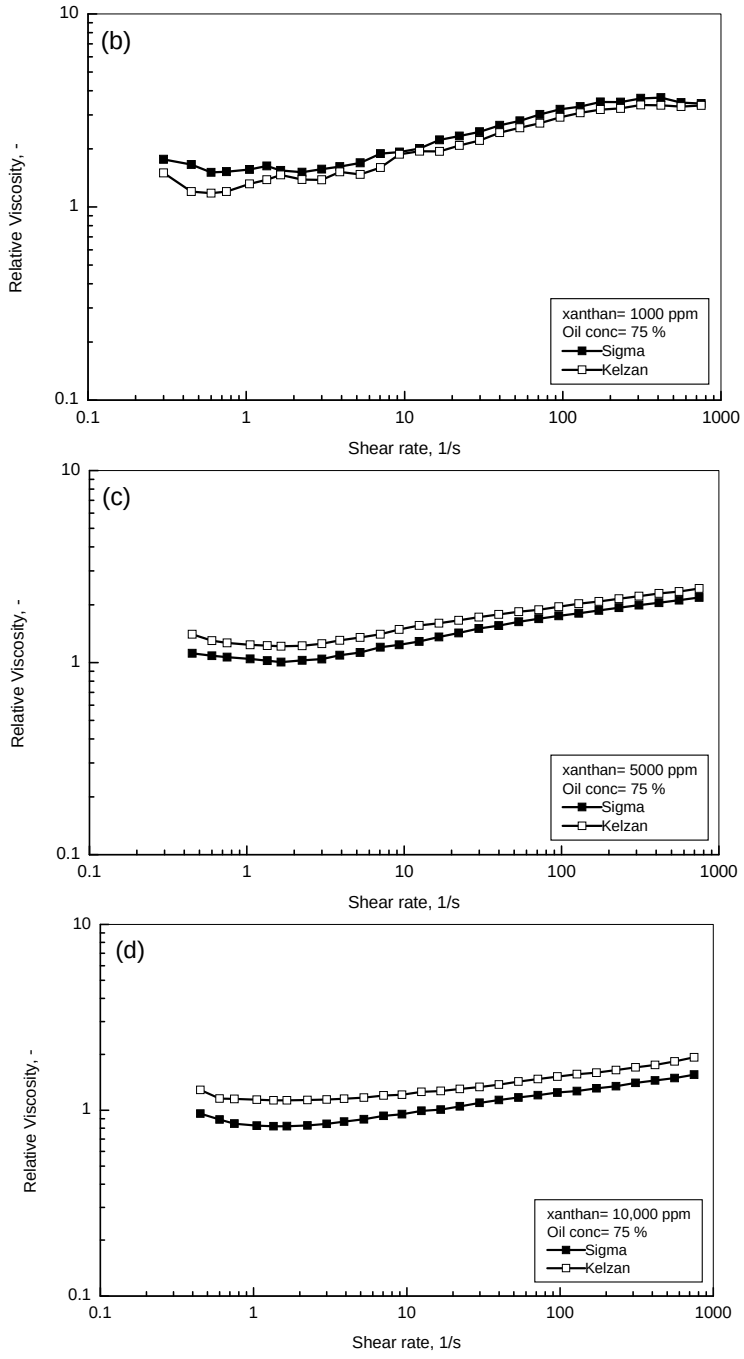

Figure 12. Comparison between the relative viscosity of 75% emulsions.

From the above discussion, at a lower temperature such as the room temperature of 22 °C, the viscosity of the xanthan aqueous solutions increases strongly with the gum concentration. On the other hand, the viscosity of the xanthan solutions decreases strongly with increasing temperature especially at low ionic strength of electrolyte.[36] The strong temperature effect can be attributed to a conformational transition of xanthan chains from helical at low temperatures to random coil at high temperatures.[37] The aqueous solutions of xanthan gum display good resistance to the effect of high temperatures. It was reported that the solution viscosity of the commercial gum remained relatively constant at 80°C.[38] Reduction of solution viscosity occurs at temperatures above 100 °C. Many investigations have examined the temperature effect on the viscosity of the xanthan solutions. In order to display resistance to the effect of temperatures up to 90°C, the ionic strength of the solutions has to be relatively high.[39-41]

Hester et al.[42] and Masuda et al.[43] reported that the elastic property of the polymer solutions influence the displacement process in the heterogeneous reservoirs. The enhancement of the mobility ratio of oil and water

in reservoirs and the increase of sweep efficiency with polymer flooding would be characterized with viscosity. Demin et al.[44] mentioned that the displacement of residual oil can be related to the effect of drawing, pulling and carrying ability of polymer solutions on the residual oil in the microscopic displacement process. They have concluded that the residual oil could not be driven only by the viscous properties of the glycerin flooding solutions. However, the oil driven out of the reservoir by polymer solutions is almost four times more than by glycerin solutions. The reason was that the elastic properties of the polymer solutions could improve extracting the oil out the reservoir.

Conclusions

Water soluble polymer of xanthan type is one of the most widely used polymers in the enhanced oil recovery. The process of injecting xanthan solution into the oil reservoir usually causes the formation of crude oil-xanthan emulsions, which is the presence of oil droplets phase within the aqueous polymer phase. A rheological investigation in terms of viscosity versus shear rate and shear stress versus shear rate for crude oil-xanthan gum emulsions was accomplished. The flow behavior of the crude oil-xanthan emulsions depends upon the crude oil concentration, polymer concentration, polymer type, and shear rate. Newtonian behavior was observed for a light concentration of crude oil-water emulsion, whereas non-Newtonian of shear thinning behavior was found for the crude oil concentration of higher than 25%. All aqueous solutions of Sigma and Kelzan showed non-Newtonian with shear thinning behavior in which the measured apparent viscosity decreased with shear rate. The flow behavior of crude oil-xanthan gum emulsion is characterized by non-Newtonian with shear thinning profile. The viscosity and shear stress of these emulsions depends mainly on the shear rate and xanthan concentration. The effect of gum concentration is more pronounced at low shear rate. At high shear rate, the hydrodynamic effect is more dominant than the gum concentration. Casson model can be used with enough confidence to predict the flow behavior of crude oil–xanthan emulsions. The apparent viscosities of the crude oil emulsions are higher than their corresponding aqueous solutions. For a shear rate of less than 100 s^{-1}, the viscosity profiles of the crude oil-xanthan emulsions are much higher than the same concentration of crude oil-water emulsion. Both Sigma and Kelzan emulsions exhibited similar viscosity profiles for the crude oil concentration of ≤ 25% and gum concentration of ≤ 1000 ppm. For the higher concentrations of crude oil (75%) and/or higher concentration of gum (5000 ppm), Kelzan emulsions exhibited viscosity profiles slightly higher than the Sigma emulsions.

REFERENCES

[1] Sherman, P. Industrial Rheology; Academic Press: London, 1970.

[2] Kang, K.S.; Pettitt, D.J. Xanthan, Gellan, Wellan, and Rhamsan; in Industrial Gums, 3rd ed., edited by Whistler, R. L.; DeMiller, J.N.; Academic: San Diego, 1993.

[3] Speers, R.A.; Tung, M.A. J Food Sci 1986, 51, 96.

[4] Ryles, R.G. SPE Res Eng 1988, 3, 23.

[5] Richardson, R.K.; Ross-Murphy, S.B. Int J Biological Macromolecules 1987, 9(5), 250.

[6] Sutherland, I.W. Extracellular polysaccharides; In Rehm, H.J.; Reed, G. (Ed.) Vol. 6; Biotechnology; Weinheim: VCH, 1996.

[7] Rodd, A.B.; Dunstan, D.E.; Boger, D.V. Carbohydrate Polymers 2000, 42, 159.

[8] Whistler, R.L.; BeMiller, J.N. Carbohydrate Chemistry for food scientists. Eagan Press: St Paul, MN, 1997.

[9] Milas, M.; Rinaudo, M. Carbohydrate Research 1979, 76, 189.

[10]Coviello, T.; Kajiwara, K.; Burchard, W.; Dentini, M.; Crescenzi, V. Macromolecules 1986, 19, 2826.

[11]Morris, E.R. Bacterial polysaccharides; In Stephen, A.M. (Ed.) Food polysaccharides and their applications; Marcel Dekker Inc: New York, 1995.

[12]Norisuye, S.; Fujita. Macromolecules 1984, 17, 2696.

[13]Sherman, P. Encyclopedia of a Emulsion Technology, P. Becher (Ed.) Vol. 1, Dekker: New York, 1983.

[14]Plegue, T.; Frank, S.; Fruman, D.; Zakin, J. J Colloid Interface Sci 1986, 114, 88.

[15]Pal, R.; Rhodes, E. J Rheol 1989, 33, 1021.

[16]Princen, H. J Colloid Interface Sci 1983, 91, 160.

[17]Princen, H. J Colloid Interface Sci 1985, 105, 150.

[18]Princen, H.; Kiss, A. J Colloid Interface Sci 1986, 112, 427.

[19]Han, C.; King, R. J Rheol 1980, 24, 213.

[20]Pal, R. J. Rheol. 1992, 36, 1245.

[21]Ghannam, M. J Chem Eng Japan 2003, 36, 35.

[22]Sosa-Herrera, M.G.; Berli, C.L.A.; Martinez-Padilla, L.P. Food Hydrocolloids 2008, 22, 934.

[23]Tanaka, H.; White, J. Poly Eng Sci 1980, 20, 949.

[24]Chan, D.; Powell, R. J Non-Newt Fluid Mech 1984, 15, 165.

[25]Metzner, A. J Rheol 1985, 29, 739.

[26]Gupta, R.; Seshadri, S. J Rheol 1986, 30, 503.

[27]Poslinski, A.; Ryan, M.; Gupta, R.; Seshadri, S.; Frechette, F. J Rheol 1988, 32, 703.

[28]Chhabra, R.; Richardson, J. Non-Newtonian Flow in the Process Industries, Butterworth-Heinemann: Oxford, 1999.

[29]Lee, H.; Lee, J.; Park, O. J Colloid Interface Sci 1997, 185, 297.

[30]Lopez, M.J.; Vargas-Garcia, M.C.; Suarez-Estrella, F.; Moreno, J. J Food Engineering 2004, 63, 111.

[31]Martinez-Padilla, L.P.; Lopez-Araiza, F.; Tecante, A. Food Hydrocolloids 2004, 18, 471.

[32]Kayacier, A.; Dogan, M. J. Food Engineering 2006, 72, 261.

[33]Cao, Y.; Dickinson, E.; Wedlock, J.D. Food Hydrocolloids 1990, 4, 185.

[34]Dickinson, E.; Golding, M.; Povey, J.W.M. J Colloid Interface Sci 1997, 185, 515.

[35]Yaseen, E.I.; Herald, T.J.; Aramouni, F.M.; Alavi, S. Food Research International 2005, 38, 111.

[36]Choppe, E.; Puaud, F.; Nicolai, T.; Benyahia, L. Carbohydrate Polymers 2010, 82, 1228.

[37]Paoletti, S.; Cesaro, A.; Delben, F. Carbohydrate Research 1983, 123, 173.

[38]Kierulf, C.; Sutherland, I.W. Carbohydrate Polymers 1988, 9, 185.

[39]Lambert, F.; Rinaudo, M. Polymer 1985, 26, 1549.

[40]Seright, R.S.; Henrici, B.J. SPE Reservoir Eng. 1990, 1, 52.

[41] Wellington, S.L. Soc. Pet. Eng. J. 1983, 23, 901.

[42]Hester, R.D.; Flesher, L.M.; McCormick, C.L. SPE 1994, 27823, 17.

[43]Masuda, Y.; Tang, K.C.; Miyazawa, M.; Tanaka, S. SPERE 1992, 24, 7.

[44]Demin, W.; Jiecheng, C. SPE 2000, 63227, 1.

doi: 10.14355/jpsr.2014.0301.02

Matlab Based Performance Evaluation of Natural Gas Transmission System due to Corrosion

Abraham D. Woldeyohannes*[1], Mohd Amin A. Majid[2], Chong Feng Chyuan[3], Aklilu T. Baheta[4]

[1]Caledonian College of Engineering, PO Box 2322, CPO Seeb 111, Sultanate of Oman

[2,4] Mechanical Engineering Department, Universiti Teknologi PETRONAS, Bandar Seri Iskandar, 31750 Tronoh, Perak, Malaysia.

[3]Curtin University Sarawak Malaysia, School of Engineering and Science, CDT 250, 98009 Miri, Sarawak, Malaysia

*[1]abraham@caledonian.edu.om ; [2]mamin_amajid@petronas.com.my; [3] chyuan_6192@hotmail.com; [4]aklilu.baheta@petronas.com.my

Abstract

Pipe corrosion is one of the serious issues associated with transportation of gases using old pipes. As a result of internal corrosion due to the accumulation of various corrosive materials, the performance of the transmission pipes is affected with ages. This paper aimed to evaluate the effect of the age of pipes on the performance of natural gas transmission pipeline network system. A simulation model was developed for looped pipeline configuration using MATLAB programming code. Newton Raphson method was used to determine the unknown pressure and flow parameters which are essential to evaluate the performance of the pipeline networks. The mathematical model was derived from the principles of fluid flow, mass conservation, and compressor characteristics. The pipe flow equations were modified to incorporate the effect of the age of pipes for evaluating the performance of the pipeline networks with respect to ages. Analyses performed on a looped pipeline network systems demonstrated that age has significant effect on the performance of the network. It was noted that the flow capacities reduced by 5.06 and 6.75% when the service life of the pipeline network reached 15 and 20 years, respectively. With the current rising price of natural gas, the reduction in flow capacity could result huge amount of cost for the nation operating large volume of gases. The results of the simulation model have been verified and validated using the techniques available in the area of pipeline network simulation.

Keywords

Age of Pipe; Corrosion; Looped Pipeline Networks; Natural Gas; Pipe Roughness; Simulation Model

Introduction

Natural gas is one of the cleanest energy sources as the SO_2 and NOx emissions are relatively low and almost no particulate or ash is produced during the combustion of natural gas (Safitri and Mannan, 2011). Natural gas is widely used in manufacturing of materials such as steel, glass, paper and bricks (Sánchez-Úbeda and Berzosa, 2007). Furthermore, natural gas is widely used due to its low-price. However, the transportation of natural gas is a great challenge due to its large specific volume. It can be transported through pipeline network system and by truck in the form of liquefied natural gas (LNG). However, pipeline network system is more preferable for short distance gas transportation as it is more economical. In addition, the LNG transportation requires high liquefaction costs no matter how long the distance of transportation is(Woldeyohannes and Majid, 2011a).

Corrosion of steel pipes is one of the critical issues in oil and gas industry as it can seriously affect the performance of the natural gas transmission pipeline network system. It was reported that $5.4 to $8.6 billion had been invested annually in the inspection and prevention of corrosion to the transmission pipeline industry (Koch et al., 2001). An increase in the service life of pipes can result in higher degree of pipe roughness as there are various elements accumulated around the internal surface of the pipes (Worthingham et al., 2001, Menon, 2005). As the service life of pipes increases, corrosive elements are accumulated around the internal surface of the pipes. This can actually increase the roughness and friction factor of the pipes. Consequently, the pressure drop along the gas pipeline increases. Associated with this, the quantities of natural gas flowing through the pipeline network system decreases.

There are several factors leading to corrosion;

including the nature of the material or alloy, surface roughness, composition, moisture absorptivity, environment, temperature, humidity and corrosive elements (Revie and Uhlig, 2008). These elements can actually react chemically and electrochemically with the pipes and lead to corrosion. Corrosion of pipeline can occur either externally or internally. The internal corrosion may occur in the form of uniform corrosion, pitting corrosion or erosion-corrosion depending on the transfer velocity and the natural characteristic of the corrosive liquid or condensates (Koch et al., 2001). In addition to accumulation of various elements around the internal surface of the pipe, another factor leading to corrosion of the gas pipes is the content of water in the natural gas. During the production of gas in the reservoir, the gas is saturated by water too. Moreover, water is produced in the gas by condensation when the pressure and temperature change during production and transmission of natural gas. The presence of water in the content of natural gas can actually cause an increase in pressure drop in the pipeline and frequently leads to corrosion problems (Shirvany et al., 2010).

There are two types of corrosions that may cause internal corrosion in pipelines which are stray current corrosion and microbiologically influenced corrosion (Koch et al., 2001). As corrosion has significant effect on the pipeline network system performance, many attempted researches on pipeline networks. Bullard (Bullard et al., 2005) carried out a soil corrosion monitoring near a gas pipeline under cathodic protection. Woldeyohannes and Majid (Woldeyohannes and Majid, 2011b) and Woldeyohannes and Chyuan (Woldeyohannes and Chyuan, 2011) had developed a simulation model to carry out analyses and evaluation on the effect of age of pipes on the performance of the branched pipeline network system. An experiment was conducted by Zhou (Zhou, 1993) to study about the effect of the fluid properties and flow conditions on the characteristic of flow as well as the corrosion rates. Nesic (Nesic et al., 2004) had developed a simulation model for an integrated CO2 corrosion–multiphase flow. Riemer (Riemer, 2000) developed a mathematical model which is able to describe appropriately the complicated relationships within cathodic protection of complex pipeline networks.

The development of digital computer facilitated the accurate solution of the nonlinear equations for different components in a gas pipeline network using numerical simulation (Wu et al., 2000). There are different simulations models for natural gas transmission and distributions networks developed under various conditions (Carter et al. 1990; Woldeyohannes and Majid, 2009; Gonzalez et al. 2009; Dorao and Fernandino, 2011; Abdolahi et al., 2007). However, most of the simulation models are developed for optimization purposes particularly in minimizing the energy consumption and maximizing the flow rate through pipes. Therefore, it is important to have a simulation model to analyze the effect of age of pipes on the performance of transmission pipelines of natural gas.

The objective of this paper is to evaluate the performances of looped transmissions pipeline networks system as the service life of pipes increases. The effect of corrosion on changes in flow capacity, nodal pressures, and compression ratio and horse power requirement has been evaluated on the basis of the looped pipeline network system. The flow equations in the model have been modified to include the effect of corrosion of the pipes with respect to the service life of the pipes. The simulation model is developed based on Newton Raphson method and implemented by using MATLAB programming. A graphic user interface (GUI) was developed to make the simulation model to be more user-friendly and flexible.

Modelling and Solution Strategy

This section discusses the procedure for the performance evaluation of looped pipeline network system as the age of the pipes increases. A simulation model developed in Woldeyohannes and Majid (Woldeyohannes and Majid, 2011a) and the methods developed in (Woldeyohannes and Majid, 2011b) and (Woldeyohannes and Chyuan, 2011) for integrating corrosion with pipeline flow equations were adopted here to assist the performance evaluation for the looped pipeline networks. Mathematical formulation and solution technique are the two key elements for developing the simulation model for analyzing transmission pipeline network problems.

Mathematical Formulation

Looped pipeline network systems are complex network system (Wu et al., 2000). Therefore, basic governing equations include equations related to the gas flow through pipes and equations related to compressors' performance characteristic, the principles of mass conservation and equations related to looping conditions (Woldeyohannes and Majid, 2011a). In order to integrate the effect of age of pipes into the simulation model, the corrosion effect with respect to

the roughness of internal surface of pipe against the service year is incorporated into the flow equations (Woldeyohannes and Majid, 2011b; Woldeyohannes and Chyuan, 2011) .

The first basic component of the model is to generate the flow equations. General flow equation is used for the analysis of the pressure difference and gas flow in pipes due to its frequent application in gas industry (Woldeyohannes and Majid, 2011a). The flow through the pipes is influenced by the gas properties, friction factor and the geometry of the pipes. In this paper, the flow is assumed to be in steady state and isothermal so the gas temperature is constant and the kinetic energy is negligible. The flow equation which relates the up-stream pressure Pi, downstream pressure Pj and flow through pipe Q_{ij} can be expressed (Woldeyohannes and Majid, 2011a) as:

$$P_i^2 - P_j^2 = K_{ij} Q_{ij}^2 \tag{1}$$

where K_{ij} takes different forms depending on the dimensions of the parameters used in the flow equations. K_{ij} represents several parameters such as gas gravity G [dimensionless], average flowing temperature T_f [K], base temperature T_b [K], base pressure P_b [kPa] and gas compressibility factor Z and other decision parameters which are length L [km], diameter of the pipes D [mm] and friction factor f . K_{ij} takes the form as:

$$K_{ij} = 9.0174 \times 10^9 \, f \, \frac{L}{D^5} \tag{2}$$

The second component of the simulation model is the equation which is used to represent compressor stations as discussed in (Woldeyohannes and Majid, 2011a). Centrifugal compressor is used for modelling as it is widely used in natural gas pipeline transmission network application due to its low installation and maintenance cost (Menon, 2005). In general, the data related to compressor can be obtained from the compressor performance characteristic map. It involves four basic quantities which are inlet volumetric flow rate Q, compressor speed S, adiabatic head H and adiabatic efficiency η. The basic component of compressor equation for multiple compressors operating in parallel is given as (Woldeyohannes and Majid, 2011a);

$$\left(\frac{P_d}{P_s}\right)^m = \frac{mS^2}{ZRT_S}\left[A_H + B_H\left(\frac{Q/n}{S}\right) + C_H\left(\frac{Q/n}{S}\right)^2 + D_H\left(\frac{Q/n}{S}\right)^3\right] + 1 \tag{3}$$

where n is the number of compressors working in parallel within the station, $m = (k-1)/k$ with k to be specific heat ratio, R is gas constant, T_s is suction temperature and Z is gas compressibility factor, A_H , B_H , C_H and D_H are constants .

The third and fourth components of the mathematical formulation are the mass balance at junction nodes and the looping conditions. As discussed in (Woldeyohannes and Majid, 2011a), the mass balance equation is used to generate additional sets of equation for each junction based on the principles of conservation of mass. Similarly, the looping condition is used to generate another form of equation which is important for the simulation model as developed (Woldeyohannes and Majid, 2011a).

The fifth component in the simulation model is to integrate the corrosion effect to the flow equation. As the service life of pipe increases, the surface roughness of the pipe tends to increase due to the accumulation of various elements such as corrosion elements around the internal surface of the pipe, which leads to degradation in performance of the pipeline networks. The friction factor in the flow equation is modified by incorporating the corrosion effect with respect to the service life of pipe. To express the corrosion effect, the equation which relates the service life of the pipe and the surface roughness of inner part of the pipe is established based on the coated pipe fouling data collected from (Worthingham et al., 1993) via curve fitting technique. The friction factor f which is used in Eq. (2) is modified and approximated as function of roughness as (Woldeyohannes and Majid, 2011b; Woldeyohannes and Chyuan, 2011):

$$f = \frac{1}{\left[2\log_{10}\left(\frac{3.7D}{r}\right)\right]^2} \tag{4}$$

where r is surface roughness of the pipe which varies based on the age of the pipes and D is the diameter of the pipe.

Solution Strategy

In order to solve the mathematical model of the looped pipeline network problem, the solution strategy for the simulation model is developed based on Newton Raphson method. To solve a system of n governing simulation equations which are non-linear in n unknown pressure and flow variables, numerical method by using the centred finite-divided-difference approximation was implemented (Chapra and Canale, 2006; Keffer, 1999; Kiusalaas, 2005). The solution strategy developed in (Woldeyohannes and Majid, 2011a; Woldeyohannes and Majid, 2011b; Woldeyohannes

and Chyuan, 2011) was adopted and implemented using MATLAB programming. Fig. 1 shows the flow chart of the simulation model based on Newton Raphson method. In order to make the simulation model to be more user-friendly, a graphic user interface was developed by using MATLAB programming. In the GUI developed, users can input any desired values for different parameter and guess values as shown in Fig. 2. Furthermore, users are provided with the recommended ranges for the input parameters in order to make a valid analysis as well to avoid divergence particularly the initial guess values for the pressure and flow variables. Moreover, extra features are added into the GUI that a pop up window would appear if the divergence occurs or the calculated compression ratio has exceeded the ideal range i.e. between 1.5 and 2. Its purpose is to remind users to re-input more appropriate values for the desired parameters in order to obtain reasonable results. Moreover, it has the advantage that users can simply change any of the input parameters in order to investigate the performance of the gas pipeline networks under different conditions.

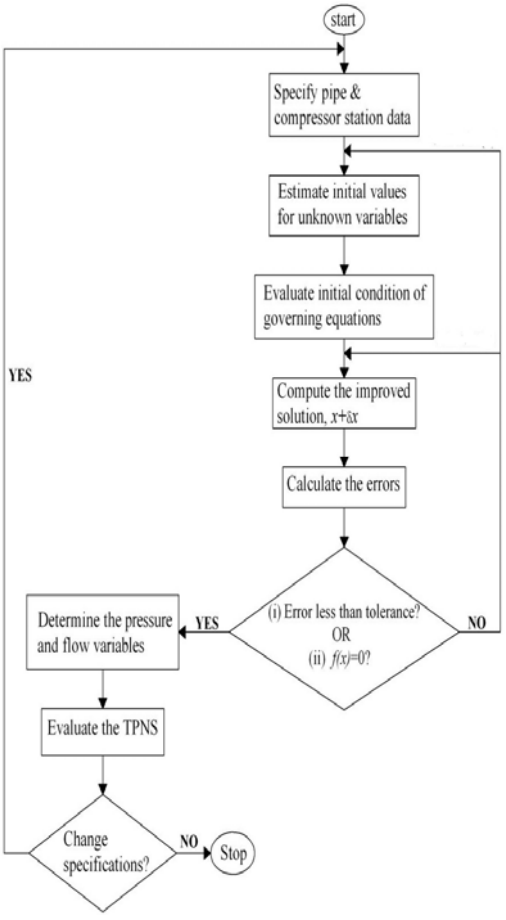

FIG. 1 FLOW CHART OF THE SIMULATION MODEL BASED ON NEWTON RAPHSON METHOD

Based on the input parameters, the simulation results for a new looped pipeline network and comparisons of result with respect to different service life of pipes will be displayed in the GUI. Three types of graphs which are flow capacity against age of pipes, compression ratio against age of pipes and horse power against age of pipes can be plotted based on the input parameters.

Results and Discussions

The simulation model developed was used to evaluate part of the existing gas transmission pipeline network which is categorized as looped pipeline network as shown in Fig. 3. The given network basically consists of 8 clients i.e. power plants, 16 pipes, 1 compressor station and 7 junctions. As a result, there are 8 nodal pressures and 16 flow parameters to be determined. Moreover, the network has a looped pipeline allocated between node 2 and 7 which is installed to reduce overall pressure drop within the system. In order to develop the simulation model which is based on Newton Raphson Method to solve the network, 24 independent equations were formed including 15 pipe flow equations, 7 mass balance equations, 1 looping condition equation and 1 compressor station.

In the numerical evaluations, the following data were used throughout the analysis. Due to the limited access to the compressor working in the field, a centrifugal compressor data from the manufacturer was used for the simulation model. By using curve fitting technique, the coefficients for the approximation of the performance map of the compressor are determined to be (Dos Santos and Lubomirsky, 2006): $A_H = 1.20\times10^{-6}$, $B_H = -2.48\times10^{-9}$, $C_H = -4.60\times10^{-12}$, $D_H = -3.17\times10^{-13}$. All units within the compressor stations are assumed to be identical and connected in parallel. Besides, the pipeline network problem was solved based on the pipe data tabulated in Table 1.

TABLE 1 PIPE DATA

Node	Length, L (km)	Diameter, D (mm)
0-1	232	914.4
2-3	180	508
3-D1	20	508
3-D2	28	508
2-4	60	914.4
4-5	40	508
5-D3	20	508
5-D4	17	508
4-6	106	914.4
6-D5	18	508
6-7	75	914.4
7-D6	50	508
7-8	184	914.4
8-D7	18	508
8-D8	20	508

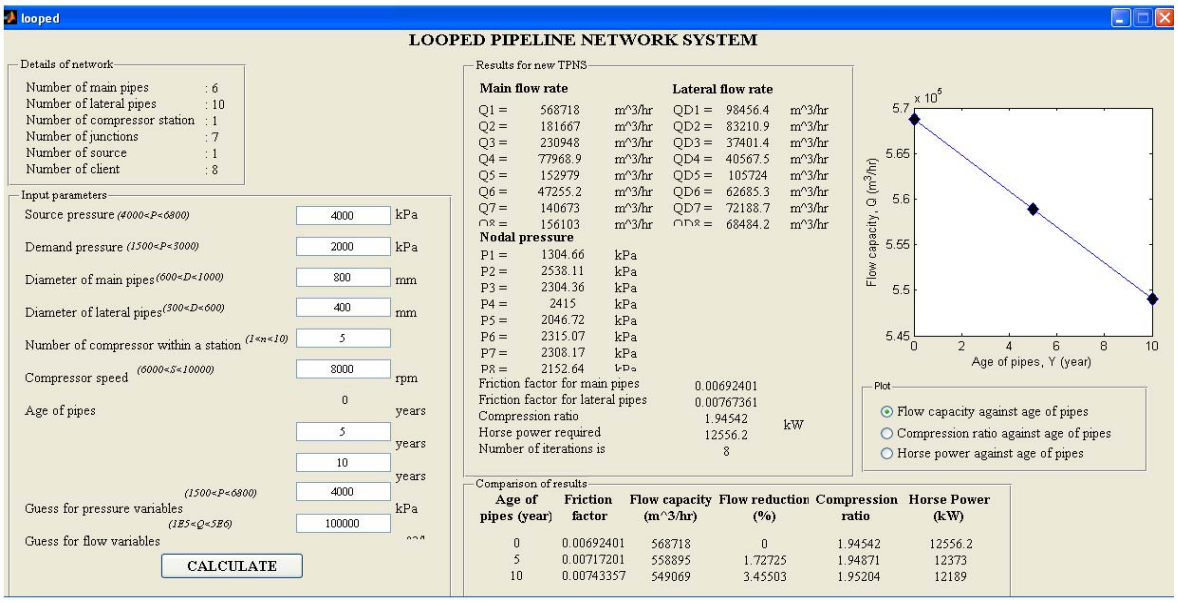

FIG. 2 SCREENSHOT OF GUI FOR LOOPED PIPELINE NETWORK SYSTEM

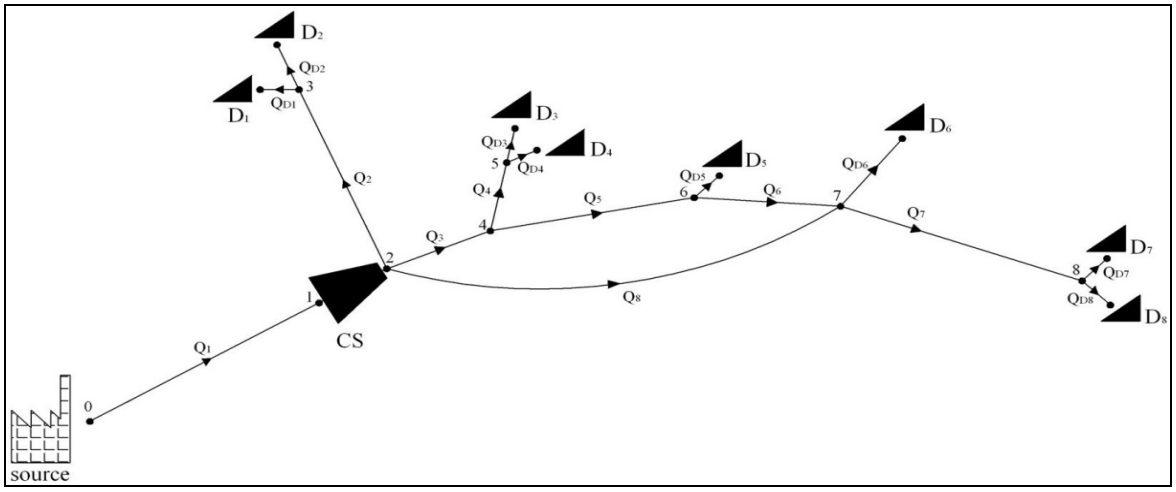

FIG. 3 LOOPED PIPELINE NETWORK

TABLE 2 VARIATION OF FLOW VARIABLES WITH AGES OF PIPES

Age of pipe, Y (Year)	Friction factor, f	Flow resistance, K_{ij} (×10-5)	Main flow rate, Q1 (m3/hr) (×105)	Flow capacity reduction percentage (%)
0	0.00679	2.2228	8.6983	-
5	0.00703	2.3016	8.5517	1.685
10	0.00729	2.3847	8.4050	3.372
15	0.00756	2.4724	8.2581	5.061
20	0.00784	2.5650	8.1111	6.751

TABLE 3 VARIATION OF PRESSURE VARIABLES WITH AGES OF PIPES

Age of pipe (Year)	Suction pressure, P_1 (kPa)	Discharge pressure, P_2 (kPa)	Compression ratio, *CR*	Horse power, HP (kW)
0	1852.7	3353.9	1.810	16985
5	1848.8	3354.3	1.814	16767
10	1844.9	3354.9	1.818	16546
15	1841.0	3355.4	1.823	16323
20	1837.1	3355.9	1.827	16098

The simulation model was used to determine the pressure and flow variables for the looped pipeline networks system. The analysis was done based on source pressure of 4500 kPa and demand pressure requirement 3000 kPa. The temperature of the gas is assumed to be constant while 4 compressors with the speed of 8000 rpm were working for the system. The results showed that the solutions to nodal pressure

and flow parameters were obtained after 11 iterations with relative percentage errors of 2.49×10-11%.

The simulation model was utilized to analyze the effect of the age of the pipe on the performance of the given network. The flow capacity, compression ratio and horse power required were the main performances evaluated. The simulation results are shown in Table 2 and Table 3.

At the compressor speed of 8000 rpm, the results of the simulation analysis showed that a decrement of 1.685, 3.372, 5.061 and 6.751% flow capacities for the 5, 10, 15 and 20 years pipes respectively as shown in Table 2. This is because the friction factor of the pipes increased and consequently led to a rise in flow resistance along the pipeline as the age of the pipes increased. Similar observations have been noted for the flow capacity to reduce as the age of pipes increase when the compressors were operating at speed of 7500 and 8500 rpm.

In addition, Table 3 shows that as the age of the pipe increases, the compression ratio increases as well owing to a decrease in suction pressure and a slight increase in discharge pressure. The reason for the decrement of suction pressure was due to the corrosion effect which could raise the friction factor of the pipes. As the friction factor of the pipes increases, it creates higher resistance to the flow thus enhancing the pressure drop along the pipelines. On the contrary, the power consumption of the compressors decreased due to significant decrement of flow capacity of the system as shown in Table 3. However, the reduction in power consumption of the pipeline network does not bring any benefit as the reduction in flow capacity obviously causes insufficiency of the gas supply.

The simulation model developed was also verified using various techniques such as conceptual model validation, computerized model verification and operational validation. The technique used for the computerized model validation was compared to the other model which had been validated. In fact, there were a lot of simulation model available for gas pipeline network system but they were developed for different intended purposes and objectives. The model proposed by Woldeyohannes and Majid (2011a) was used to validate the developed simulation model as its objective was closer to the objective of this work. However, the difference occurred in the friction factor used in modelling the flow equation and the implementing software. Visual C++ was used by Woldeyohannes and Majid (2011a) to implement the mathematical model whereas in this project, MATLAB program was used to develop the programming code of the simulation model. In order to show the comparison between the two models, the same network structure reported in Woldeyohannes and Majid (2011a) was used for comparison approach. Furthermore, the same compressor data, pipe data and gas properties were used. The analysis was performed with compressor speed of 8000 rpm, 4 compressors within a station and the pipes were assumed to be new. Moreover, the analysis was conducted using the performance characteristics of the compressors taken from Kurz and Ohanian (2003). The results for pressure variables were basically the same as the analysis was performed under the same source and demand pressure. However, there were some differences in the results of flow rates at several nodes as shown in Fig. 4.

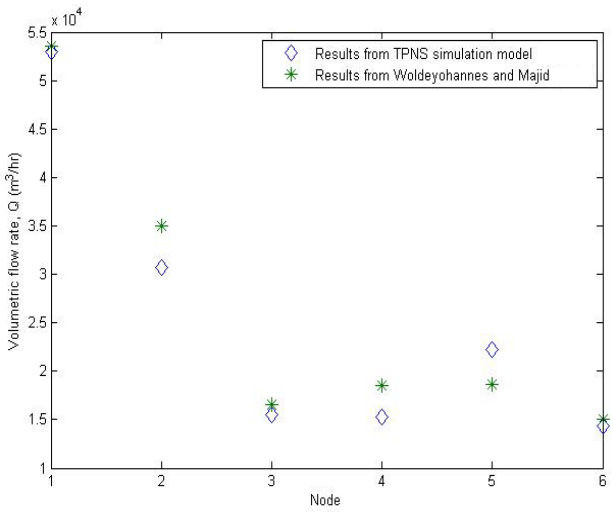

FIG. 4 COMPARISON OF MAIN FLOW RATES BETWEEN TWO MODELS

Although there were some variations in the comparison of flow rates between two models, the trends of the results were still the same between the models. The variations of the simulation results could be as a result of the different friction factor that was used in analysis. The friction factor used in this simulation model took into account of the corrosion effect where roughness is a function of service year of the pipes. In addition, the pipe's friction factor is dependent on the diameter. On the other hand, constant friction factor was used for analysis in the model developed by Woldeyohannes and Majid (2011a) where the friction factor is independent on the pipe's diameter.

Conclusions

The simulation model was capable to perform the

analysis of looped pipeline network configurations under various operating conditions. Based on the effect of age of the pipes, the performance of the network was evaluated. Analyses of the looped networks with different operating conditions showed that significant corrosion effects on the performance were observed for the five groups of pipes with respect to age i.e. new, 5, 10, 15 and 20 years pipes. The results showed a decrease in flow capacity of 1.69%, 3.37%, 5.06% and 6.75% for the 5, 10, 15 and 20 years pipes respectively. Furthermore, the performances of the system including the power consumption and compression ratio were also analyzed based on the parameters obtained. Therefore, the developed model was not only served as a tool for evaluating the performance of the system based on the age of the pipes but also can assist in decisions making in the design and operation of various looped pipeline network configurations.

REFERENCES

Abdolahi F., Mesbah A., Boozarjomehry R. B., and Svrcek W. Y., 2007, The effect of major parameters on simulation results of gas pipelines, International Journal of Mechanical Sciences.

Bullard S. J., Covino B. S., Cramer J. S. D., Holcomb G. R., and Ziomek-Moroz M., 2005, Soil corrosion monitoring near a pipeline under CP, U.S. Department of Energy, DOE/ARC 2005-082.

Carter R. G., Schroeder D. W., and Harbick T. D., 1990, Some causes and effect of discontinuities in modelling and optimizing gas transmission networks, PSIG.

Chapra S. C. and Canale R. P., 2006, Numerical Methods for Engineers Fifth ed. New York: McGraw-Hill.

Dorao C. A. and Fernandino M., 2011, Simulation of transients in natural gas pipelines, Journal of Natural Gas Science and Engineering, Vol (3): 349-355.

Dos Santos S. P. and Lubomirsky M., 2006, Gas Composition Effect on Centrifugal Compressor Performance, 35th Annual Meeting of Pipeline Simulation Interest Group (PSIG),Williamsburg, Virginia.

Gonzalez A.H.,Cruz J.M.D.L., Andres-Toro B.D., Martin J.L.R., 2009, Modelling and simulation of gas distribution pipeline network, Applied Mathematical Modelling. Vol (33): 1584–1600.

Keffer D., 1999, Advanced numerical techniques for the solution of single nonlinear algebraic equations and systems of nonlinear algebraic equations, University of Tennessee, Knoxville .

Kiusalaas J., 2005, Numerical Methods in Engineering with MATLAB, First ed. New York: Cambridge University Press.

Koch G. H., Brongers M. P. H., Thompson N. G., Virmani Y. P., and Payer J. H., 2001, Corrosion Costs and Preventive Strategies in the United States, FHWA-RD-01-156.

Kurz R. and Ohanian S., 2003, Modelling turbo machinery in pipeline simulations, 35th Annual Meeting of Pipeline Simulation Interest Group (PSIG), Bern, Switzerland.

Menon E. S., 2005, Gas Pipeline Hydraulics, First ed. Boca Raton: CRC Press.

Nesic S., Wang S., Cai J., and Xiao Y., 2004, Integrated CO2 Corrosion - Multiphase Flow Model, SPE International Symposium on Oilfield Corrosion, Aberdeen, UK.

Revie R. W. and Uhlig H. H. , 2008, Corrosion and corrosion control: an introduction to corrosion science and engineering, Fourth ed. Hoboken New Jersey: John Wiley & Sons, Inc.

Riemer D. P., 2000, Modelling Cathodic Protection for Pipeline Networks, PhD Thesis, University of Florida, Chemical Engineering Department.

Safitri A., Gao X., and Mannan M. S., 2011, Dispersion modelling approach for quantification of methane emission rates from natural gas fugitive leaks detected by infrared imaging technique, Journal of Loss Prevention in the Process Industries. Vol (24): 138-145.

Sánchez-Úbeda E. F. and Berzosa A., 2007. Modelling and forecasting industrial end-use natural gas consumption, Energy Economics. Vol (29): 710-742.

Shirvany Y., Zahedi G., and Bashiri M., 2010, "Estimation of sour natural gas water content, Journal of Petroleum Science and Engineering. Vol (73):156-160.

Woldeyohannes A. D. and Majid M. A. A., 2011a, Simulation model for natural gas transmission pipeline network system, Simulation Modelling Practice and Theory. Vol. (19): 196-212.

Woldeyohannes A. D. and Majid M. A. A., 2011b, Effect of Age of Pipes on Performance of Natural Gas Transmission Pipeline Network System, Journal of Applied Science.

Woldeyohannes, A. D. and Chyuan C. F., 2011, Predictive Model for Evaluating the Effect of Service Life of Pipes on Performance of Natural Gas Transmission Pipelines, 3rd CUTSE International Conference, Sarawak, Malaysia.

Woldeyohannes A. D. and Majid M. A. A., 2009, Simulation of natural gas transmission pipeline network system performance, Journal of Energy and Power engineering.Vol (3): 19-30.

Worthingham R. G., Asante B., Carmichael G., and Dunsmore T., 1993, Cost justification for the use of internal coatings, Proceedings of the 25th Annual Meeting of Pipeline Simulation Interested Groups, Pittsburgh, Pennsylvania.

Wu S., Ríos-Mercado R. Z., Boyd E. A., and Scott L. R., 2000, Model relaxations for the fuel cost minimization of steady-state gas pipeline networks, Mathematical and Computer Modelling, Vol (31): 197-220.

Zhou X., 1993, Experimental Study of Corrosion Rate and Slug Flow Characteristics in Horizontal, Multiphase Pipeline, M.Sc Thesis, Faculty of the College of Engineering and Technology, Ohio University.

doi: 10.14355/jpsr.2014.0301.03

Development of an Advisor Auditor Computer Program for the Acidizing Operation Design

Yasser A. Ahmed[1], Mahmoud Abu El Ela[*2], El Sayed El Tayeb[3], Abdel Aziz Osman[4]

Petroleum Engineering Department, Faculty of Engineering, Cairo University, Egypt

[*2]Mahmoud.abuelela@worleyparsons.com

Abstract

Acidizing operation is an irreversible process and may cause a serious problem if carried out in a wrong manner. It may fail due to many reasons such as: bad design, poor quality control or any operational problems. The acidizing operation depends mainly on field experience: there is no systematic methodology for the evaluation of the acidizing programs design.

This paper presents a new developed computer program (acidizing auditor advisor program: AAA program) that can be used as an auditor and advisor to evaluate the design of the acidizing operations before its implementation. The developed program can be also used to recommend proper design conditions to achieve successful acidizing operations. AAA program has been tested, validated and applied. It has been used to audit the design of eight acidizing programs.

This work presents the results of the application of AAA program in only three acidizing operations. It was found that the results of AAA program are consistent with the performance of the actual acidizing operations. It successfully predicts the behavior of the acidizing operations and it recommends the necessary preventive actions to mitigate the reasons of any failure. Therefore, it saves time and money, and reduces the risk of acidizing operations failure.

Keywords

Acidizing; Acidizing Auditor Program; Acidizing Operation Design; Stimulation

Introduction

Acidizing is a chemical stimulation technique involving the injection of an acid solution at pressure below the fracture pressure of the formation to remove the formation damage, restore the permeability to its original state and enhance the flow by creating new passes (Civan, 2000).

Commercial application of acidizing occurred in the Gulf Coast of Mexico in 1940, when Dowell introduced mud acid (mixture of hydrochloric acid, HCl; and hydrofluoric acid, HF). Following this event, the application of acidizing has grown rapidly and developed as follows (Ahmed, 2011):

- During 1950s and 1960s, the application of acidizing expanded and numerous acid additives and systems were developed.
- During 1970s and 1960s, the work on the physics of acidizing in limestone and the secondary reactions of sandstone acidizing have been performed. Foam diversion, oil soluble resins and coiled tubing placement were introduced to improve zone coverage. The emphasis for clay problems shifted from clay swelling to clay migration. Numerous clay control agents were developed.
- Since 1990s till now, environmentally friendly additives have been introduced and better understanding of the acidizing chemistry has been achieved. In addition, a lot of research has been performed to study all phases of the acidizing process: candidate selection, treatment design, monitoring of the execution (real-time evaluation of skin effect evolution) and post-treatment evaluation.

Acidizing Auditor Advisor (AAA) Program

To achieve good acidizing operation design, several types of data should be accurately collected and considered as follows:

1. Well data including well deviation, completion type, minimum inside diameter, completion size, flowing bottom hole pressure, tubing end, perforated interval, tubing volume, casing volume, and total depth;
2. Production data including gross production rate, water cut, productivity index, specific gravity, gas lift mandrel on/off, H2S content, oil viscosity, and oil formation volume factor;

3. Reservoir data including skin factor, reservoir permeability, drive mechanism, formation porosity, reservoir pressure, fracture pressure, gas oil contact, reservoir temperature, damage radius, and reservoir radius;
4. Mineralogical data including formation type, clays types and percentages, formation damage type, and cementing material;
5. Historical data including drilling fluid and last operation executed; and
6. Lab data including solubility and compatibility tests (emulsion and sludge tendency).

Generally, previous experiences and analogy concept are used to design the acidizing programs. This work presented a developed computer program (AAA program) that can be used as an auditor and advisor to evaluate the design of the acidizing operations before its implementation. AAA program was developed in Visual Basic Language Version 6. Fig. 1 shows the flow chart of this program which mainly consists of five steps as follows:

1. The first step is "Data Entry of the Candidate Well" in which the data of the candidate well (well data, production data, reservoir data, and mineralogy data) is fed to AAA program. Fig. 2 presents, as an example, the interface of this step in the developed program.
2. The second step is "Data Entry of the Proposed Acidizing program" in which the data of the proposed acidizing program (acidizing technique, design steps, placement technique, volume of acid, type and quantities of additives, pumping pressure, and pumping rate) is fed into AAA program.

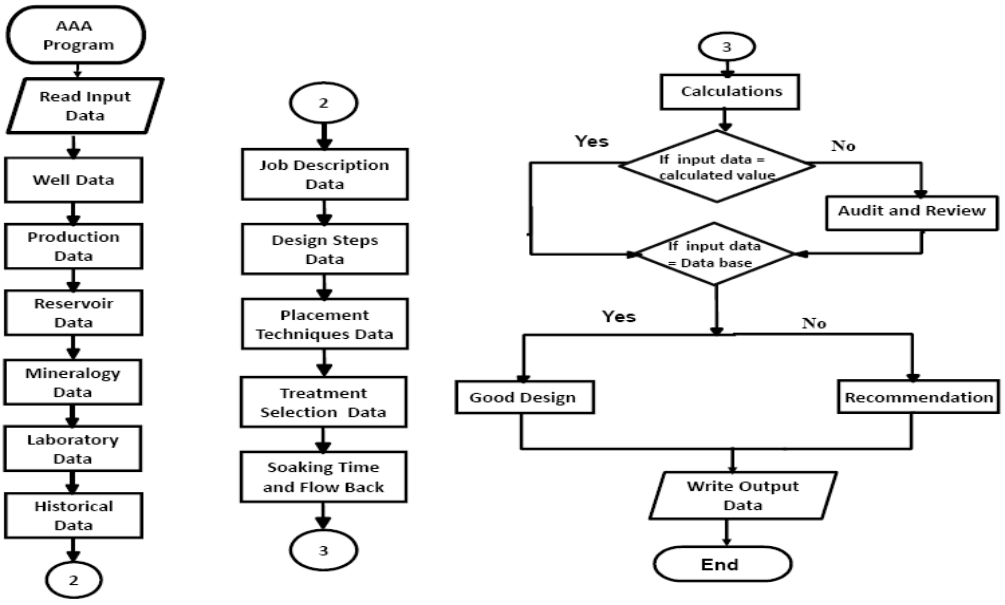

FIG. 1 FLOW CHART OF AAA PROGRAM

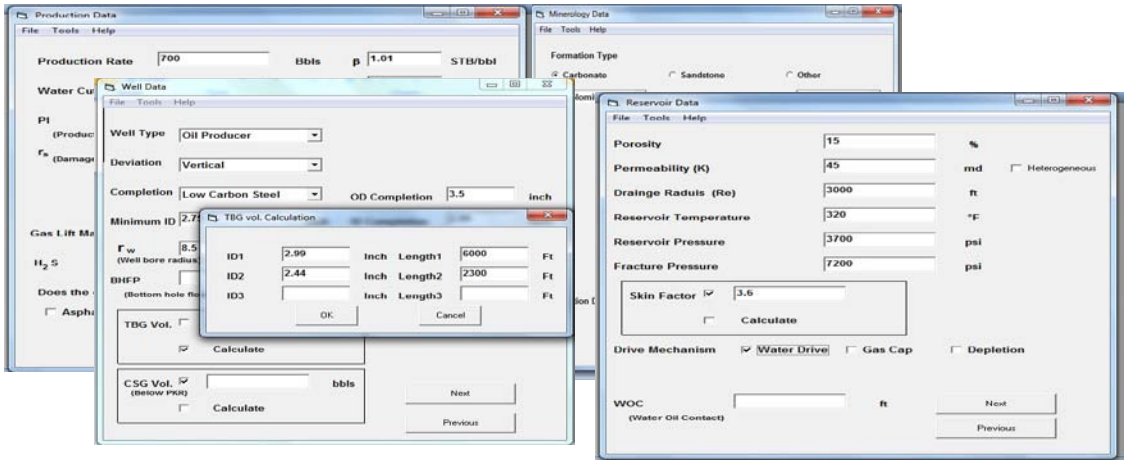

FIG. 2 INTERFACE OF AAA PROGRAM

TABLE 1 MODEL EQUATIONS

No.	Equation
1	$Q_{max} = \frac{4.916 \times 10^{-6}\ Kh\ (P_{frac} - P_{res} - P_{safe})}{\left(\mu B\ ln\frac{r_e}{r_w} + S\right)}$
2	$Q_{min} = \frac{(Vol_{acid} - Vol_{pump})}{42 \times 60\ t_{CI}}$
3	$P_s = P_{frac} + P_{fric} - P_{hyd} - P_{safe}$ $P_{fric} = 518\ \frac{\rho^{0.79} q^{1.79} \mu^{0.207}}{ID^{4.79}}$ $P_{hyd} = 0.052 \times \rho d \times h$
4	$Vpickling = 4.68743 \times t_s \times L \times F \times (ID + t_s)$
5	$V_{tbg} = \frac{ID^2}{1029} \times L$
6	$S = \left(\frac{K}{K_d} - 1\right) \ln\frac{r_d}{r_w}$

β: Formation volume factor of the injection fluid, res bbl/STB;
D: Inside diameter, in;
F: Safety factor, (1.1 is assumed);
h: Net height of the formation, ft;
H: True vertical depth, ft;
ID: Inside diameter, in;
k = Undamaged permeability, md;
k_d = Damaged permeability, md;
L = Length of tubing, ft;
P_{safe}: Safe margin, 200 to 500 psi;
P_{frac}: Fracture pressure, psi;
P_{fric} : Friction pressure, psi;
P_{hyd}: Hydrostatic pressure, psi;
P_{res}: Average reservoir pressure, psi;
P_s : Well head pressure, psi;
q: pumping rate, bbl/min;
Q_{max}: Max injection rate, bbl/min;
Q_{min}: Minimum allowable pumping rate, bbl/min;
R_d = Damage radius, ft;
r_e: Drainage radius, ft;
r_w: Wellbore radius, ft;
S: Skin factor, dimensionless;
t_{CI} : Corrosion inhibition time, hr.;
t_s : Thickness of mill, in;
Vol_{acid}:Total acid volume, gal;
Vol_{pump}: Total pumped acid, gal;
$V_{pickling}$ = Pickling volume, gal;
V_{tbg}: Tubing volume, bbl;
μ: Viscosity of the injection fluid, cp;
ϱ: Fluid density, gm/cc; and
ϱd: Fluid density, ppg.

3. The third step is "Calculations". Calculations step is one of the major steps in the AAA program which assesses the values fed in the first and second steps. During this step, AAA program calculates the maximum pumping pressure, minimum pumping rate, maximum pumping rate, pickling volume and skin. The relevant equations for the model calculations are presented in Table 1 (Ahmed, 2011; Al-Mutairi and Nasr El Din, 2005; Al-Mutairi et al., 2005; Economides and Nolte, 1989; Muecke, 1982).

4. The fourth step is "Evaluation and Modification". During this step, AAA program compares (a) the data of the candidate well and the proposed acidizing operation, and (b) the screening criteria of the acidizing operations in the database. In this step, the causes of the unsuccessful design are defined. The comparison is carried out according to specific database on AAA program. The database includes screening criteria for the data of the well, reservoir, production, mineralogy, lab, and concentrations range of the acid additives. Tables 2 to 7 present a summary for these screening criteria (Ahmed, 2001; Ahmed, 2011; Al-Mutairi and Nasr El Din, 2005; Al- Mutairi et al., 2005; Al-Mutawa et al., 2003; Buijse and van Domelen, 1998; Chang et al., 2007; Civan, 2000; Economides and Nolte, 1989; El-Halib, 2010; Gdanaski, 2005; Guidry et al., 1989; Hill and Rossen, 1994; Don Hill et al., 2000; Jones et al., 2001; Kalfayan and Metcalf, 2000; King, 1996; McLeod, 1989; Muecke, 1982; Sahara Petroleum Service Company Ltd, 2010; Shokry and Tawfik, 2010; Shuchart and Gdanski, 1996; Subero and Holder, 1996; Toseef et al. 2010; Williams et al., 1979). The database has been collected from field experience, acidizing manuals, books, SPE papers, and SPE Monograph Volume 6. The database of the program can recommend the optimum acid volume and the percentage of its additives.

5. The fifth step is "Output Data". At the end of each run, AAA program presents a report concerning the evaluation of the acidizing operation design, as being either "Successful or Unsuccessful". If the proposed acidizing design is unsuccessful, the report highlights the reasons of the failure and proposes the alternative solutions to adjust and improve the acidizing design.

TABLE 2 SCREENING CRITERIA OF THE WELL DATA

Property	Parameter	Actions / Recommendations
Well type	Oil well	Flow back step should be executed.
	Water well	Flow back step should be executed. If flow back step will be cancelled and the solubility test is 100 %, the over-flush volume should be duplicated.
Completion type	Cr, Ni	Pickling steps should be avoided and use coiled tubing as a placement technique to protect the completion.
Paz zone length	>100 ft	Diversion technique should be used.
Minimum inside diameter (ID)	Coiled tubing outside diameter OD	If outside diameter of coiled tubing is equal or larger than the minimum ID of completion, the coiled tubing string should be changed.
Total depth (TD)	Coiled tubing length	If the coiled tubing technique will be used, the coiled tubing should be taller than TD.

TABLE 3 SCREENING CRITERIA OF THE RESERVOIR DATA

Property	Parameter	Actions / Recommendations
Reservoirtemperature	200 °F >Tres>300 °F	Acid inhibitor aid should be added.
	>300 °F	Organic acid or combined acid should be used.
	T >250 °F	VESCO diversion technique cannot be used because of over limit of temperature.
	T >300 °F	Insute gel acid technique cannot be used because of over limit of temperature.
Reservoir permeability	Heterogonous	The diversion technique should be used.
	Gas reservoir	<1 md, cannot be stimulated.
	Oil or water reservoir	<20 md, cannot be stimulated.
Reservoir. pressure	Less than the hydrostatic pressure	If the reservoir pressure is less than the hydrostatic pressure, the lifting system (such as Nitrogen Lifting or Gas Lifting Mandrel) should be used to flow back the well.
Drive mechanism	Water drive	If the retarded acidizing is used, the water-oil contact (WOC) should be away (greater than 100 ft).
	Gas cap	If the retarded acidizing is used, the gas-oil contact (GOC) should be away (greater than 100 ft).
	Gas cap and water drive	If retarded acidizing is used, the WOC/GOC should be away (greater than 100 ft).
Pumping pressure	Max pumping pressure	If $P_s > P_{frac} + P_{fric} - P_{hyd} - P_{safe}$ Stop operation.

TABLE 4 SCREENING CRITERIA OF THE PRODUCTION DATA

Property	Parameter		Actions / Recommendations
Water cut	>40 %		It is not recommended to stimulate the well.
Format--ion damage	Organic	Paraffin	It does not require a stimulation job; the right solution is mixture of organic solvent and diesel.
		Asphaltine	
	Inorganic	Calcium carbonate	HCl / Organic acid should be used.
		Iron carbonate	
		Iron sulfide	It does not require a stimulation job; the right solution is a mechanical solution.
		Iron sulfate	
		Gypsum	
		Barium sulfate	
		Strontium sulfate	
		Fill	
	Other	Emulsion	It does not require a stimulation job.
		Water blockage	
		Sludge	
		Bacteria	
		Wettability change	
Damage radius (Rd), ft	Rd ≤ 0.5		Matrix acidizing should be used.
	0.5<Rd<1		Acid wash techniqueshould be used.
	1>Rd>3		Regular acidizing technique should be used.
	3>Rd>6		Retarded acid technique should be used.
	Rd>6		
H2S	50,000> H2S > 0 ppm		Add H2S scavenger.
	H2S > 50,000 ppm		From field experiences, coil tubing is not capable to work in this environment.

TABLE 5 SCREENING CRITERIA OF THE LAB DATA

Property	Parameter	Actions / Recommendations
Compatibility data	Emulsion tendency	Demulsifies should be added
	Sludge tendency	Anti-sludge should be added

TABLE 6 SCREENING CRITERIA OF THE MINERALOGICAL DATA

Property	Parameter	Actions / Recommendations
Formation types	Carbonate	Never ever choose HF acid.
		HCl or organic acid should be used.
	Sandstone	If the carbonate content is greater than 15 %, it is recommended to consider the formation as carbonate formation.
		If the carbonate content is less than 15 %: • HF system should be used, and • Pre-flush by HCl or organic acid should be used.
		If HF is used, the pre flush should contain NH4Cl to avoid the contact between HF and formation water.
		If the carbonate content is less than 15 %: • HF system should be used, and • Over-flush by HCl or organic acid should be used.
		Mutual solvent should be added in the over-flush to alert the wettability: change the formation to be water wet.
		If the high quartz content is greater than 80 % and the clay content is greater than 5%, 12:3 HF should be used.
		If the cementing material is carbonate, it is not recommended to use HCl greater than 10%.
		If the high feldspar is greater than > 20 %, 13.5:1.5 HF should be used.
		If the high clay is greater than 10 %, 6.5:1 HF should be used.
		High Iron chlorite Clay, 3: 0.5 HF should be used.
Clays types	Ellite	It is not recommend to use HCl.
	Chlorite	Iron control should be added.
	Semictite	Fresh water should be avoided.
	Kaolinite	Fresh water should be avoided. NH4Cl should be added to avoid a swelling problem.
	Dolomite	It needs more than one hour of soaking time.

TABLE 7 NORMAL CONCENTRATIONS RANGE OF THE ACID ADDITIVES

Property	Additives	Range%
Additives range	Acid inhibitor	0.2>Acid inhibitor >2
	Surfactant	0.1> Surfactant>0.5
	Mutual solvent	5>Mutual solvent>10
	Clay stabilizer	0.1>Clay control >0.2
	NH4Cl solution	2>NH4Cl>5
	KCl solution	2>KCl>5
	Demulsifier	0.1>Demulsifier>0.5
	Inhibitor aid	0.2>Acid inhibitor >2
	Anti-sludge	5> Anti sludge >25
	Non emulsion	0.2> Non emulsion >2
	Emulsifier	1> Emulsifier >4
	Organic solvent/ Acid	30:70
	Iron control	4> Iron control>8
	H2S scavenger	0.5>Anti sludge > 2.5
	Friction reducer	0.1> Friction reducer >0.5
	Foaming agent	0.1> Foaming agent >0.5

Database of AAA Program

The database of the AAA program was collected from the field experience, published data, acidizing manuals, handbooks, and the results of 93 previous acidizing operations. The database represents different basins, well types, and lithologies. 43% of these acidizing operations were executed in Egyptian oil fields; and the rest were executed in the Libyan oil fields. The case studies of the database are classified according to their results as follows: 73% of these acidizing operations represent successful acidizing programs, and the rest (27% of which about 25 are

acidizing operations) represents unsuccessful acidizing programs. There are various reasons for the failure of these acidizing programs. Fig. 3 represents the percentage of the failure reasons in the selected acidizing programs. A brief description of the major failure reasons is listed below:

1. Inappropriate acid type: Some wells are stimulated by wrong acid type. If HF is used in sandstone formation or carbonate formation, severe formation damage may occur from by-product precipitation. Moreover, in high temperature wells, it is not recommended to use HCl more than 15% by weight as it will be highly-corrosive to the metal in the wells.

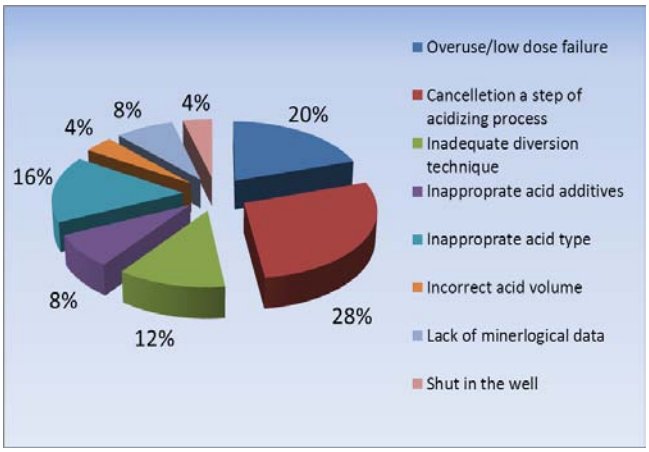

FIG. 3 PERCENTAGES OF THE FAILURE REASONS IN THE SELECTED ACIDIZING PROGRAMS DATABASE

2. Inappropriate acid additives: All additives which are used in the acidizing operations have benefits as well as side effects. If inappropriate additives are used, formation damage occurs.
3. Additive overuse or low-dose: Acid inhibitor is used to minimize the corrosion rate. However, using over-dose of acid inhibitors changes the formation wettability due to the adsorption of acids inside the formation. On the other hand, a low-dose of the acid inhibitor may increase the corrosion rate.
4. Improper placement technique: Two placement techniques are used to pump the acid in the well. The first technique is Coiled Tubing (CT: concentric tube ranges from 1 to 4.5 inch). This technique can be applied to depth of 20,000 ft or more. When the pay zone contains several layers, it is recommended to use CT to spot the acid cross the perforation and reciprocated against the pay zone to make good contribution. The second technique is Bull Heading (BH)which is cheap. The pumping rate with bull heading technique is better than coiled tubing in case of normal conditions.
5. Lack of the mineralogical information: it may cause more damage. If the formation has some types of clays like illite, and the formation is stimulated by 15% HCl, the problem of fine migration shall occur.
6. Cancelation of any step of the acidizing sequence: The acidizing steps sequence are pressure test, pickling, pre-flush, main treatment, over-flush, soaking time, and flow back. Each step has an important role in the acid operation (Al-Mutairi and Nasr El Din, 2005).
7. Inadequate of diversion technique: A critical factor to the success of the acidizing treatment is the proper placement of the acid. If a significant variation exists in the reservoir permeability, the acid tends to flow primarily into the highest-permeability zones, leaving less permeable zones virtually untreated. Thus, the distribution of the acid into the formation is an important consideration in the acidizing operation. Therefore, the design should include plans for acid placement (Chang et al., 2007; Hill and Rossen, 1994).
8. Incorrect acid volume: The relation between the damage and the volume of acid is direct. Increasing the volume of acid increases the etched penetration which depends on the fluid loss and reaction rates (Subero and Holder, 1996).
9. Incorrect calculations: Accurate calculations for the design parameters (such as pumping pressure and pumping rate) are very important to get successful acid design.

Model Assumptions and Considerations

AAA program is developed based on the following assumptions and considerations:

1. Fluid flow is steady-state radial flow;
2. The well type is oil well or water injector;
3. The model is single phase flow
4. The well is vertical well;
5. The movement of the fluid in the pipe and the formation is piston-like (no disturbance, cross-flow, or fingering occurs at the interface of any two fluids);

6. Reservoir type is a single reservoir;
7. The program deals with formation (sandstone , carbonate)
8. Maximum temperature is 400°F;
9. Occurrence of one type of damage; and
10. If the data of the reservoir radius, well bore radius, water viscosity, and oil formation volume factor are not available; AAA program assumes them as the following:
    - Reservoir radius (Re)= 3000 ft
    - Well bore radius (Rw)= 6 in
    - Water viscosity (μ_w)= 1 cp
    - Oil formation volume factor (Bo)= 1.01 STB/bbl

Case Studies

AAA program has been tested, validated and applied. Till now, AAA program has been used to audit and evaluate the design of eight acidizing programs. It was found that the results of AAA program are consistent with the actual performance of the acidizing operations after their implementation. AAA program successfully predicts the behavior of the acidizing operations. It also recommends the necessary preventive actions to mitigate the reasons of the failure. This work presents only the results of the application of AAA program in three acidizing operations for Well I, Well II and Well III.

Well I

This well is located in Sirte Basin in Libya. Table 8 presents the data of this well. The initial production rate of Well I is 500 bbl/d with zero water cut (Feb. 2008). In May 2010, the production rate was 410 bbl/d. After the implementation of a workover operation in May 2010; formation damage was formed around the well bore and the production rate became 120 bbl/d.The field also suffered calcium carbonate scale. Therefore, it was recommended to acidize this well.

TABLE 8 DATA OF WELL I

Well data			
Deviation	0	Tubing volume	105.1 bbl
Completion type	Steel	Casing volume below packer	28.2 bbl
Outside diameter of the completion	3.5 in	Open hole or cased hole	Cased hole
Inside diameter of the completion	2.99 in	Perforated interval	13211-13248ft
Minimum inside diameter	2.25 in	Primary cementing	No
Well bore radius	5 in	True vertical data	13605ft
Tubing end	12094 ft		
Production data			
Production rate	120bbl/d	H2S	0
Water cut	0	Bo	1.01
Damage radius	0.5 ft	Viscosity	15 cp
Does the oil contain asphaltin?			No
Does the oil contain paraffin?			No
Reservoir data			
Porosity	14%	Skin factor	1.5
Permeability	55 md	Drive mechanism	Water drive
Reservoir pressure	4800 psi	Reservoir temperature	240^{0}F
Fracture pressure	9000 psi		
Mineralogy data			
Formation type	Dolomite	Is the cementing material carbonate?	No
Clays content	0%	Formation damage type	Calcium carbonate
Lab data and rig operation			
Emulsion	No	Sludge	No

TABLE 9 DATA OF THE ORIGINAL ACIDIZING PROGRAM FOR WELL I

Program procedures			
Job description	Acid wash	Do you use diversion?	No
Acidizing technique	Regular	Placement technique	CT
Design steps	Pressure test - main treatment - over-flush soaking time - flow back		
Coil tube outside diameter	1.5 in	Coil tubelength	10,000ft
Treatment design			
Pressure test	5000 psi	Pickling volume	0
Main treatment additives			
Volume	3700gal	Treatment	15 % HCl
Surfactant	0.20%	Iron control	0.50%
Inhibitor	0.0%		
Viscosity	1 cp	Density	8.4 ppg
Pumping pressure	1000 psi	Pumping rate	0.6 bbl/min
Over-flush additives			
Volume	4200 gal	Treatment	KCl 2 %
Viscosity	1 cp	Density	8.45
Pumping pressure	1000 psi	Pumping rate	0.6
Soaking time and flow back			
Flow back type	Coil tube and N2	Soaking time	90 Min

Table 9 presents the data of the original acidizing program prepared to remove the formation damage. After the preparation of the acidizing program; AAA program was used to audit it. Table 10 presents the output data of AAA program. It is clear from Tables 9 and 10 that the pumping pressure and pumping rate of the acid in the proposed program are reasonable. However, Table 10 identifies four inaccurate design parameters and proposes four corresponding recommendations as follows:

TABLE 10 OUTPUT DATA OF AAA PROGRAM FOR WELL I

Job Identification
Company Name:E
Field/Well Name:Sirte Basin 7
Job Description
Acid wash is not suitable, Matrix acidizing should be used
Design Steps
The pickling step should be done for coiled tubing string
Placement Technique
The coiled Tubing sting should be taller than TD
Pickling
Preflush
Main Treatment
Acid inhibitor aid should be added
The max pumping rate is:3.6 bbl/min
The max pumping pressure:2571 psi
The minimum pumping rate:0.24 bbl/min
Over flush
Soaking time & Flow back

1. The original acidizing program indicates that the acidizing operation shall be conducted with acid wash. However, AAA program is recommended to use matrix acidizing because the damage radius in the formation is about 0.5 ft. It should be mentioned that the comparison between the damage radius (0.5 ft as shown in Table 8) against the screening criteria of the production data (Table 4) led the program to provide this recommendation.

2. The proposed acidizing program does not include the pickling step. AAA program is recommended to include pickling step in the acidizing program to avoid the movement of rust, scale, wax, and pipe dope into the formation and cause severe damage. It is clear that the value of the pickling volume in Table 9 (zero) led the program to provide this recommendation. Cancelation of any step of the acidizing sequence might lead to a failure in the acidizing program.5

3. The coiled tubing string in the proposed acidizing program is shorter than the total depth of the well. AAA program highlights this issue and indicates that the coiled tubing string should be taller than the total depth of the well. It should be stated that the comparison between the total depth of the well (13,605 ft) and the length of the CT (10,000 ft) in Tables 8 and 9 against the screening criteria of the well data (Table 2) led the program to provide this recommendation.

4. The proposed acidizing program does not include acid inhibitor aid. AAA program recommends to use acid inhibitor aid (as the temperature is high) to avoid the corrosion of the casing and tubing. It should be mentioned that the HCl is very corrosive at high

temperatures (Don Hill et al., 2000). The comparison between the reservoir temperature (240°F as shown in Table 8) and the value of the inhibitor in Table 9 (zero) against the screening criteria of the reservoir data (Table 3) led the program to provide this recommendation.

After the implementation of the acidizing program with the recommendations of AAA program; the acidizing operation was successfully performed. The production rate of the well increased from 120 bbl/d to 485 bbl/d and the well head pressure increased from 25 to 90 psi as shown in Table 11.

Well II

This well located in Sirte Basin in Libya was drilled in 2007 and started its production with a rate of 1300 bb/d and zero water cut. Table 12 presents the data of this well. In Jan 2009, workover operation was performed to repair the casing leakage. The production rate in Jan 2009 declined from 1180 to 700 bbl/d with zero water cut. The formation was damaged due to the presence of calcium carbonate in the workover fluid. Therefore, it was recommended to acidize this well.

Table 13 presents the data of the proposed acidizing program. After the preparation of the acidizing program, AAA program was used to audit it. Table 14 presents the output data of AAA program. AAA program confirms the adequacy of the proposed acidizing program without any recommendations. Table 14 confirms also that the pumping pressure and pumping rate of the acid in the proposed program (Table 13) are reasonable.

After the implementation of the acidizing program, it was found that the results of AAA program are consistent with the actual behavior of the formation and the job is successful as shown in Table 15. The production rate increased after the acidizing operation from 700 bbl/d to 1135 bbl/d. Moreover, the well head pressure increased from 80 psi to 230 psi.

TABLE 11 WELL HEAD PRESSURE AND PRODUCTION RATE OF WELL I

Parameter	Initial conditions (Feb.2008)	Before the damage before the workover (May 2010)	After the workover before the acidizing (May 2010)	After the acidizing (June 2010)
Production rate,* bbl/day	500	410	120	485
Well head pressure, psi	95	80	25	90

* Note: water cut is zero

TABLE 12 DATA OF WELL II

Well data			
Deviation	0	Tubing volume	78 bbl
Completion type	Steel	Casing volume below packer	7 bbl
Outside diameter of the completion	3.5 in	Open hole or cased hole	Cased hole
Inside diameter of the completion	2.99in	Perforated interval	8910 - 8970ft
Minimum inside diameter	2.25 in	Primary cementing	Normal
Well bore radius	8.5in	True vertical depth	9000ft
Tubing end	8000ft		
Production data			
Production rate	700	H2S	0
Water cut	0	Bo	1.01
Damage radius	2 ft	Viscosity	15 cp
Does the oil contain paraffin?			No
Does the oil contain asphaltin			No
Reservoir data			
Porosity	15%	Skin factor	3.6
Permeability	25md	Drive mechanism	Water Drive
Reservoir temperature	320ºF	Fracture pressure	6100psi
Reservoir pressure	3700psi		
Mineralogy data			
Formation type	Carbonate	Is the cementing material carbonate?	No
Clays content	0%	Formation damage type	Calcium carbonate
Lab data and rig operation			
Emulsion	No	Sludge	No

TABLE 13 DATA OF THE ORIGINAL ACIDIZING PROGRAM FOR WELL II

Program procedures					
Job description	Matrix	Do you use diversion?		Yes	
Acidizing technique	Retarder combined	Type of diversion		Foam	
Design Steps	Pressure test - pickling - main treatment - over-flush soaking time - flow back				
Placement technique	Coil tube	Coil tube outside diameter	1.5in	Coil tube length	15,000 ft
Treatment design					
Pressure test	4500psi	Pickling volume		800 gal	
Pickling additives					
15 % HCl	800 gal	Surfactant		0.20%	
Inhibitor	0.80%				
Density	8.35ppg	Displaced by		Water	
Main Treatment additives					
Volume	4500gal	Treatment		Combined acid	
Mutual solvent	5%	Iron control		0.50%	
Inhibitor	0.50%	Inhibitor aid		0.50%	
Viscosity	1cp	Density		8.33 ppg	
Pumping pressure	1000 psi	Pumping treatment		0.5 bbl/min	
Over flush additives					
Volume	1600 gal	Treatment		KCl 2 %	
Viscosity	1 cp	Density		8.45 ppg	
Pumping pressure	1000 psi	Pumping rate		1 bbl/min	
Soaking time and flow back					
Flow back type	Coil tube and N2	Soaking time		60 Min	

TABLE 14 OUTPUT DATA OF AAA PROGRAM FOR WELL II

Job Identification
Company Name:A
Field/Well Name:Sirte Basin 3
Job Description
Design Steps
Placement Technique
Pickling
Preflush
Main Treatment
The max pumping rate is:1.2 bbl/min
The max pumping pressure:1589 psi
The minimum pumping rate:0.3 bbl/min
Over flush
Soaking time & Flow back

TABLE 15 WELLHEAD PRESSURE AND PRODUCTION RATE OF WELL II

Parameter	Initial conditions (Sep. 2007)	Before the damage before the workover (Jan 2009)	After the workover before the acidizing (Jan 2009)	After the acidizing (Jan 2009)
Production rate,* bbl/day	1300	1180	700	1135
Well head pressure, psi	260	190	80	230

* Note: water cut is zero

Well III

This well was drilled and completed in 1981 at the Sirte Basin in Libya. After excessive production with ESP; the water cut increased to 95%. Then, it was converted into a water injection well in 2006. The injection rate started with 3000 bbl/day. Then, it declined to 2000 bbl/day in February 2010. The production logging tools (PLT) was executed to evaluate the injection rate profile for the perforated intervals. The PLT showed that the upper interval (from 5615 to 5642 ft) received around 75% of the total injection rate; while the lower interval (from 5672 to 5688 ft)received the rest. Therefore, the operating company took a decision to stimulate the lower zone.

Tables 16 and 17 present the data of the well and the data of the proposed acidizing program, respectively. The main idea in the proposed acidizing program is the usage of bull heading placement technique with in-situ gelled acid as a chemical diversion to direct the acid into the low permeable zone (damaged zone). In the damaged zone, the regular acid is used with its additives to remove the formation damage and create new wormholes.

After the preparation of the acidizing program, AAA Program was used to audit it. Table 18 presents the output data of AAA program, which confirms the adequacy of the proposed acidizing program without any recommendations. Table 18 indicates also that the pumping pressure and pumping rate of the acid in the proposed program (Table 17) are reasonable.

After the implementation of the acidizing program, it was found that the results of AAA program are consistent with the actual behavior of the formation and the Job is successful. The injection rate increased after the acidizing job from 2000 bbl/d to 2920bbl/d. The acidizing job increased the injection rate to almost the normal injection rate. Moreover, the well head pressure decreased from 370 psi to 110 psi. The PLT which was conducted after the acidizing job indicated that the injection profile came back to its normal behaviour.

TABLE 16 DATA OF WELL III

Well data			
Deviation	0	Tubing volume	27.4 bbl
Completion type	Steel	Casing volume below packer	2.7 bbl
Outside diameter of the completion	3.5 in	Open hole or cased hole	Cased hole
Inside diameter of the completion	2.99 in	Perforated interval	5672-5688ft
Minimum inside diameter	2.19 in	Primary cementing	Normal
Well bore radius	6.276 in	True vertical depth	5700 ft
The depth of Tubing end	5300 ft		
Production data			
Injection rate	2000 bbl/day	H2S	0
Damage radius	1ft	Viscosity	1 cp
Does the oil contain paraffin?			No
Does the oil contain asphaltin			No
Reservoir data			
Porosity	19%	Skin factor	6
Permeability	40 md	Reservoir pressure	1950 psi
Reservoir temperature	170^{0}F	Fracture pressure	4900 psi
Mineralogy data			
Formation type	Limestone	Is the cementing material carbonate?	No
Clays content	0 %	Formation damage type	Inorganic scale
Lab data and rig operation			
Emulsion	No	Sludge	No

TABLE 17 DATA OF THE ORIGINAL ACIDIZING PROGRAM FOR WELL III

Program procedures			
Job description	Matrix	Do you use diversion?	Yes
Acidizing technique	Regular	Type of diversion	In-situ gel acid
Design steps	Pressure test - Pickling - Pre-flush - Main treatment - Over-flush - Soaking time		
Treatment design			
Pressure test	3000 psi	Pickling volume	500 gal
Pickling additives			
15 % HCl	500 gal	Surfactant	0.20%
Inhibitor	0.40%	Iron control	0.60%
Density	8.3 ppg		
Pre-flush additives			
Volume	400 gal	Treatment	2% KCl
Viscosity	1 cp.	Density	8.45 ppg
Pumping pressure	1000 psi	Pumping rate	0.4bbl / min
Main treatment additives			
Volume	1250 gal.	Treatment	15% HCl
Iron control	0.60%	Surfactant	0.30%
Mutual solvent	7%	Inhibitor	0.40%
Viscosity	1 cp.	Density	8.3 ppg
Pumping pressure	1000psi	Pumping rate	0.4 bbl/min.
Over flush additives			
Volume	3200 gal	Treatment	KCl 2 %
Viscosity	1cp	Density	8.45ppg
Pumping pressure	1000 psi	Pumping rate	0.4 bbl/min
Soaking time and flow back			
Flow back type	No	Soaking time	60 Min

TABLE 18 OUTPUT DATA OF AAA PROGRAM FOR WELL III

Job Identification
Company Name:D
Field/Well Name:Sirte Basin 1
Job Description
Design Steps
Placement Technique
Pickling
Preflush
The max pumping rate is:0.5 bbl/min
The max pumping pressure:1900psi
Main Treatment
The max pumping rate is:0.5 bbl/min
The max pumping pressure:1944 psi
The minimum pumping rate:0.08 bbl/min
Over flush
Soaking time & Flow back

Conclusions

This paper has presented a new developed computer program (Acidizing Auditor Advisor program: AAA program) that can be used as an auditor and advisor to evaluate the design of the acidizing operation before its implementation. The developed program can be also used to recommend proper design conditions to achieve successful acidizing operations. AAA program has been tested, validated and applied.

Three case studies have been presented in this work. It was found that the results of AAA program are consistent with the performance of the actual acidizing operations, the behavior of the acidizing operations were successfully predicted and the necessary preventive actions were recommended to mitigate the reasons of any failure.

REFERENCES

Ahmed, Tarek. "Reservoir Engineering Handbook." 2nd Edition, Gulf Professional Publishing, Houston, Texas, USA, 2001.

Ahmed, Yasser. "Development of an Advisor Auditor Computer Program for Acidizing Job Design.", M.Sc. Thesis, Faculty of Engineering, Cairo University, Egypt, 2011.

Al-Mutairi, Saleh H., and Hisham Nasr El Din. "Tube Pickling Pocedures: Case History." Paper SPE 95004-MS presented at the SPE European Formation Damage Conference, Sheveningen, The Netherlands, May 25-27, 2005.

Al-Mutairi, Saleh H. et al. "Pickling Well Tubulars Using Coiled Tubing: Mathematical Modelling and Field Application." Paper SPE 94124-MS presented at the SPE/ICoTA Coiled Tubing Conference and Exhibition, The Woodlands, Texas, USA, April 12-13, 2005.

Al-Mutawa, Majdi et al. "Zero-damaging Stimulation and Diversion Fluid: Field Cases from the Carbonate Formation in North Kuwait." Paper SPE 80225-MS presented at the International Symposium on Oilfield Chemistry, Houston, Texas, USA, February 5-7, 2003.

Buijse, Martin A., and Mary S. Van Domelen. "Novel Application of Emulsified Formations Acids to Matrix Stimulation of Heterogeneous." Paper SPE 39583-MS presented at the SPE Formation Damage Control Conference, Lafayette, Louisiana, USA, Feb. 18-19, 1998.

Chang, Frank F. et al. "Chemical Diversion Techniques used for Carbonate Matrix Acidizing: an Overview and Case Histories." Paper SPE 106444-MS presented at the SPE International Symposium on Oilfield Chemistry, Houston, USA, Feb. 28 - March 2, 2007.

Civan, Faruk. "Reservoir Formation Damage: Fundamentals, Modeling, Assessment, and Mitigation." 2nd Edition, Gulf Professional Publishing, Texas, USA, 2000.

Don Hill, George et at. "Formation Damage Origin, Diagnosis and Treatment Strategy." in: Economides, Michael J., and Kenneth G. Nolte (ed.), Reservoir Stimulation, Third Edition, NY, USA, 2000.

Economides, Michael J., and Kenneth G. Nolte. "Reservoir Stimulation." 2nd Edition, Prentice Hall, NJ, USA, 1989.

El-Halib, Ismail M. "Production Improvement of Formation Damaged Wells by Proper Acid Treatment." Paper SPE 128433-MS presented at North Africa Technical Conference and Exhibition, Cairo, Egypt, Feb. 14-17, 2010.

Gdanaski, Rick. "Recent Advances in Carbonate Stimulation." Paper SPE 10693-MS presented at the International Petroleum Technology Conference, Doha, Qatar, November 21-23, 2005.

Guidry, G.S. et al. "SXE/N2 Matrix Acidizing." Paper SPE 17951-MS presented at the Middle East Oil Show, 11-14 March, Bahrain, 1989.

Hill, A. Daniel, and W.R. Rossen. "Fluid Placement and Diversion in Matrix Acidizing." Paper SPE 27982-MS presented at the University of Tulsa Centennial Petroleum Engineering Symposium, USA, Aug. 29-31, 1994.

Jones, A.T. et al. "An Engineered Approach to Matrix Acidizing HTHP Sour Carbonate Reservoir." Paper SPE 68915-MS presented at the SPE European Formation Damage Conference, The Hague, Netherlands, 21-22 May, 2001.

Kalfayan, L.J., and A.S. Metcalf. "Successful Sandstone Acid Design Case Histories: Exceptions to Conventional Wisdom." Paper SPE 63178-MS presented at the SPE Annual Technical Conference and Exhibition, Dallas, Texas, USA, October 1-4, 2000.

King, George E. "An Introduction to the Basic of Well Completion Stimulations and Workover." 2nd Edition, George E. King, Tulsa, Oklahoma, USA, 1996.

McLeod, H.O. "Significant Factors for Successful Matrix Acidizing." Paper SPE 20155-MS presented at the SPE Centennial Symposium at New Mexico Tech, Socorro, New Mexico, USA, October 16-19, 1989.

Muecke, T.W. "Principle of Acid Stimulation." Paper SPE 10038-MS presented at the International Petroleum Exhibition and Technical Symposium, Beijing, China, March 17-24, 1982.

Sahara Petroleum Service Company Ltd. "Well Service Operating Manual." Rev. 1.1, SAPESCO, 2010.

Shokry, F., and O. Tawfik. "Acid Stimulation Results of Arab Carbonate Reservoirs in Offshore Field, U.A.E.: 10 Years of Review, How to Prepare the Future Challenges Linked to Stimulation." Paper SPE 138357-MS presented at Abu Dhabi International Petroleum Exhibition and Conference, Abu Dhabi, UAE, November 1-4, 2010.

Shuchart, C.E., and R.D. Gdanski. "Improved Success in Acid Stimulations with a New Organic-HF System." Paper SPE 36907-MS presented at the European Petroleum Conference, Milan, Italy, October 22-24, 1996.

Subero, D., and G. Holder. "Design, Execution and Evaluation of Matrix acid Stimulation Jobs Using Chemical Diversion and Bullheading." Paper SPE 36111-MS presented at the SPE Latin America/Caribbean Petroleum Engineering Conference, Port-of-Spain, Trinidad, April 23-26, 1996.

Toseef, A. et al. "Viscoelastic Surfactant Diversion: an Effective Way to Acidize Low-Temperature Wells." Paper SPE 136574-MS presented at Abu Dhabi International Petroleum Exhibition and Conference, November 1-4, Abu Dhabi, UAE, 2010.

Williams, Bert B. et at. "Acidizing Fundamentals." SPE Monograph Volume 6, 1979.

Yasser A. Ahmed is CT Stimulation Technical Leader at Weatherford Oil Tool Middle East. He got his B.Sc. and M.Sc. degrees from the Petroleum Engineering Department at Cairo University, Egypt. His area of research includes well stimulation and formation damage removal. He is a member of the Egyptian Engineers Syndicate and SPE.

Mahmoud Abu El Ela is an associate professor at the Petroleum Engineering Department, Cairo University, Egypt, and works also as a manager of projects "Acting" at WorleyParsons Engineers Egypt Ltd. Previously, he was a lead process engineer at WorleyParsons, assistant professor at the Petroleum Engineering Department at Cairo University, petroleum process consulting engineer for Khalda Petroleum Co., and a research engineer at Woodside Research Foundation (Curtin University of Technology, Australia). Since 1997, he has been a technical consultant in petroleum engineering for national and international companies. Abu El Ela holds a B.Sc. and M.Sc. in petroleum engineering from Cairo University, and a Ph.D. from Curtin University of Technology. He is a member of the Egyptian Engineers Syndicate and SPE.

El Sayed El-Tayeb is a professor in the petroleum engineering department, Cairo University; and also works as a professor within Petroleum and Petrochemicals Engineering Consultants (PPEC) Group - Cairo University. He is the director of the Mining Studies & Research Center (MSRC) at Cairo University. Since 1998, he has been a Consultant Engineer in the areas of petroleum reservoir engineering and enhanced oil recovery. El-Tayeb holds a BSc and MSc in petroleum engineering from Cairo University and a PhD from Laboratories des Sciences du Genie Chimique, ENSIC Nancy University - Nancy – France. He is a member of the Egyptian Engineers Syndicate and SPE.

Abdel Aziz Osman is a professor in the petroleum engineering department, Cairo University. Since 1970's, he has been a consultant in petroleum geology. Osman holds BSc, MSc and PhD from Cairo University in Petroleum Geology. In addition he hold Diplome Ingenier from ENSPM, France.

doi: 10.14355/jpsr.2014.0301.04

Water-in-Oil Emulsions: Formation and Prediction

Merv F. Fingas

Spill Science
1717 Rutherford Point, S.W., Edmonton, AB, Canada T6W 1J6
*1fingasmerv@shaw.ca

Abstract

The formation of water-in-oil emulsions was described. Research has shown that asphaltenes are the prime stabilizers of water-in-oil emulsions and that resins are necessary to solvate the asphaltenes. It has also been shown that other factors play a role, including the amount of saturates and the oil viscosity and density. Essentially, water droplets injected into the oil by turbulence or wave action can be stabilized temporarily by the oil viscosity and on a longer-term basis by resins and then asphaltenes. Depending on the starting oil properties, four types of water-in-oil types are created: meso-stable and stable emulsions, entrained water-in-oil and unstable or those-that-do-not-form types. Each type with unique properties was described. For most oils, loss of lighter components by evaporation is necessary before the oils form a water-in-oil type.

It was noted that variability in emulsion formation is, in part, due to the variation in types of compounds in the asphaltene and resins groups. Certain types of these compounds form more stable emulsions than others within the same asphaltene/resin groupings.

A review of numerical modelling schemes for the formation of water-in-oil emulsions was given. A recent model was based on empirical data and the corresponding physical knowledge of emulsion formation. The density, viscosity, asphaltene and resin contents were correlated with a stability index.

Keywords

Oil Spill Emulsification; Emulsion Formation; Emulsion Modeling

Introduction

Water-in-oil emulsions sometimes form after oil products are spilled. These emulsions, often called "chocolate mousse" or "mousse" by oil spill workers, can make the cleanup of oil spills very difficult (NAS 2002). When water-in-oil emulsions form, the physical properties of oil change dramatically. As an example, stable emulsions contain from 60 to 80% water, thus expanding the spilled material from 2 to 5 times the original volume. Most importantly, the viscosity of the oil typically changes from a few hundred mPa.s to about 100,000 mPa.s, an increase by a factor of 500 to 1000. A liquid product is changed into a heavy, semi-solid material. These emulsions are difficult to recover with ordinary spill recovery equipment.

Types of Emulsions

Fingas and Fieldhouse found that four clearly-defined water-in-oil types are formed by crude oil when mixed with water (Fingas and Fieldhouse 2009, 2011). This was shown by water resolution over time, by a number of rheological measurements, and by the water-in-oil product's visual appearance, both on the day of formation and one week later. Some emulsions were observed over a year, with the same results. The types are named stable water-in-oil emulsions, mesostable water-in-oil emulsions, entrained water, and unstable water-in-oil types. The differences among the four types are quite large based on at least two water content measurements and five rheological measurements. More than 400 oils or petroleum products were studied.

The four water-in-oil types formed by crude oils and petroleum products are stable, meso-stable, entrained and unstable (Fingas and Fieldhouse 2009, 2011; Fingas 2011).

Stable emulsions are reddish-brown semi-solid substances with an average water content of about 70-80% on the day of formation and about the same one week later. Stable emulsions remain stable for at least 4 weeks under laboratory conditions. All of the stable emulsions studied remained at least one year. The viscosity increase following formation averages 400 times the original viscosity and one week later averages 850 times the original viscosity.

Meso-stable water-in-oil emulsions are reddish-brown viscous liquids with an average water content of 60-65% on the first day of formation and less than 30% one week later. Meso-stable emulsions generally break

down to about 20% water content within one week. The viscosity increases over the initial viscosity on the day of formation averages a factor of 7 and one week later averages 2.

Entrained water-in-oil types are black viscous liquids with an average water content of 40-50% on the first day of formation and less than 28% one week later (Fingas and Fieldhouse 2009). The viscosity increase over the day of formation averages a multiple of two and one week later still averages two. Unstable water-in-oil emulsion types or those oils that do not form any of the other three types are characterized by the fact that the oil does not hold significant amounts of water following mixing with water.

Stable emulsions, on average, begin at a high level of water content (about 78%) and lose little water over one year (Fingas and Fieldhouse 2009). Meso-stable emulsions, on the other hand, begin at about 65% and lose most of this water within a few days. Entrained water-in-oil types pick up only about 40% water and only slowly lose this over one year. Unstable water-in-oil types pick up only a few percent of water and this does not change much over one year. The apparent viscosity of stable emulsion increases over the period of one year and the others generally decline or only increase a small amount. Thus, after a few months, the stable emulsion will have the greatest viscosity. The unstable-type of water-in-oil products change, becoming more viscous than elastic. The stable emulsion has about the same viscous and elastic components over the year. All other water-in-oil types show a much greater viscous component than the elastic component.

Stability Indices

Fingas and Fieldhouse (2009) carried out tests of several indices of stability, a single value that could provide good discrimination between water-in-oil types even on the first day. This was necessary as the water content alone was not entirely discriminating because some of the water loss occurs within hours or days, especially for meso-stable emulsions. It was found that all of these indices could be used to some extent to differentiate the four water-in-oil types. The chosen stability index proved to be the index that best differentiated all four water-in-oil types on the day of formation and afterwards. The baseline used was the water content one week after formation. Figure 1 shows the stability index and the slight overlaps between groups.

The calculation of the stability index, is shown in Table 1. The stability index can be simply calculated from rheological data and that it can be used, along with some basic property data such as density and viscosity, to classify the water-in-oil types.

Table 1 Calculation of a Stability Value

Step	
1	Carry out rheological studies on the water-in-oil product measuring Complex Modulus and Elastic Modulus
2	Calculate the cross product (Xpr) of the complex modulus and elastic modulus divided by the starting oil viscosity
	$Xpr = \frac{\text{Complex Modulus}}{\text{Starting Oil Viscosity}} \times \frac{\text{Elastic Modulus}}{\text{Starting Oil Viscosity}}$
3	Correct the cross product (Xpr) to yield Stability (sometimes referred to as Stability C)
	$\text{Stability} = \ln((Xpr/10000)*(Xpr/10000))$

Relation of Stabilities to Water-in-Oil Type

Calculated Stability				Calculated
Minimum	Maximum	Starting Oil Properties	Water-in-oil Type	Average Stability
4	29		Stable	13
-10	5		Meso-stable	-2
-20	3	**density >0.94 or <1.0 viscosity > 6000**	Entrained	-7
-4	-18	**density <0.85 or >1.0 viscosity<100 or >800000 Asphaltenes or Resins <1.5%**	Unstable	-15

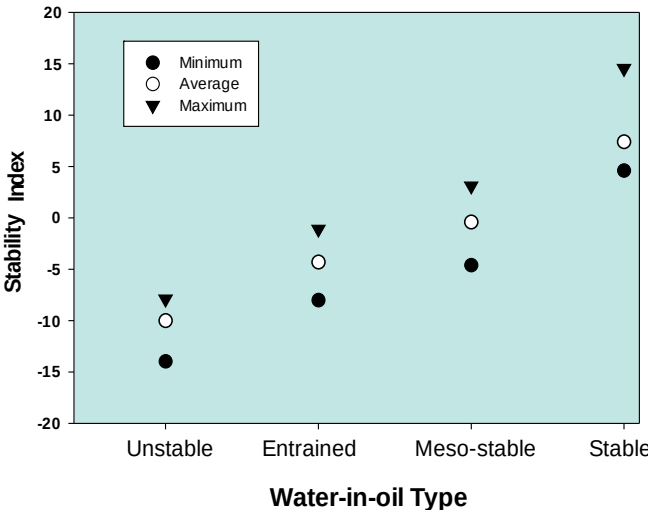

FIGURE 1 A PLOT OF THE MINIMUM, AVERAGE AND MAXIMUM STABILITY INDEX VALUES FOR EACH WATER-IN-OIL TYPE ON THE DAY OF FORMATION.

Figure 1 shows that the averages are different and there is little overlap between minimum and maximum values.

Formation of Emulsions

The Role of Asphaltenes

Some researchers reported that asphaltenes were a major factor in water-in-oil emulsions more than 40

years ago (Fingas 2011). The specific roles of asphaltenes in emulsions were not defined until recently. Currently, the basics of water-in-oil emulsification are now understood to a much better degree (Sjöblom et al. 2003, Czarnecki 2009). The fundamental process is that water-in-oil emulsions are stabilized by the formation of high-strength visco-elastic asphaltene films around water droplets in oil. Resins could also form emulsions, but resins do not form stable emulsions, and actually aid in asphaltene emulsion stability by acting as asphaltene solvents and by providing temporary stability during the time of the slow asphaltene migration. Overall, a wide spectrum of scientists has found that oil composition is the key factor in water-in-oil emulsion formation including the amounts and types of asphaltene, resin, and saturate contents.

Asphaltenes represent a very broad category of substances. Graham et al. (2008) separated resins and asphaltenes into two classes of binding and non-binding, and found that the binding component formed emulsions, whereas the non-binding did not. Czarnecki (2009) analysed several fractions and found that there were differences in the oxygen and sulphur contents of the different fractions studied. Further, he noted that the composition of rag, a persistent emulsion often left behind after an emulsion is broken, consisted of multiple emulsion droplets, a number of water droplets unable to break through the interface and flocculated fine solids. Varadaraj and Brons (2012) found that rag, the residual of a broken emulsion, contains high proportions of asphaltenes; then noted that water-in-oil emulsions, solids-in-oil dispersions, oil-in-oil dispersions and oil-in-water-in-oil multiple emulsions coexist in the rag.

Several scientists reviewed emulsions and concluded that the asphaltene content is the most important factor in the formation of emulsions (Gu et al. 2002, Yarranton et al. 2000, Kilpatrick and Spiecker 2001). Even in the absence of any other possibly-synergistic compounds such as resins, asphaltenes were found to be capable of forming rigid, elastic films which are the primary agents in stabilizing water-in-crude oil emulsions. The exact conformations by which asphaltenes organize at oil-water interfaces and the corresponding intermolecular interactions have not been elucidated. Workers studying only crude oil emulsions concluded that water-in-oil emulsions are exclusively stabilized by asphaltenes, although the specific stability was not measured (Kilpatrick and Spiecker 2001). Even though the emulsions contain inorganic solids, waxes and other organic solids, the main stabilization comes from asphaltenes. Other workers have noted that solid particles, such as clays, when present, can stabilize or enhance the stability of emulsions (Sztukowski and Yarranton 2004). This is true of emulsions formed by clay-containing bitumens. These clay-stabilized emulsions may have differences from the crude oil and petroleum product emulsions noted in this paper.

Asphaltenes are a class of substances defined only by their precipitation from oil in pentane, hexane, or heptane. The specific structure of asphaltenes is unknown, however, the molecular weight averages about 750 Daltons or more and there is a planar aromatic structure surrounded by alkane groups, some with heteroatoms, S, N and O (Groenzin and Mullins 2007). Studies of the time dependency of film strength by viscosity measurements showed that the complex modulus increased by about 2-fold between 2 to 4 hours. This indicated an increased film strength, probably due to asphaltene aggregation and cross-linking. The mechanism by which emulsions form begins when asphaltenes migrate to the oil-water interface, a process that is regulated by the diffusion of the soluble asphaltenes. At the interface, the asphaltenes self-assemble to produce an elastic, rigid, stable film (Lobato et al. 2007, Zhang et al. 2005). This is the source of stability for water-in-oil emulsions.

Recent work on asphaltenes has shown that separation of asphaltenes into fractions results in more information on the fraction that forms emulsions. Arla and co-workers (2007) noted that the acid fractions of the asphaltenes formed more stable water-in-oil emulsions than some other compounds.

The adsorption of asphaltenes at the water-oil interface proceeds for a long time and may still proceed after a year (Fingas and Fieldhouse 2006). This implies that the adsorption at the interface lowers the net energy of the system and is thus favoured thermodynamically. The bulk concentration of asphaltenes is important and drives the amount that is adsorbed at the interface. Asphaltenes have their greatest tendency to adsorb and make the strongest interfacial film at their limit of solubility, otherwise they would stay in solution (Fingas and Fieldhouse 2006). Several workers noted that there were differences in the stability of emulsions, depending on the fractions of asphaltenes taken and also by the amount of asphaltene aggregation present (Spiecker et al. 2003, Yang et al. 2004). Asphaltene aggregation may be an important topic in emulsion stability.

Asphaltenes may self-associate in a manner that is oligimerization rather than simple stacking, implying that some form of bonding takes place.

The Role of Resins and Other Components

Several researchers studied the role of resins in water-in-oil formation (Fingas and Fieldhouse 2009). They noted that the main role appears to be solvation of the asphaltenes in the oil solution. Research was conducted which showed that the addition of resins at ratios of 2:1 (resins:asphaltenes) could increase the stability of the water-in-oil emulsions by as much as twice as that without the resins (Kilpatrick and Spiecker 2001). Others have noted that resins and asphaltenes are somehow correlated in emulsion stability. Some researchers note that with increasing asphaltene:resin ratio, the emulsions in well heads were more stable (Ali and Alqam 2000). The interfacial properties of asphaltenes in several Norwegian offshore crude oils were studied (Nordli et al. 1991). Asphaltenes were shown to be the agent responsible for stabilizing the crude oils tested, however the resins were also noted as being important. Pereira et al. (2007) noted that resins can determine whether asphaltenes stabilize or destabilize emulsions depending on the type of resins and asphaltenes. Resin adsorption experiments were carried out on different substrates including silica substrates and asphaltenes. Some resins were found to adsorb much more on the same surface areas. The experiments showed a high self-interaction and were suggested as being the key factor in determining whether the resins would stabilize asphaltenes against aggregation or not.

Silset and co-workers (2003) noted that many of the stability differences in emulsions can be explained by the interactions between asphaltenes and resins. The authors noted that asphaltenes are believed to be suspended as colloids in the oil with stabilization by resins. Each particle is believed to consist of one or more sheets of asphaltene monomers and absorbed resins to stabilize the suspension. Under certain conditions, the resins can desorb from the asphaltenes leading to increased asphaltene aggregation and precipitation of the larger asphaltene aggregates. Several workers note that there is significant interplay between asphaltenes and resins and that resins solvate the asphaltenes (Spiecker et al. 2003).

Waxes have not been found to stabilize oil water-in-oil emulsions but have been found to play a role in other types of emulsions, such as food formulations, but only if they are molten or deformed (Binks and Rocher 2009).

Methods to Study Emulsions

The availability of methodologies to study emulsions is very important. In the past 15 years, dielectric methods and rheological methods and many other methods have been used to study formation mechanisms and stability of emulsions (Nordi et al. 1991). Standard chemical techniques, including Nuclear Magnetic Resonance (NMR), chemical analysis techniques, Near-infrared spectroscopy (NIR), microscopy, interfacial pressure, and interfacial tension, are also being applied to emulsions. These techniques have largely confirmed findings noted in the dielectric and rheological mechanisms.

Most researchers studied the stability of emulsions by measuring the amount of water resolved with time (Fingas and Fieldhouse 2009, Aguilera et al. 2010, Rondon et al. 2010, Borges et al. 2009). This method certainly is the baseline method. Some researchers also subjected the emulsions to centrifugation removing water, to assess stability.

The use of high pressure NIR has been used by one group to study asphaltene aggregation of live crude oils (Kallevik et al. 2000). NIR information on the amount of asphaltenes and resins was tied to the emulsion stability. Araujo et al. (2008) studied the use of NIR and found that NIR was both sensitive to the water content and droplet size, and models were proposed to estimate both water content and droplet size from NIR data. Many of the measurements can now be inter-correlated. NMR provides the best method of measuring water droplet size in emulsions (Araujo et al. 2008). Standard optical techniques suffer from the fact that the continuous medium, oil, is not transparent. Therefore, only the surface droplets are measured using optical techniques.

The NMR method is known as pulse field gradient with diffusion editing (PFG-DE) NMR (Aichele et al. 2008). Results from recent measurements of a water-in-oil emulsion shows a change in droplet size from the revolution rate of the mixing vessel. The average water droplet size in one experiment varied with mixing energy-from about 12 to 30 micrometers.

Dielectric spectroscopy has been used to study emulsions. The electrical permittivity of the emulsion can be used to characterize an emulsion and assign a stability (Midttun 2000). The Sjöblom group has measured the dielectric spectra using the time domain spectroscopy (TDS) technique (Midttun 2000). A

sample is placed at the end of a coaxial line to measure total reflection. Reflected pulses are observed in time windows of 20 ns and Fourier transformed in the frequency range from 50 MHz to 2 Ghz.

Many studies on the rheology of emulsions have been performed (Johnsen and Rønningsen 2003, Spiecker and Kilpatrick 2004). Emulsions stabilized by surfactant films (such as resins and asphaltenes) behave like hard sphere dispersions and display viscoelastic behaviour. Relaxation time can be determined for the system, which increases with the volume fraction of the discontinuous phase. It has been noted that the emulsion stability is highly dependent on the rheological properties of the water/oil interface and that a high elasticity will increase the level of stability.

Many researchers studied emulsification by using model oils or modified crude oils. Other researchers studied emulsions as thin layers or by droplets (Ridi et al. 2009). Hemmingsen et al. (2005) studied the water-in-oil emulsions formed from 27 crude oils of different origins. They found that there is an increase in stability as viscosity increases. Viscosity also correlated with the SARA (Saturates, Aromatics Resins and Asphaltenes) data taken on the crude oil. Aske et al. (2002) studied 16 crudes from the North Sea and 5 from North Africa. Stability was measured using the results from an electric field cell. A voltage was applied to the cell until coalesence was observed using a microscope. The value of the voltage at the critical point was taken as a measure of stability. Fingas and Fieldhouse (2011) studied more than 400 oils at various weathering stages using rheological measurements.

The Overall Theory of Emulsion Formation

The data indicate that the water-in-oil types are stabilized by both asphaltenes and resins, but for greater stability, resin content should exceed the asphaltene content slightly (Fingas and Fieldhouse 2009). However, excess resin content (A/R > about 0.6) apparently destabilizes the emulsion. This does not consider the question of different types of asphaltenes or resins. A high asphaltene content (typically > 10%) increases the viscosity of the oil such that a stable emulsion will not form. Viscous oils will only uptake water as entrained water and will slowly lose much of this water over a period of about one week. Viscous oils (typically >1000 mPa.s) will not form stable or meso-stable emulsions. Oils of low viscosity or without significant amounts of asphaltenes and resins will not form any water-in-oil type and will retain less than about 6% water. Oils of very high viscosity (typically > 10,000 mPa.s) will also not form any of these water-in-oil types and thus are classified as unstable. This is probably due to the inability of water droplets to penetrate the oil mass.

The discussion in 4.1 and 4.2 above certainly shows that asphaltenes and resins combine to stabilize water droplets in emulsions. This can be seen in Figure 2. Figure 2 shows a simplified plot of oil composition and viscosity and the types of emulsions that result from this combination. This figure shows that even a very simplified presentation can highlight the importance of the starting oil viscosity and resin and asphaltene contents.

The information given in section 4 highlights the formation process. The start of the process is the injection of water droplets into the oil mass. This would typically occur as the result of turbulence or wave action. This also could occur as the result of oil injection into water, such as from an underwater blowout. Once in the oil mass, the water droplets may coalesce and sink to the bottom unless these water droplets are somehow stabilized. Asphaltenes probably reside in the oil in the form of resin-solvated agglomerates. They are not likely to stabilize the water droplets immediately as the large asphaltene-resin agglomerates migrate too slowly. If, however, the oil has a viscosity between about 50 to 5000 mPa.s, the water droplets will move slowly, allowing time for some chemical stabilization. It is thought that resins, weakly stabilize the water droplets initially. Resins are also polar compounds and can become associated with polar water. Once stabilized by resins, the large asphaltenes will move toward the water droplets and will form elastic films around the water droplets. The ratio of asphaltene to resins can affect this process. If the quantity of resins is too high, they will solvate the asphaltenes to the extent that their migration is affected and will also create a barrier between the asphaltenes and the water droplets. Thus in the case of too high resin content, destabilization will also occur. It is thought that this destabilization is the origin of meso-stable emulsions.

If the viscosity of the oil is too high, water droplets cannot penetrate the oil mass to a great extent and thus emulsions are not formed. At moderate oil viscosities, about 1000 to 10,000 mPa.s, the water droplets may be retained by viscosity alone. This is possibly the origin of the entrained water-in-oil type.

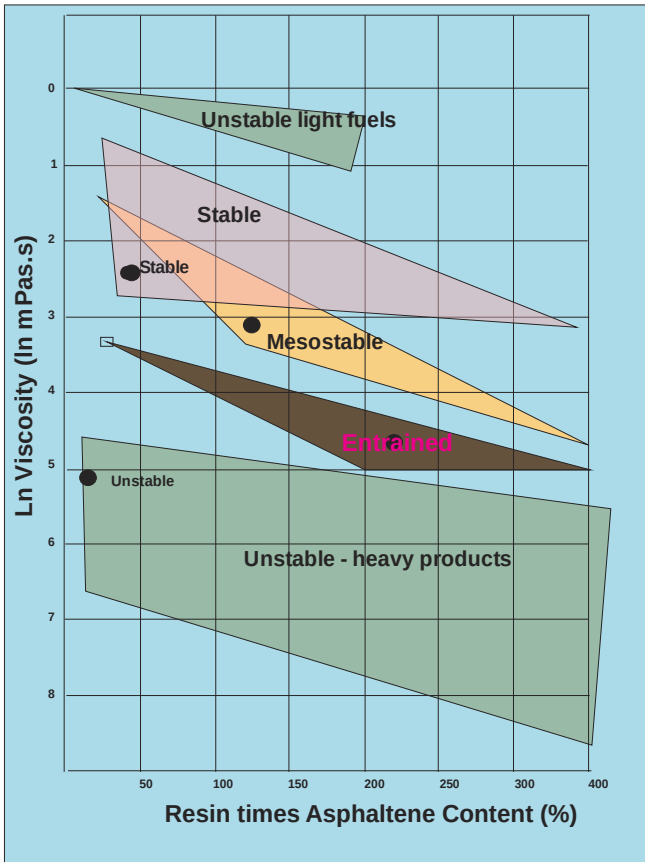

FIGURE 2 A PLOT OF THE STARTING OIL VISCOSITY VERSUS THE ASPHALTENE TIMES THE RESIN CONTENT OF THE STARTING OIL. THE SHADED REGIONS SHOW ALL AREAS WHERE THE PARTICULAR WATER-IN-OIL TYPE EXISTS. THIS SIMPLE COMPARISON SHOWS THAT THERE ARE APPROXIMATE REGIONS OF STABILITY WITH ONLY THESE THREE FACTORS. ANOTHER IMPORTANT FACTOR IS THE ASPHALTENE/RESIN RATIO AND THIS FACTOR HELPS SEPARATE ANY OVERLAPS. THIS PLOT USES DATA ON THE DAY OF FORMATION.

The Role of Weathering

Most crude oils and petroleum products require weathering (evaporation) before they will form emulsions (Fingas and Fieldhouse 2011). Some heavy oils will make transitions from stable to entrained and further on to being unable to form a water-in-oil mixture (unstable - heavy oil type) upon weathering. Most typical crude oils require weathering to make the transition from the basic crude to a meso-stable or stable emulsion. The weathering is necessary to increase the viscosity and the asphaltene/resin content to the point where the next water-in-oil type is possible.

It should be noted that once a water-in-oil type is formed, it cannot make a transition to another type even if extensive weathering or mixing takes place. This is felt to be a result of the exacting conditions for each type. Further, asphaltenes appear to be tied up in the form of 'rag' in broken meso-stable emulsions. This 'rag' formation appears to prohibit the formation of other types of emulsions.

Modeling the Formation of Water-in-oil Emulsions

Older Models

The emulsification processes described above were not apparent until about 15 years ago and have since been translated into modelling equations (Fingas 2011). The different water-in-oil states dictate that one simple equation is not adequate to predict formation. Information on the kinetics of formation at sea and other modeling data was less abundant in the past. It is now known that emulsion formation is a result of surfactant-like action of the polar asphaltene and resin compounds. While these are similar compounds that both behave like surfactants when they are not in solution, asphaltenes form much more stable emulsions. Emulsions begin to form when the required chemical and viscosity conditions are met and when there is sufficient sea energy. Further, as pointed out above, three different water-in-oil types are formed, depending on the oil type and its composition. Some oils do not form any water-in-oil types and this fact is stated to be a fourth type.

In the distant past, the rate of emulsion formation was assumed to be first-order with time. This was approximated with a logarithmic (or exponential) curve. The physical assumption was that all oils uptake water on a first-order basis. Although not consistent with the knowledge of how emulsions form, this assumption was used extensively in oil spill models. As was shown in comparisons, this does not yield correct results (Fingas and Fieldhouse 2011). The old models and comparison with newer models are described in the literature (Fingas 2011). This comparison shows that most of the older approaches are not reliable and can result in inaccurate predictions.

In summary, there are two basic ingredients to the formation of water-in-oil types: sea energy, and the correct chemical conditions in an oil. Often an oil must lose certain components by evaporation before it can form an emulsion or entrained water type.

New Models

Several new models for the prediction of water-in-oil emulsions were recently developed by the present author (Fingas 2011, Fingas and Fieldhouse 2004), Yetilmezsoy et al. 2011). These models used empirical

data to predict the formation of emulsions using a continuous function and employing the physical and chemical properties of oil. The emulsification properties of more oils were measured and the properties of some of the oils in the existing oil set have been re-measured. This enables the models to be recalculated with sound data on over 400 discreet oil samples.

The basis of these models is the result of the knowledge demonstrated above–namely, that models are stabilized by asphaltenes, with the participation of resins. Findings of this group and other groups show that the entire SARA (Saturates, Aromatic, Resins, and Asphaltene) distribution effects the formation of emulsions. The prime stabilizers, asphaltenes and secondarily resins, are only available for emulsion formation when the concentration of the saturates and aromatics are at a certain level and when the density and viscosity are correct.

The approaches to model development were implemented and are detailed in the literature (Fingas 2011, Fingas and Fieldhouse 2004, Yetilmezsoy et al. 2011). The empirical data including oil content data, viscosity, density and the resulting water-in-oil type stability were used to develop mathematical correlation. The value for each parameter was correlated in a series of models using DataFit (Oakdale Engineering), which calculates linear models. A two-step process is necessary as DataFit is not able to calculate the specific mathematical function with more than 2 variables, due to the large number of possibilities. The steps to produce the first models are summarized in earlier papers (Fingas 2011). First of all, the parameters available were correlated one at a time. The latest model used the new stability index as the target of the correlation. This new approach used a multi-regression program directly, using various multi-functional transformations of the input oil property data.

A transformation is needed to adjust the data to a singular increasing or decreasing function. Regression methods will not respond correctly to a function that varies both directly and inversely with the target parameter. Most parameters have an optimal value with respect to class, that is, the values have a peak function with respect to stability or class. After this correction is made to the values, the regression coefficient increases. The arithmetic converts values in front of the peak to values behind the peak, thus yielding a simple declining function. The optimal value of this manipulation is found by using a peak function. This peak function fit is available from TableCurve software.

The arithmetic to perform the transformation is: 1. if the initial value is less than the peak value, then the adjusted value is the peak value less the initial value; 2. and if the initial value is more than the peak value, the adjusted value is the initial value less the peak value. It should be noted that the exponential of density was used and the natural log of the viscosity. Previous modeling work had shown that these mathematical changes are necessary to achieve higher correlations.

Having the transformed values, the new model development proceeds by fitting a multiple linear equation to the data. The functionalities of square, logarithmic or exponential curves are achieved by correlating the straight value of the input properties plus their expanded values, taken here as the exponential of the starting value; and their companded values, the natural log (ln). Each parameter is correlated with the stability index in five sets of mathematical statements. This is similar to the standard Gaussian expansion regression technique (Kozachenko et al. 2011). In this method, the regression is expanded to functionalities above and below linear until the entire entity is optimized. For example, a linear function would be included, then a square and a square root and so on until tests of the complete regression show that there are no more gains in increased expansions. Using this technique, six input parameters: exponential of density, ln of viscosity, saturate content, resin content, asphaltene content and the asphaltene/resin ratio (A/R) were found to be optimal. Thus with 4 transformation and the original values of these input parameters, there are six times five or 30 input combinations.

Using Datafit, a multiple regression software, a maximum of 20 of these could be taken at a time to test the goodness-of-fit. Values that yield Prob(t) factors of greater than 0.9 were dropped until all remaining factors could be calculated at once. The Prob(t) is the probability that input can be dropped without affecting the regression or goodness-of-fit. Over twenty regressions were carried out until the resulting model was optimal. The r^2, the regression coefficient, was 0.82, which is high considering many potential sources of error, etc.

The present model was developed by adding multiple data sets to force the parameters to lower values. The similarities and differences between older models include:

1. The Gaussian expansion is simplified further to one term expansion and one term compression,

2. Three terms are also not rationalized in the same manner as above, this includes density, viscosity and asphaltene/resin ratio. These are felt to be continuous functions as they are and thus can be used as such,

3. The input values are also used directly as well as the Gaussian expansion,

4. There are two less terms, and

5. The resulting equation terms are mostly of values less than 100, leading to a greater stability.

The first step is to transform the input data so that it forms a continuous declining or increasing function. It should be noted that the 'greater than' can also be read as greater or equal to.

Density: in g/mL, *not transformed-just take the exponential, abbreviated Den,*

Viscosity: in mPa.s, *not transformed-just take the natural log, abbreviated Visc,*

Saturate Content: (%) *If the saturate content is less than 45, then the saturate content parameter is 45 less the saturate content and if it is greater than 45, it becomes the saturate content less 45. The value used in the equation is this transformed value.* (1)

Resin Content: (%) *If the resin content is less than 10, then the resin content parameter is 10 less the resin content and if it is greater than 10, it becomes the resin content less 10. The value used in the equation is this transformed value. If the value of the resins is zero, then this value is set to be 20.* (2)

Asphaltene Content: (5) *If the asphaltene content is less than 4, then the asphaltene content parameter is 4 less the asphaltene content and if it is greater than 4, it becomes the asphaltene content less 4. The value used in the equation is this transformed value. If the value of the asphaltene content is zero, then the value is set to be 20.* (3)

A/R or Asphaltene/Resin Ratio: *not transformed*

The class of the resulting emulsion is then calculated as follows:

Stability = -15.3 +1010*Den -3.66*Visc +0.174*Rst -0.579*Ast +34.4*A/R +1.02*exp(Den) -7.91*exp(A/R) -2740*ln(Den) +12.2*ln(Visc) -0.334*ln(Sst) -3.17*ln(Rst) +0.99*ln(Ast) -2.29*ln(A/R) (4)

Where: Stability is the stability of the resulting water-in-oil type on the day of formation,

Den is the untransformed exponential of the density,

Visc is the untransformed natural logarithm (ln) of the viscosity,

Rst is the transformed resin content as calculated in equation (2),

Ast is the transformed asphaltene content as calculated in equation (3),

A/R is the (untransformed) asphaltene/resin ratio,

Exponential den is the exponential of the exponential of density,

Exponential (A/R) is the exponential of the asphaltene/resin ratio,

Ln (natural logarithm) of the exponential of density,

Ln (natural logarithm) of the natural logarithm of viscosity,

Ln (natural logarithm) of the transformed saturates as calculated in equation (1),

Ln (natural logarithm) of the transformed resins as calculated in equation (2),

Ln (natural logarithm) of the transformed asphaltenes as calculated in equation (3)

Ln (natural logarithm) of the (untransformed) (A/R) ratio.

TABLE 2 VISCOSITY INCREASES FROM STARTING OIL AND TYPICAL WATER CONTENT

	Viscosity increase on		
	First Day	**Week**	**Year**
Entrained	1.9	1.9	2.1
Meso-stable	7.2	11	32
Stable	405	1054	991
Unstable	0.99	1.0	1.0
	Typical water content		
	First Day	**Week**	**Year**
Entrained	44.5	27.5	6
Meso-stable	64.3	30	6
Stable	81	78	70
Unstable	6.1	6	5

The values of stability which are assigned to each class are given in Table 1. The viscosities and water contents of the resulting products can be taken as the average of the types at a given time as shown in Table 2. The regression table is given in Table 3. The calculations for this model are summarized in Table 4. The new procedure is that the density and viscosity data are first applied to remove the unstable and entrained types. The calculation in equation 4 is used to separate the stable and meso-stable types.

A comparison of data is given in Table 5. The comparison of calculated stability compared to actual

stability (measured by rheology) shows good correlation. This shows how the new model can predict the water uptake.

Table 3 Regression Results for the Emulsification Model

Regression Variable Results

Variable	Value	Standard Error	t-ratio	Prob(t)	Input Variable	Math Applied
a	1006	210	4.79	0.0	Density	exp
b	-3.66	0.839	-4.36	0.00002	Viscosity (ln)	ln
c	0.175	0.100	1.76	0.079	Resins	adjusted
d	-0.579	0.142	-4.08	0.00005	Asphaltenes	adjusted
e	34.4	9.56	3.60	0.00035	A/R	
f	1.02	0.389	2.63	0.0089	exp Density	**exp**
g	-7.91	3.10	-2.55	0.011	exp A/R	
h	-2740	535	-5.12	0.0	ln Density	**ln**
i	12.2	5.01	2.43	0.0155	ln Viscosity	
j	-0.334	0.183	-1.82	0.0687	ln Saturates	
k	-0.317	0.237	-1.34	0.182	ln Resins	
l	0.990	0.358	2.76	0.00594	ln Asphaltenes	
m	-2.29	1.83	-1.25	0.212	ln A/R	
n	-15.3	41.6	-0.37	0.713	Constant	

Table 4 Summary of Calculations for Model

Basic Inputs	Symbol	Units
Density	D	g/mL
Viscosity	V	mPa.s
Saturate content	S	%
Resin content	R	%
Asphaltene content	A	%
First Calculation		**Description**
Density	Den	take exponential of density
Viscosity	Visc	take natural logarithm of viscosity
Asphaltene/Resin ratio	A/R	Divide asphaltene content by resin content
Second Step - Rationalization (converts units to simple declining or increasing functions)		
Saturate content	Sst	if(S<45, 45-S, S-45)
Resin content	Rst	if(R<10, 10-R, R-10)
Asphaltene content	Ast	if(A<4, 4-A, A-4)
Third Step - Parsing Zeros from SARA numbers*		
Resin content	Rst	replace zero's at rationalization stage with '20.1'
Asphaltene content	Ast	replace zero's at rationalization stage with '20.1'
Fourth Step - Calculate Gaussian Expansion Steps		
Exponential of density	exp(Den)	exponential of the exponential of density
Exponential of resin content	exp(Rst)	exponential of rationalized resin content
Exponential of A/R ratio	exp(A/R)	exponential of A/R ratio
natural logarithm of density	ln(Den)	natural logarithm (ln) of the exponential of density
natural logarithm of viscosity	ln(Visc)	natural logarithm (ln) of the natural logarithm of viscosity
natural logarithm of saturates	ln(Sst)	natural logarithm (ln) of the rationalized saturate content
natural logarithm of resins	ln(Rst)	natural logarithm (ln) of the rationalized resin content
natural logarithm of asphaltenes	ln(Ast)	natural logarithm (ln) of the rationalized asphaltene content
natural logarithm of A/R ratio	ln(A/R)	natural logarithm (ln) of the A/R ratio

* zeros must be purged from numbers as they cause problems in division and with logarithmic expressions

Table 5 Comparison of Model Predictions with Actual Values

Oil	Oil Evaporation	Actual Stability	Model Prediction	Density	Viscosity	Saturates	Aromatics	Resins	Asphaltenes	Actual Stability	Model
	%			(@15C)	mPa.s	%	%	%	%		
Albian Heavy Synthetic	0	stable	stable	0.9372	156	41	27	26	6	19.0	4.9
Arabian Light	0	stable	stable	0.8658	14	51	39	6	3	23.3	24.1
Arabian Medium	0	stable	stable	0.8783	29	54	32	7	6	21.0	25.0
Canolimon	0	stable	stable	0.8817	46	60	24	8	8	27.2	23.8
Canolimon	6.97	stable	stable	0.8961	103	57	25	8	9	19.9	20.0
Canolimon	13.5	stable	stable	0.9077	254	56	25	8	10	15.1	16.5
Canolimon	21.0	stable	stable	0.9200	1350	51	28	10	11	9.9	7.4
Cook Inlet - Swanson River	39.7	stable	stable	0.9143	152	56	29	7	7	14.8	16.0
Fuel Oil #5 (2000)	0	stable	stable	0.9883	1410	44	40	8	8	10.2	5.2
Fuel Oil #5 (2000)	7.25	stable	stable	1.0032	4530	40	39	8	13	7.0	1.5
Garden Banks 426	37.7	stable	stable	0.8993	136	56	32	10	3	6.7	7.2
Hebron M-04	8.8	stable	stable	0.9344	676	46	32	9	13	4.0	8.9
Hebron M-04	16.4	stable	stable	0.9423	1442	40	35	12	14	5.2	5.1
Hondo	0	stable	stable	0.9356	735	33	31	24	12	10.1	2.8
Hondo	16.7	stable	meso	0.9674	9583	27	33	29	12	0.9	-6.2
Lago Treco	0	stable	stable	0.9230	272	38	38	14	11	11.4	9.1
Lucula	0	stable	stable	0.8574	43	67	22	8	4	20.9	26.4
Lucula	15.4	stable	stable	0.8904	6118	62	26	9	4	3.6	7.1
Malongo	11.8	stable	stable	0.8970	6359	60	28	10	3	0.6	0.7
Mississippi Canyon 72	26.2	stable	stable	0.9095	195	52	34	11	3	9.5	6.0
Neptune [2009]	0	stable	stable	0.9244	402	58	13	19	10	4.0	6.2
Neptune Spar (Viosca Knoll 826)	22.6	stable	stable	0.8986	187	61	29	8	2	15.6	7.9
Platform Gail (Sockeye)	0	stable	stable	0.9297	406	39	28	21	12	3.6	5.5
Point Arguello Comingled	0	stable	stable	0.9248	533	36	25	23	16	10.6	5.8
Point Arguello Comingled	9.05	stable	meso	0.9528	4988	31	33	19	17	2.0	-1.3
Point Arguello Heavy	0	stable	stable	0.9447	3250	32	32	17	19	1.4	1.2
Point Arguello Light	0	stable	stable	0.8739	22	57	27	9	7	22.7	23.5
Point Arguello Light	10.2	stable	stable	0.8979	76	54	30	9	8	24.3	17.5
Point Arguello Light	19	stable	stable	0.9132	183	48	31	12	9	20.9	11.7
Point Arguello Light	28.3	stable	stable	0.9289	671	45	32	12	11	10.7	9.0
Prudhoe Bay (1995)	9.32	stable	stable	0.9048	55	51	35	10	3	19.0	7.0
Sockeye	0	stable	stable	0.8965	45	48	31	13	8	29.1	15.6
Sockeye	12.5	stable	stable	0.9166	163	44	32	15	9	17.3	10.3
Sockeye	22.1	stable	stable	0.9264	628	39	34	15	11	12.3	6.8
Sockeye Comingled	0	stable	stable	0.9350	550	34	32	21	13	2.0	4.2
Sockeye Sour	0	stable	stable	0.9409	821	38	29	20	13	0.5	3.1
Sockeye Sweet	26.9	stable	stable	0.9229	321	48	33	14	6	11.0	6.4
Takula	0	stable	stable	0.8637	110	65	22	8	2	17.8	18.4
Takula	11	stable	stable	0.8860	844	62	24	10	4	10.5	9.9
Takula	18	stable	stable	0.8961	3148	60	25	11	4	5.1	5.8
Viosca Knoll 826	24	stable	stable	0.9067	325	59	29	8	3	9.3	7.9
Viosca Knoll 990	35.2	Stable	stable	0.8905	91	62	28	8	2	9.5	10.7

Table 5 (Ctd.) Comparison of Model Predictions with Actual Values

Oil	Oil Evaporation	Actual Stability	Model Prediction	Density	Viscosity	Saturates	Aromatics	Resins	Asphaltenes	Actual Stability	Model
	%			(@15C)	mPa.s	%	%	%	%		
Carpenteria	10.3	meso	meso	0.9299	755	40	30	19	11	-1.0	4.7
Carpenteria	14.9	meso	meso	0.9482	3426	31	36	22	11	-4.8	-1.7
Dos Cuadras	11.2	meso	meso	0.9270	187	42	31	20	7	-9.1	6.2
Dos Cuadras	20.3	meso	entrain	0.9359	741	41	31	19	9	-4.2	3.3
Gail E019	24.4	meso	meso	0.9346	1357	59	21	12	8	6.8	2.9
Garden Banks 387	23.3	meso	meso	0.9287	579	46	40	13	2	-9.3	0.3
Genesis	23.1	meso	meso	0.9364	543	48	28	21	3	-5.2	2.0
Green Canyon 184	38.2	meso	meso	0.9043	117	54	34	11	1	1.5	4.6
Green Canyon 200	30.7	meso	meso	0.9071	121	77	13	9	1	3.9	3.5
Green Canyon 65	7.7	meso	meso	0.9509	457	38	42	15	5	3.3	0.9
Green Canyon 65	13.1	meso	meso	0.9559	800	36	44	15	4	0.0	-1.1
Green Canyon 65	22.9	meso	meso	0.9716	4250	32	45	16	8	-5.6	-3.7
Gulfaks	29.8	meso	meso	0.9129	202	46	42	12	1	2.1	3.3
Hibernia [2000]	22.8	meso	stable	0.8893	99	61	29	8	2	10.4	11.0
Hibernia [2000]	33.5	meso	meso	0.9075	773	56	29	11	4	9.4	6.1
Lucula	10.7	meso	stable	0.8821	5214	64	23	8	4	-0.8	11.2
MARS - TLP	8.42	meso	stable	0.9122	93	55	28	11	6	-0.4	10.3
MARS - TLP	17.2	meso	meso	0.9331	404	50	30	13	7	-4.4	5.3
MARS - TLP	26.2	meso	stable	0.9520	2237	49	29	13	10	-5.2	1.6
Mississippi Canyon 72	18	meso	stable	0.8966	76	58	32	9	2	-0.8	8.5
Mississippi Canyon 807	0	meso	stable	0.8894	41	47	35	12	6	3.1	16.4
Mississippi Canyon 807	8.67	meso	stable	0.9187	127	39	41	13	7	-0.8	9.1
Mississippi Canyon Block 807	11.8	meso	stable	0.9202	165	70	16	8	6	1.5	11.5
Mississippi Canyon Block 807	22.4	meso	meso	0.9562	396	66	17	10	7	-0.6	1.7
Mississippi Canyon Block 807	35.9	meso	meso	0.9693	1472	63	16	11	10	-2.8	1.5
Morpeth EW921	15.2	meso	meso	0.9426	551	66	18	10	6	-0.3	1.6
Morpeth EW921	24.0	meso	meso	0.9619	3697	60	19	13	8	-3.2	-2.0
North Slope (Middle Pipeline)	30.5	meso	meso	0.9418	900	42	38	12	7	0.7	3.0
North Slope (Northern Pipeline)	31.1	meso	meso	0.9402	748	44	37	12	7	1.2	3.9
North Slope (Southern Pipeline)	29.6	meso	meso	0.9431	961	42	39	13	7	2.5	2.4
Prudhoe Bay (1995)	0	meso	stable	0.8837	22	53	34	10	4	4.5	14.6
Prudhoe Bay (1995)	27.3	meso	meso	0.9352	623	43	38	15	5	3.6	2.8
Sakhalin	42.0	meso	meso	0.9201	52	56	32	10	2	8.4	1.7
Santa Clara	0	meso	meso	0.9202	304	36	22	29	13	-7.7	6.6
Santa Clara	11.4	meso	meso	0.9479	1859	32	28	27	13	5.3	-0.7
Santa Clara	21.6	meso	meso	0.9672	22760	28	32	23	17	-8.5	-7.2
Sockeye (2000)	0	meso	meso	0.9354	761	50	18	18	15	2.9	5.1
Sockeye (2000)	7	meso	meso	0.9537	2720	47	17	19	16	-1.3	0.5
Sockeye Sweet	17.5	meso	stable	0.9089	103	50	32	13	5	4.3	9.8
Waxy Light Heavy Blend	12	meso	meso	0.9582	2002	32	38	24	6	-9.9	-2.3
Waxy Light Heavy Blend	19.6	meso	meso	0.9749	17280	30	35	28	6	-10.2	-7.8
West Texas (2000)	21	meso	stable	0.8827	38	76	15	8	1	6.3	11.3
West Texas (2000)	31	meso	meso	0.8973	112	75	14	10	2	7.9	4.9

Model Certainty

It is noted that there is little error for more stable types, but more error for the unstable types or those that do not form any of the other three types. This was noted in previous modeling as well (Fingas 2011). It is suspected that the reasons for this are:

a) Unstable types or those oils that do not form any of the other three types, generally consist of three widely separate classes of oils or fuels, very light oils such as the fuels which have little or no resins or asphaltenes; those very heavy oils which are so viscous that they will not uptake water; and those oils that have the incorrect ratio or amounts of resins or asphaltenes. It is difficult to mathematically incorporate all three of these variances into one grouping. The new procedure is that the density and viscosity data are first applied to remove the unstable and entrained types. The calculation in equation 4 is used to separate the stable and meso-stable types.

b) Some of the oils may be able to form different water-in-oil types, but emulsion inhibitors or asphaltene suspenders have been added to the products. These types of oils make prediction very difficult, and

c) There are many different asphaltenes some of which make much more stable emulsions than others. Recent work has shown that there are hundreds of asphaltene sub-components varying very much in composition and molecular size (Fingas 2011). Thus the percent of asphaltenes (or resins) certainly does not tell the whole story about the emulsion-stabilizers.

The regression table is given in Table 3.

Conclusions

Water-in-oil emulsions are formed as a result of asphaltene and resin surfactant characteristics in oil of moderate viscosity (50 to 2000 mPa.s). Four types of water-in-oil products are formed: stable and meso-stable emulsions, entrained water in oil and unstable (or those that do not form any of the other three types) types. Each of these types has unique characteristics and is thought to be non-convertible to other types once formed.

The knowledge that water-in-oil types exist and that a new scheme to classify their stability, herein called stability, enables the development of new and much more accurate emulsion formation models. The density, viscosity, asphaltene and resin contents are used to develop a regression equation to stability, which in turn predicts either an unstable or entrained water-in-oil state or a meso-stable or stable emulsion.

The new model can provide accurate prediction of class about 90% of the time. This can be compared with the older models where the fit varied from about 60 to 80% of cases (Fingas and Fieldhouse, 2011). The new procedure is that the density and viscosity data are first applied to remove the unstable and entrained types. The calculation in equation 4 is used to separate the stable and meso-stable types. The major inaccuracy lies with the unstable types because of the fact that there are three distinct types of oils or fuels in this class, each very different, as well as the possible presence of emulsion breakers or asphaltene suspenders in the oils.

REFERENCES

Aguilera, B.M., J.G. Delgado, and A.L. Cardenas, "Water-in-Oil Emulsions Stabilized by Asphaltenes Obtained from Venezuelan Crude Oils", *Journal of Dispersion Science and Technology*, pp. 359-363, 2010.

Aichele, C.P., W.G. Chapman, L.D. Rhyne, H.J. Subramani and W.V. House, "Analysis of the Formation of Water-in-Oil Emulsion", *Energy & Fuels*, pp. 3674-3680, 2009.

Ali, M.F. and M.H. Alqam, "The Role of Asphaltenes, Resins and Other Solids in the Stabilization of Water in Oil Emulsions and its Effects on Oil Production in Saudi Oil Fields", *Fuel*, Vol. 79, pp. 1309-1316, 2000.

Araujo, A.M., L.M. Santos, M. Fortuny, R.L.F.V. Melo, R.C.C. Coutinho, and A.F. Santos, "Evaluation of Water Content and Average Droplet Size in Water-in-Crude Oil Emulsions by Means of Near-Infrared Spectroscopy", *Energy & Fuels*, pp. 3450- 3458, 2008.

Arla, D., A. Singuin, T. Palermo, C. Hurtevent, A. Graciaa, and C. Dicharry, "Influence of pH and Water Content on the Type and Stability of Acidic Crude Oil Emulsions", *Energy & Fuels*, pp. 1332-1342, 2007.

Aske, N., H. Kallevik and J. Sjöblom, "Water-in-Crude Oil Emulsion Stability Studied by Critical Electric Field Measurement: Correlation to Physico-Chemical Parameters and Near-Infrared Spectroscopy", *Journal of Petroleum Science and Engineering*, Vol. 36, pp. 1-17, 2002.

Binks, B.P. and A. Rocher, Effects of Temperature on Water-in-oil Emulsions Stabilized Solely by Wax Microparticles, *Colloids and Interface Science*, 94, 2009.

Borges, B. M. Rondon, O. Sereno, and J. Asuaje, "Breaking of

Water-in-Crude-Oil Emulsions: Influence of Salinity and Water-Oil Ratio on Demulsifier Action", *Energy & Fuels*, pp. 1568-1574, 2009.

Czarnecki, J., "Stabilization of Water in Crude Oil Emulsions. Part 2", *Energy & Fuels*, pp. 1253-1257, 2009.

Fingas, M. and B. Fieldhouse, "Formation of Water-in-oil Emulsions and Application to Oil Spill Modelling", *Journal of Hazardous Materials*, Vol. 107, pp. 37-50, 2004a.

Fingas, M. and B. Fieldhouse, "Studies on Crude Oil and Petroleum Product Emulsions: Water Resolution and Rheology", *Colloids and Surfaces A: Physicochemical and Engineering Aspects*, Vol. 333, pp. 67-81, 2009.

Fingas, M., "Models for Water-in-Oil Emulsion Formation", Chapter 10, in *Oil Spill Science and Technology,* M. Fingas, Editor, Elsevier Publishers, NY, NY, pp. 243-273, 2011.

Fingas, M., B. Fieldhouse, "Studies on Water-in-oil Products from Crude Oils and Petroleum Products," *Mar. Pollut. Bull*., Vol: 64, pp. 272-283, 2011.

Fingas, M.F. and B. Fieldhouse, A Review of Knowledge on Water-in-oil Emulsions, *AMOP*, pp. 1-26, 2006

Graham, B.F., E.F. May and R.D. Trengove, "Emulsion Inhibiting Components in Crude Oil", *Energy & Fuels*, pp. 1093-1099, 2008.

Groenzin, H. and O.C. Mullins, "Asphaltene Molecular Size and Weight by Time-Resolved Fluorescence Depolarization", in *Asphaltenes, Heavy Oils and Petroleomics*, O.C. Mullins, E.Y. Sheu, A. Hammami, and A.G. Marshall, Editors, Springer Publications, pp. 17- 40, 2007.

Gu, G., Z. Xu, K. Nandakumar and J.H. Masliyah, "Influence of Water-Soluble and Water-Insoluble Natural Surface Active Components on the Stability of Water-in-Toluene-Diluted Bitumen Emulsion", *Fuel*, Vol. 81, pp. 1859-1869, 2002.

Hemmingston, P.V., A. Silset, A. Hannisdal and J. Sjöblom, "Emulsions of Heavy Crude Oils. I: Influence of Viscosity, Temperature and Dilution", *Journal of Dispersion Science and Technology*, Vol. 26, pp. 615-627, 2005.

Johnsen, E.E. and H.P. Rønningsen, "Viscosity of 'Live' Water-in-Crude-Oil Emulsions: Experimental Work and Validation of Correlations", *Journal of Petroleum Science and Engineering*, Vol. 38, pp. 23-36, 2003.

Kallevik, H., O.M. Kvalheim and J. Sjöblom, "Qualitative Determination of Asphaltenes and Resins in Solution by Means of Near-Infrared Spectroscopy: Correlations to Emulsion Stability", *Journal of Colloid and Interface Science*, Vol. 225, pp. 494-504, 2000.

Kilpatrick, P.E., and P.M. Spiecker, "Asphaltene Emulsions", in *Encyclopedic Handbook of Emulsion Technology*, Ed. J. Sjoblom, Marcel Dekker, Inc., New York, pp. 707-730, 2001.

Kozachenko, Y., A. Olenko, A., and O. Polosmak, "Uniform Convergence of Wavelet Expansions of Gaussian Random Processes", *Stochastic Analysis and Applications*, 29 (2), pp. 169-184, 2011.

Lobato, M.D., J.M. Pedrosa, A.R. Hortal, B. Martinez-Haya, R. Lebron-Aguilar, and S. Lago, "Characterization and Langmuir Film Properties of Asphaltenes Extracted from Arabian Light Crude Oil", *Colloids and Surfaces*, A, pp.72-79, 2007.

Midttun, O., H. Kallevik, J. Sjoblom and O.M. Kvalheim, "Multivariate Screening Analysis of Water-in-Oil Emulsions in High External Electric Fields as Studied by Means of Dielectric Time Domain Spectroscopy", *Journal of Colloid and Interface Science*, Vol. 227, pp. 262-271, 2000.

NAS, *Oil in the Sea III, Inputs, Fates and Effects*, National Research Council, National Academies Press, Washington, D.C., 2002

Nordli, K.G., J. Sjöblom, and P. Stenius, "Water-in-Crude Oil Emulsions from the Norwegian Continental Shelf: 4. Monolayer Properties of the Interfacially Active Crude Oil Fraction", *Colloids and Surfaces*, Vol. 57, pp. 83-98, 1991.

Pereira, J.C., I. Lopez, R. Salas, F. Silva, C. Fernandez, C. Urbina, and J.C. Lopez, "Resins, The Molecules Responsible for the Stability/Instability Phenomena of Asphaltenes", *Energy & Fuels*, pp. 1317-1321, 2007.

Ridi, F., N. Verdal, P. Balioni and E.Y. Sheu, "Phase Separation Kinetics of Maya Asphaltene Emulsion and Free-to-bound Water Transformation", *Fuel*, 319, 2009.

Rondon, M., J.C. Pereira, P. Bouriat, A. Graciaa, J. Lachaise and J-L. Salagar, "Breaking of Water-in-Crude-Oil Emulsions. 2. Influence of Asphaltene Concentration and Diluent Nature on Demulsifier Action", *Energy & Fuels*, pp. 702-707, 2008.

Silset, A., A. Hannisdal, P. Hemmingsen, and J. Sjöblom, "Emulsions of Heavy Crude Oils. II. Viscous Responses

and Their Influence on Emulsion Stability Measurements", *Journal of Dispersion Science andTechnology*, 1432, 2010.

Sjöblom, J., N. Aske, I.H. Auflem, O. Brandal, T.E. Havre, O. Saether, A. Westvik, E.E. Jonsen and H. Kallevik, "Our Current Understanding of Water-in-Crude Oil Emulsions: Recent Characterization Techniques and High Pressure Performance", *Advances in Colloid and Interface Science*, Vol. 100-102, pp. 399-473, 2003.

Spiecker, P.M. and P.K. Kilpatrick, "Interfacial Rheology of Petroleum Asphaltenes at the Oil-Water Interface", *Langmuir*, Vol. 20, pp. 4022-4032, 2004.

Spiecker, P.M., K.L. Gawrys, C.B. Trail and P.K. Kilpatrick, "Effects of Petroleum Resins on Asphaltene Aggregation and Water-in-Oil Emulsion Formation", *Colloids and Surfaces*, Vol. 220A, pp. 9-27, 2003.

Spiecker, P.M., K.L. Gawrys, C.B. Trail and P.K. Kilpatrick, "Effects of Petroleum Resins on Asphaltene Aggregation and Water-in-Oil Emulsion Formation", *Colloids and Surfaces*, Vol. 220A, pp. 9-27, 2003.

Sztukowski, D.M. and H.W. Yarranton, "Characterization and Interfacial Behaviour of Oil Sands Solids Implicated in Emulsion Stability", *Journal of Dispersion Science and Technology*, Vol. 25, pp. 299-310, 2004.

Varadaraj, R. and Brons, C. "Molecular Origins of Crude Oil Interfacial Activity. Part 4: Oil-water Interface Elasticity and Crude Oil Asphaltene Films", *Energy and Fuels*, 26 (12), pp. 7164-7169, 2012.

Yang, X., H. Hamza and J. Czarnecki, "Investigation of Subfractions of Athabasca Asphaltenes and Their Role in Emulsion Stability", *Energy Fuels*, pp. 770-779, 2004.

Yarranton, H.W., H. Hussein and J.H. Masliyah, "Water-in-Hydrocarbon Emulsions Stabilized by Asphaltenes at Low Concentrations", *Journal of Colloid and Interface Science*, Vol. 228, pp. 52-63, 2000.

Yetilmezsoy, K, M. Fingas, and B. Fieldhouse, "Modeling Water-in-Oil Emulsion Formation Using Fuzzy Logic", *Journal of Multiple-Valued Logic Soft Computing*, pp. 1-25, 2011, 2011.

Zhang, L.Y., R. Lopetinsky, Z. Xu and J.H. Masliyah, Asphaltene Monolayers at a Toluene/Water Interface, *Energy Fuels*, 1330, 2005

Merv F. Fingas scientist living in Edmonton, Alberta, Canada, Dr. Fingas has a PhD in environmental physics from McGill University (1996), three masters degrees; that is, chemistry (1984), business and mathematics (1978), all from University of Ottawa. He also has a bachelor of science in Chemistry from Alberta (1974) and a bachelor of arts from Indiana (1968).

He was Chief of the Emergencies Science Division of Environment Canada for over 30 years in Ottawa, Ontario and is currently working on research in Edmonton, Western Canada as an independent researcher. He has published more than 840 papers. Merv has prepared 7 books on spill topics and is working on 2 others.

Dr. Fingas is a member of the American Chemical Society and the American Association for the Advancement of Science. He has been active in the American Society for Testing and Materials.

doi: 10.14355/jpsr.2014.0301.05

Estimating Required Combustion Air and Fuel Gas in a Sulfur Recovery Unit (SRU) Containing Lean Acid Gas Feed

Hamid Reza Mahdipoor [*1a], Saeed Hassan Boroojerdi [2a], Amir Erfani [3b], Hooman Javaherizadeh [4a]

[a] Department of Process Development and Equipment Technology, Research Institute of Petroleum Industry, West Bld. of Azadi Stadium, Tehran, Iran

[b] School of chemical, gas and petroleum engineering, Semnan university, Semnan, Iran

[*1] mahdipoorhr@ripi.ir; [2] hassanboroojerdi@ripi.ir; [3] a.erfani@students.semnan.ac.ir; [4] Javaherizadehh @ripi.ir

Abstract

Modified Claus process is highly applied in oil refining and gas processing for recovery of sulfur from H_2S. Estimating the required air and fuel gas in reaction furnace are important in design and operation of sulfur recovery units. In this article based on some industrial SRUs design and operational conditions, variation of air and fuel flow vs. acid gas flow and concentration are investigated. As a result two simple correlations are developed for estimating the air and fuel gas demands.

Keywords

Combustion Air; Fuel Gas; Furnace Temperature; Claus Process; Sulfur Recovery Unit

Introduction

The Claus process continues to be the most widely used process for conversion of H_2S to sulfur (Paskall, 1979; Tulsa, 1987; Sames; Baehr, 1938). Sulfur recovery units (SRUs) are necessary to match increasingly stringent emission control regulations (Signor, Manenti, Grottoli, Fabbri and Pierucci, 2010). Multi step Claus process removes sulfur from hydrogen sulfide in natural gas processing, refining crude oil, gasification and synthesis gas processes (Lins , 2007; Rappold, 2010; Maddox, 1974). The modified Claus process consists of a high temperature reaction furnace, followed by catalytic reaction stages. Many researchers had worked on thermodynamic and kinetic modeling of SRUs (Hawboldt , 1999; Monnery, 2001; Nasato, 1994; Dowling, 1990), while many researches study optimum operation condition of these units (Hawboldt, 1998; ZareNezhad, 2009; Mahdipoor, 2012).Furnace flame temperature is one of the most important criteria's in SRU operation but accurate prediction of temperature and species concentrations are difficult tasks. Estimation of required combustion air and fuel gas is useful for primary sizing of the air blowers and control valves.

Aim of this research is to introduce two simple correlations for estimation of air and fuel gas flow rates. Although complete sets of data for operating and equipment conditions are not easy to find, we had the opportunity to obtain the plant data for some industrial cases.

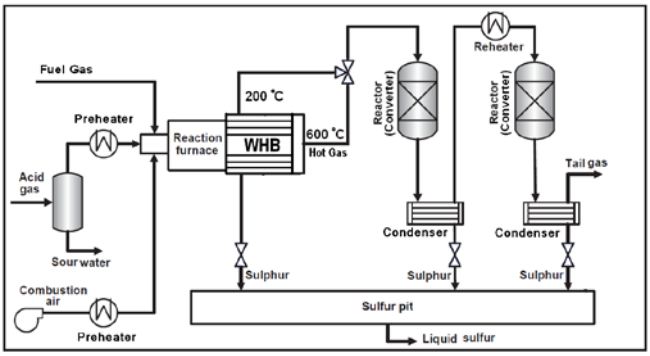

FIG. 1 PROCESS FLOW OF A MODIFIED TWO-STAGE CLAUS PROCESS

SRU Process Design

Figure 1, illustrates process flow of a modified two-stage Claus process. Numerous chemical reactions take place in reaction furnace but the overall reaction characterizing the process is oxidation of hydrogen sulfide as follows:

$$2H_2S + O_2 \Rightarrow S_2 + 2H_2O \quad (1)$$

At first approximately 1/3 of the acid gas is oxidizes:

$$H_2S + \tfrac{3}{2}O_2 \Rightarrow SO_2 + H_2O \quad (2)$$

This combustion generates large amount of heat. SO_2 also reacts away in subsequent reactions; the most important one is the Claus reaction:

$$2H_2S + SO_2 \Leftrightarrow \tfrac{3}{2}S_2 + 2H_2O \quad (3)$$

Reaction (3) is a reversible, exothermic reaction. Principally adiabatic extent of every exothermic

equilibrium reaction increases temperature, which lowers equilibrium conversion. 50-60% of the total sulfur production of the plant is generated in the reaction furnace. Effluent gas from the reaction furnace passes through waste heat boiler (WHB).

In catalytic reaction stages, unreacted H_2S reacts with SO_2, over an activated alumina catalyst to form elemental sulfur. Processing gas with low H_2S content requires some special considerations in burner. Feed containing a relatively low concentration of H_2S has flame stability problems. Also, incomplete combustion of hydrocarbons in the feed can lead to deterioration of the catalyst in the reactors due carbon deposition. Several configurations are applied to treat lean SRU acid gas feed. Most common methods are: acid gas preheating, fuel gas burner, acid gas bypass around the furnace, and oxygen enrichment of the combustion air. Table 1, summarizes design of two SRUs with different H_2S concentrations. In lean feed case, acid gas and combustion air are normally fed to plant.

TABLE 1 DESIGN OF TWO SRUS WITH DIFFERENT H2S CONCENTRATIONS

	Industrial case 1	Industrial case 2
Feed	Acid gas from MDEA trains	Sour gas
H_2S Concentration (molar)	36%	64%
Operating Furnace Temperature (°C)	1000	1009
Design Temperature (°C)	1600	1600
Pressure (barg)	0.5	0.58
Preheating	Up to 220 °C	No preheating
Fuel Gas	Always operational	Only for start-up and shut-down

TABLE 2 SPECIFICATIONS OF ACID GAS FEED FOR AN INDUSTRIAL CASE

Temperature	58 °C
Pressure	0.6 barg
Molar Flow	300 Kmol/h
Composition (molar %)	
H_2S	36
CO_2	57
H_2O	7

TABLE3, REQUIRED COMBUSTION AIR AND FUEL GAS FOR INDUSTRIAL CASES (FURNACE TEMPERATURE=1000 °C)

Flow (Kmol/h)	H_2S (mole %)	Air (Kmol/h)	Fuel Gas (Kmol/h)
350	36	374.77	11.11
325	36	348.00	10.32
300	36	321.23	9.53
275	36	294.46	8.73
250	36	267.69	7.94
300	40	323.93	6.54
300	38	322.58	8.04
300	34	319.86	11.02
300	32	318.48	12.50

Estimating the Required Air and Fuel Gas

Conditions of acid gas feed stream demands for a typical SRU is presented in table 2 and combustion air and fuel gas, for industrial cases are summarized in Table 3.

Rigorous modeling of required air and fuel should be based on minimizing Gibbs free energy based of Lagrangian multipliers, which is not in scope of this research. If we assume all furnace reactions, as one simple reaction of H_2S and fuel gas oxidation we have:

$$(a)\ H_2S + (b)\ \text{Fuel gas} + (AF)\ \text{Air} \longrightarrow \text{products} \quad (4)$$

Then we can have:

$$AF=(x)\ H_2S+(y)\ FG \quad (5)$$

In the other hand: x=HS*Ag

$$AF=a_1*(HS)*(AG)+a_2*(FG) \quad (6)$$

Which x, y, a, b and ai are all constants. Also base on most simple form of energy balance:

$$AF*(H_{AF})+AG*(H_{AG})+FG*(H_{FG})+\Delta Hr(\text{fuel gas})+\Delta Hr(\text{Acid gas})-H\text{products}=0 \quad (7)$$

From equation (7), FG can be obtained:

$$FG=a_3+a_4(AF)+a_5(AG)+a_6(HS) \quad (8)$$

Equation 5 and 8 can be solved and reformed for FG and AF, thus:

$$FG=a+b(HS)(AG)+c(AG)+d(HS) \quad (9)$$

$$AF=e+f(HS)(AG)+g(AG)+h(HS) \quad (10)$$

Utilizing least square method and table 3 data's, constants in equation 9 and 10 are obtained. Equation 11 and 12 present obtained correlations for air flow and fuel gas flow:

$$FG= 0.7500-0.0024(HS)(AG)+ 0.1190(AG)-0.0206(HS),\ r_2=0.992 \quad (11)$$

$$AF=0.9573+0.0024(HS)(AG)+0.9858(AG)-0.0271(HS),\ r_2=0.995 \quad (12)$$

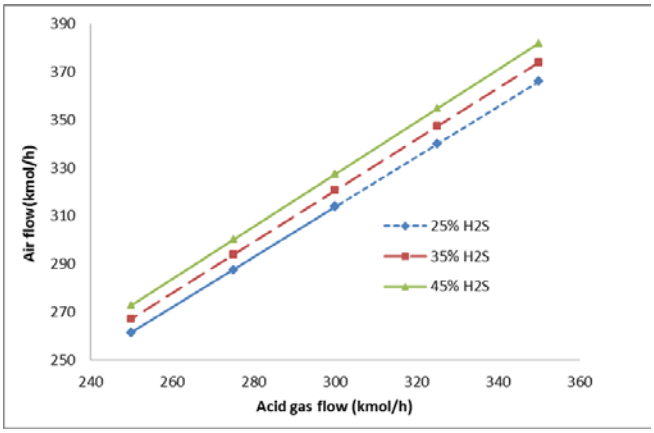

FIG. 2 VARIATION OF REQUIRED AIR VS. ACID GAS FLOW RATE AT DIFFERENT H2S CONCENTRATIONS

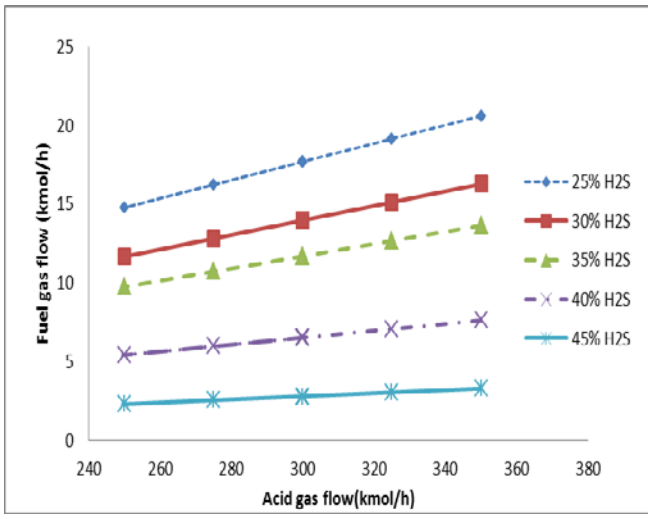

FIG. 3 THE VARIATION OF FUEL GAS VS. ACID GAS FLOW AT DIFFERENT H_2S CONCENTRATIONS

Figure 2 and 3 illustrate required air and fuel gas flow rates accordingly.

Summary and Conclusions

Estimating the required air and fuel gas in reaction furnace is important for primary sizing of the air blowers and control valves. In this paper, the variations of the air and fuel gas were illustrated against changes in SRU feed flow rate and Hydrogen Sulfide mole percent. As the result, two correlations were developed for estimating the required air and fuel gas.

Nomenclature

AF: Estimated Air Flow (Kmol/h)

AG: Acid Gas Flow (Kmol/h)

FG: Estimated Fuel Gas Flow (Kmol/h)

Hi: enthalpy of component i

ΔHr: enthalpy of reaction

HS: Hydrogen Sulfide molar percent

REFERENCES

Baehr, H. "Gas Purification by the I.G. Alkacid Process and Sulfur Recovery by the I.G. Claus Process." Refin. Nut. Gasoline Manuf. 237-244, 17, 1938.

Dowling, N. I., Hyne, J. B., and Brown, D. M., "Kinetics of the Reaction between Hydrogen and Sulfur under High-Temperature Claus Furnace Conditions", Ind. Eng. Chem. Res. 2327-2332, 29, 1990.

Hawboldt, K. A.; Monnery, W. D.; Svrcek, W. Y. "New Experimental Data and Kinetic Rate Expression for H_2S Cracking and Re-Association". Chem. Eng. Sci. 957-966, 55 (5), 1999.

Hawboldt, K. A.; Monnery, W. D.; Svrcek, W. Y. "A Study on the Effect of Quench Design on the Quality of Experimental Data". Ind. Eng. Chem. Res. 2260-2263, 38 (6), 1999.

Huisman H.M., P. van der Berg, R. Mos, A.J. van Dillen, and J.W. Geus, "Hydrolysis of Carbon Sulfides on Titania and Alumina Catalysts: The Influence of Water", Applied Catalysis A, 157-172, 115, 1994.

Laperdrix, E., I. Justin, G. Costentin, 0. Saur, J.C. Lavalley, A. Aboulayt, J.L. Ray, and C. Nedez, "Comparative Study of CS_2 Hydrolysis Catalyzed by Alumina and Titania", Applied Catalysis B: Environment, 167-173, 17, 1998.

Lins V.F.C., Guimaraes E.M. "Failure of a heat exchanger generated by an excess of SO2 and H2S in the Sulfur Recovery Unit of a petroleum refinery", Journal of Loss Prevention in the Process Industries 91–97, 20, 2007.

Maddox, R.N. "Gas and Liquid Sweetening", M. Campbell, 1974.

Mahdipoor, H. R., Ganji, H., Naderi, H., Yousefian, H., Javaherizadeh, "Adjusting the Furnace and Converter Temperature of the Sulfur Recovery Units", H., World Academy of Science Engineering and Technology, Bali, Indonesia, 24-25, October 2012.

Mahdipoor, H. R., Khorsand, K., Hayati, R., Javaherizadeh, H., "Effect of Reaction Furnace and Converter Temperatures on Performance of Sulfur Recovery Units (SRUs)", JPSR Vol. 1, No. 1 , 1-3, Apr. 2012.

Mahdipoor, H. R., Yousefian, S. H., Naderi, H., Kakavand, M.,"Investigating the Effective Parameters at Choosing an Appropriate Tail Gas Treatment Process", CTAIJ 7(3), 82-86, 2012.

Monnery, W. D., Hawboldt, K. A., Pollock, A. E. and Svrcek, W. Y., "Ammonia Pyrolysis and Oxidation in the Claus Furnace", Ind. Eng. Chem. Res. 144-151, 40, 2001.

Nasato, L. V., Karan, K., Mehrotra, A. K., and Behie, L. A., Modeling Reaction Quench Times in the Waste Heat Boiler of a Claus Plant, Ind. Eng. Chem. Res. 7-13, 33, 1994.

Paskall, H. G. "Capability of the Modified-C1ausProcess"; Department of Energy and Natural Resources: Edmonton, Alberta, Canada; Chapter IV, 1979.

Rappold T.A., Lackner K.S. "Large scale disposal of waste sulfur: From sulfide fuels to sulfate sequestration", Energy 1368–1380, 35, 2010.

Sames, J., "Sulfur recovery process fundamental", Sulfur experts Inc.

Signor, S., Manenti, F., Grottoli, M. G., Fabbri, P., and Pierucci, S., "Sulfur Recovery Units: Adaptive Simulation and Model Validation on an Industrial Plant", Ind. Eng. Chem. Res. 5714-5724, 49, 2010.

Tulsa,"Gas Processors Suppliers Association (GPSA)". Engineering Data Book; GPSA; Chapter 22, 1987.

ZareNezhad, B., "An investigation on the most important influencing parameters regarding the selection of the proper catalysts for Claus SRU converters", J. Ind. Eng. Chem. 143-147, 15, 2009.